

Dissertation zur Erlangung des Doktorgrades  
der Fakultät für Chemie und Pharmazie  
der Ludwig-Maximilian-Universität München



**Characterisation of apoptosis signal transduction  
induced by the marine compound cephalostatin 1  
in leukemic cells**

Irina Melanie Müller

aus

Forchheim / Ofr.

2004

### Erklärung

Diese Dissertation wurde im Sinne von § 13 Abs. 3 bzw. 4 der Promotionsordnung vom 29. Januar 1998 von Frau Prof. Dr. A. M. Vollmar betreut.

### Ehrenwörtliche Versicherung

Diese Dissertation wurde selbständig, ohne unerlaubte Hilfe angefertigt.

München, den 04.03.2004

---

Irina Müller

Dissertation eingereicht am:	04.03.2004
1. Gutachter:	Frau Prof. Dr. A. M. Vollmar
2. Gutachter:	Herr Prof. Dr. E. Wagner
Mündliche Prüfung am:	15.04.2004

# I. CONTENTS

I.	Contents .....	I
II.	Introduction .....	1
1.	Background - Marine Compounds in Cancer Therapy .....	1
2.	The Family of Cephalostatins .....	3
2.1	<i>Cephalodiscus gilchristi</i> Ridewood .....	5
2.2	Biological activity of cephalostatin 1 .....	7
3.	Aim of the work .....	8
4.	Apoptosis / Programmed Cell Death and Necrosis .....	8
5.	Signal transduction in Apoptosis .....	10
5.1	Caspases .....	11
5.2	Extrinsic Pathway / Death Receptor Pathway .....	13
5.3	Intrinsic Pathway / Mitochondrial Pathway .....	15
5.3.1	The Bcl-2 Family .....	17
5.3.2	Smac / DIABLO .....	19
5.4	ER-mediated Pathway .....	20
III.	Materials and Methods .....	23
1.	Materials and Solutions .....	23
2.	Cephalostatin 1 .....	23
2.1	Isolation .....	23
3.	Cell culture .....	24
3.1	Cell Lines .....	24
3.2	Cell Culture Techniques .....	24
3.2.1	Freezing and thawing .....	24
3.2.2	Determination of cell concentration .....	25
3.2.3	Splitting and seeding .....	25
4.	Cytotoxicity Assays .....	26
4.1	MTT Assay .....	26
4.2	Propidium Iodide Exclusion Assay .....	27
5.	Quantification of Apoptosis by Flow Cytometry .....	28
5.1	Introduction to Flow Cytometry .....	28
5.2	Quantification by Staining with Propidium Iodide .....	29
5.3	Quantification by Staining with Annexin V .....	31
5.4	Measurement of Mitochondrial Potential Dissipation .....	32

<b>6. Microscopy .....</b>	<b>33</b>
6.1 Light Microscopy .....	33
6.2 Fluorescence Microscopy.....	33
6.2.1 Hoechst staining.....	33
6.2.2 JC1 staining .....	34
6.3 Confocal Laser Scanning Microscopy (CLSM).....	34
6.4 Transmission Electron Microscopy.....	35
<b>7. Caspase Activity Assay.....</b>	<b>38</b>
<b>8. Western Blot Analysis .....</b>	<b>39</b>
8.1 Preparation of Samples.....	39
8.1.1 Whole cell lysates .....	39
8.1.2 Cytosolic and particulate fractions.....	40
8.2 Protein Determination.....	41
8.3 SDS-PAGE.....	42
8.4 Western Blotting and Detection of Proteins.....	44
8.5 Coomassie Staining of Gels .....	46
8.6 Membrane Stripping.....	47
<b>9. Immunoprecipitation.....</b>	<b>47</b>
<b>10. Comet Assay / Single Cell Gel Electrophoresis .....</b>	<b>48</b>
<b>11. Statistics .....</b>	<b>49</b>
<b>IV. Results .....</b>	<b>50</b>
<b>1. Cytotoxic Activity of Cephalostatin 1.....</b>	<b>50</b>
<b>2. Apoptosis-Induction by Cephalostatin 1 .....</b>	<b>50</b>
2.1 Morphologic Alterations.....	51
2.1.1 Light microscopic analysis of cephalostatin 1-treated cells ....	51
2.1.2 Morphologic analysis per flow cytometry.....	51
2.1.3 Morphologic changes of the nucleus.....	52
2.1.4 Phosphatidylserine exposure .....	53
2.2 Quantitative Analysis of Cephalostatin 1-Induced Apoptosis .....	54
<b>3. Signal Transduction in Cephalostatin 1-Induced Apoptosis .....</b>	<b>56</b>
3.1 Caspases are Essential for Cephalostatin 1-Induced Apoptosis ...	56
3.1.1 Inhibition of apoptosis by zVADfmk.....	57
3.2 Involvement of the Cd95 Pathway.....	58
3.2.1 Activation of caspase-8.....	58
3.2.2 Apoptosis induction in CD95 deficient cells.....	59
3.3 Involvement of the Mitochondria .....	61
3.3.1 Morphological alterations of cephalostatin 1-activated mitochondria.....	61
3.3.2 Alterations of the mitochondrial membrane potential .....	63
3.3.3 Activation of caspase-9.....	65

---

3.3.4	Release of apoptogenic factors from the intermembrane space .	65
3.3.5	Formation of an apoptosome .....	68
3.3.6	Necessity of caspase-9 for cephalostatin 1-induced apoptosis	69
3.3.7	Overexpression of anti-apoptotic proteins Bcl-2 and Bcl-x <sub>L</sub> .....	70
3.3.8	Inactivation of Bcl-2.....	74
3.4	Involvement of the Endoplasmic Reticulum.....	80
3.4.1	Cephalostatin 1 elicits ER stress.....	80
3.4.2	Activation of caspase-12 .....	81
<b>V.</b>	<b>Discussion.....</b>	<b>83</b>
	<b>Characterisation of the Cell Death Induced by Cephalostatin 1.....</b>	<b>83</b>
	<b>Signal Transduction Pathways in Cephalostatin 1-Induced Apoptosis .....</b>	<b>84</b>
1.1	Involvement of CD95 Pathway .....	84
1.2	Involvement of Mitochondria in Cephalostatin 1-Induced Apoptosis ..	85
1.3	Involvement of the Endoplasmic Reticulum.....	90
	<b>Regulation of Cephalostatin 1-Induced Apoptosis .....</b>	<b>93</b>
<b>VI.</b>	<b>Summary and Outlook .....</b>	<b>96</b>
<b>VII.</b>	<b>Appendix.....</b>	<b>98</b>
1.	<b>Abbreviations .....</b>	<b>98</b>
2.	<b>Alphabetical List of Companies.....</b>	<b>101</b>
3.	<b>Publications.....</b>	<b>102</b>
3.1	Abstracts .....	102
3.2	Original Publications.....	102
<b>VIII.</b>	<b>References .....</b>	<b>103</b>
<b>IX.</b>	<b>Acknowledgements.....</b>	<b>128</b>
<b>X.</b>	<b>Curriculum Vitae .....</b>	<b>129</b>



## **II. INTRODUCTION**

### **1. BACKGROUND - MARINE COMPOUNDS IN CANCER THERAPY**

In the past decades, the interest in compounds from marine origins for cancer therapy has reached a so far unknown intensity. With new and safer scuba-diving techniques, ocean regions down to a depth of 200 m became accessible and since the mid-1960s, approx. 10,000 substances have been isolated from marine microorganisms, seaweeds, sponges, soft corals and marine invertebrates. The enormous diversity of organisms in the sea is mirrored in these structures which also display an extreme variability [1]. Most possess bioactivity and, most likely, represent a chemical defence for the soft-bodied animals lacking a physical barrier [2]. Recent studies have suggested that some of the compounds are not synthesised by the organisms themselves but are taken up along with the consumed food or are produced by symbiotic bacteria [3;4].

Natural products and their derivatives play a fundamental role in cancer chemotherapy. Over 60 % of approved anticancer drugs are obtained from natural sources. However, in the period of 1981 to 2002, all new approved drugs were isolated from plants or microorganisms (Table 1). So far, no marine natural anticancer agent has been accepted to clinical use although several are in clinical trials (Table 2).

The reason for this lies in part in the difficulties to provide sufficient material for preclinical and clinical trials. Often, the collection of organisms is hampered by unfavourable circumstances (adverse currents, sharks, etc.). Besides that, the concentration of the compounds is frequently so low that large quantities of the animals have to be harvested in order to achieve sufficient material. The ecological system, however, is heavily affected by these large intrusions into a previously unharmed environment. Scientists as well as pharmaceutical

companies search intensely for solutions to this problem. Chemical synthesis or mariculture (growing of marine organisms in controlled conditions) of the organisms might provide an approach but the structural complexity of numerous compounds complicates a synthesis. Moreover, the culture techniques for marine organisms have been improved over the last years but the specific requirements for many species are not easy to meet. In those cases, where a symbiotic metabolite producer is known, cultivation of these organisms has been attempted but often the microorganisms live as obligate symbionts and cannot be grown outside their host.

**Table 1: Chemotherapeutic agents introduced from 1981 – 2002 (adopted from [5])**

<b>Drug name</b>	<b>Year of introduction</b>
Aclarubicin	1981
Arglabin	1999
BEC	1989
Masoprocol	1992
Paclitaxel	1993
Pentostatin	1992
Peplomycin	1981
Solamargine	1987

In spite of all obstacles, the results reached so far are very promising. In the development for new and highly active compounds, the marine products might play a significant role in that they can serve as templates for combinatorial chemistry coupled with high-throughput screening to identify new drug candidates [2;6].

**Table 2: Current Marine Organism-Derived Anticancer Drugs in Development (adopted from [1])**

<b>Drug name</b>	<b>Source Organism (type)</b>	<b>Development Stage</b>
Aplidine	<i>Aplidium albicans</i> (tunicate)	Phase II
Bryostatin 1	<i>Bugula neritina</i> (bryozoan)	Phase I, II
Dolastatin 10	<i>Dolabella auricularia</i> (mollusk)	Phase I, II
Ecteinascidin 743	<i>Ecteinascidia turbinata</i> (tunicate)	Awaiting approval of the EMA
Kahalalide F	<i>Elysia rubefescens</i> (mollusk)	Phase II
Squalamine	<i>Squalus acanthias</i> (dogfish shark)	Phase II

## 2. THE FAMILY OF CEPHALOSTATINS

The cephalostatins isolated from the marine organism *Cephalodiscus gilchristi* Ridewood (see 2.1) belong to the most cytotoxic marine natural products ever tested by the National Cancer Institute/USA. Up to now, 19 derivatives could be characterised all of which show the same unique cytotoxicity profile in the NCI-60 panel (see Figure 1). This panel displays the growth inhibitory potency of substances against 60 cancer cell lines of diverse origins [7;8]. All cephalostatins share this fingerprint which does not show significant correlations to any other compound neither of the standard agent database nor of the complete NCI compound database suggesting that the cephalostatins might employ novel signal transduction pathways [9].

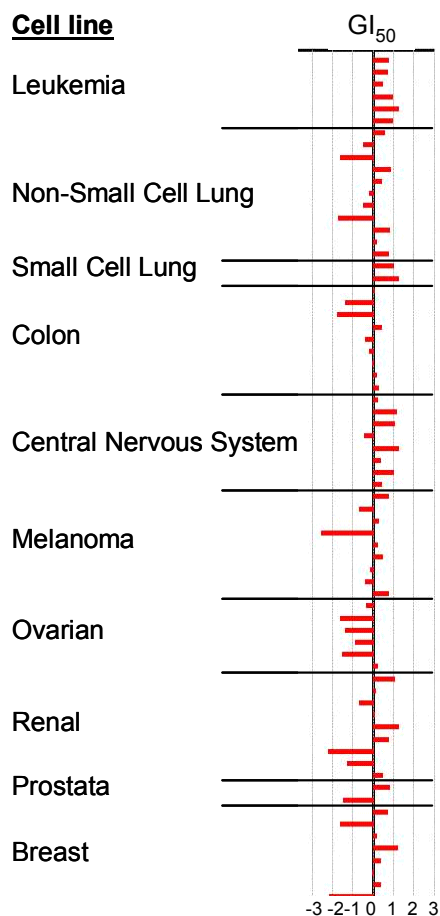


**Figure 1: Fingerprint of cytotoxic profile of cephalostatin 1 evaluated by the NCI-60 screen (September 2003).**

$GI_{50}$ , 50 % growth inhibition. The zero value represents the mean of all cell lines tested. The bars indicate the deviation of the mean data obtained from the individual cell line from the overall mean and marks the sensitivity of the cell lines for cephalostatin 1 (negative bars, less sensitive; positive bars, more sensitive).

Although the cytotoxicity profile of the cephalostatins does not differ, their potency varies depending on the chemical composition. Cephalostatin 1 (see Figure 2) proved to be the most potent form in the NCI-60 panel [10]. Cephalostatins 2-4 [11], cephalostatin 10 – 11 [12], cephalostatin 16 – 17 [13], however, show dose dependencies comparable to cephalostatin 1. These structures differ in the right side moiety or the middle part of the molecule which seems not to interfere with the biological activity. In contrast, modifications in the left side unit decrease the potency as displayed by cephalostatin 5 – 9 [14;15], cephalostatin 12 – 15 [16;17] and cephalostatins 18-19 [18].

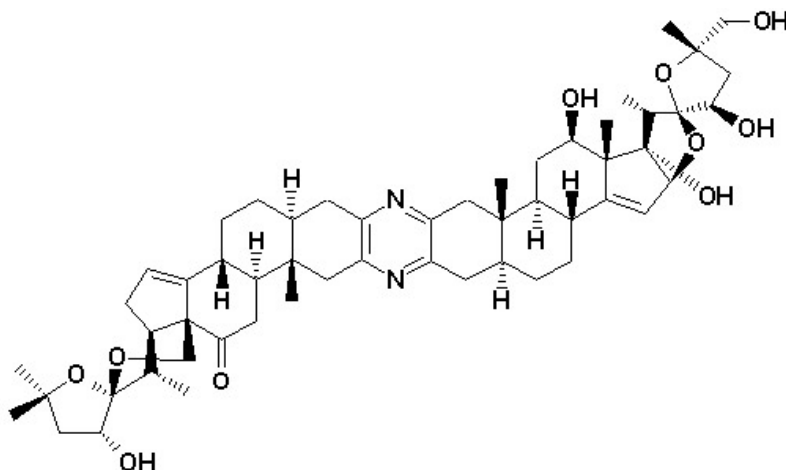
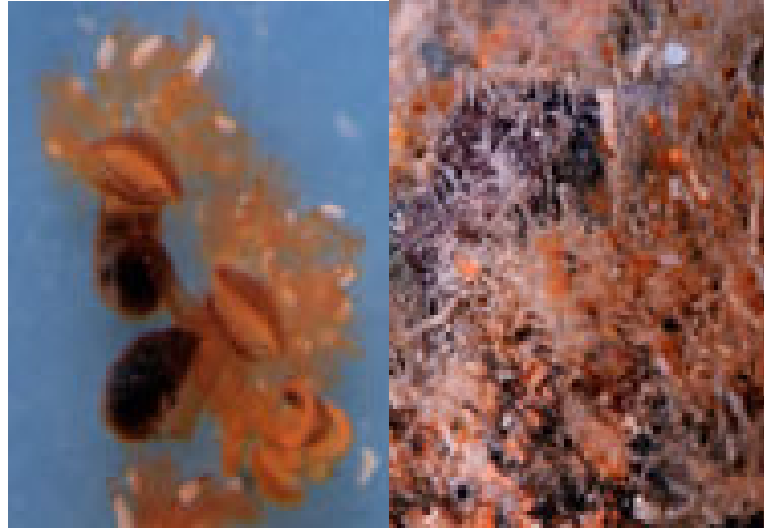


Figure 2: Chemical structure of cephalostatin 1.

## 2.1 *CEPHALODISCUS GILCHRISTI* RIDEWOOD

The marine worm *Cephalodiscus gilchristi* Ridewood (family Cephalodiscidae) (Figure 3) from which the cephalostatins were isolated belongs to the class of Pterobranchia (phylum Hemichordata). Pterobranchs are sessile colonial organisms living in tubes (coenecia) composed of a gelatinoid substance which is secreted by glands in the anterior part of their body. The colonies often contain several hundred individuals (zooids).

Their body is segmented into three parts, the prosoma, the mesosoma and the metasoma. The upper body segment, the prosoma, is modified to a cephalic shield on which the zooid is able to crawl on the inner and outer side of the coenecium (Figure 4). From the collar-like mesosoma, 4 – 10 arms, the lophophores, protrude dorsally carrying a double row of ciliated tentacles. A mucus net is formed among the tentacles in which planktonic particles are trapped. Cilia on the tentacles transport the mass towards the mouth on the ventral side of the animal. The sac-like metasoma contains the major part of the U-shaped digestive tract which is composed of a short pharynx and oesophagus



**Figure 3: Cephalodiscus sp. (family Cephalodiscidae) [19].**  
*Left panel, individual worms; right panel, colony in their coenecia.*

followed by a wide stomach. From the end of the stomach, the intestine proceeds after a loop dorsally towards the mesosoma. The mouth is located on the ventral side in the mesosoma, the anus sits directly opposite the mouth on the back. In *Cephalodiscus sp.*, one pair of gill slits opens from the lateral sides of the pharynx to the outside. On the far end of the metasoma, the body extends into a contractile muscular stalk (stolo) of several body lengths depending on the state of contraction. Together with the prosoma, the animal can use the stolo as organ of locomotion [20;21].

The animals are dioecious. In female zooids, a pair of ovaries is situated in the mesosoma. From there, two ducts lead to dorsal pores. *Cephalodiscus sp.* breeds two embryos which develop into a ciliated planula-shaped larva. Metamorphosis occurs after a short life in free suspension [22]. Although sexual reproduction is the normal method, pterobranchs are capable of asexual reproduction by budding. The buds develop out of the stalk and are released early in development. They form their own coenecium near the parent zooid thus giving rise to colonies.

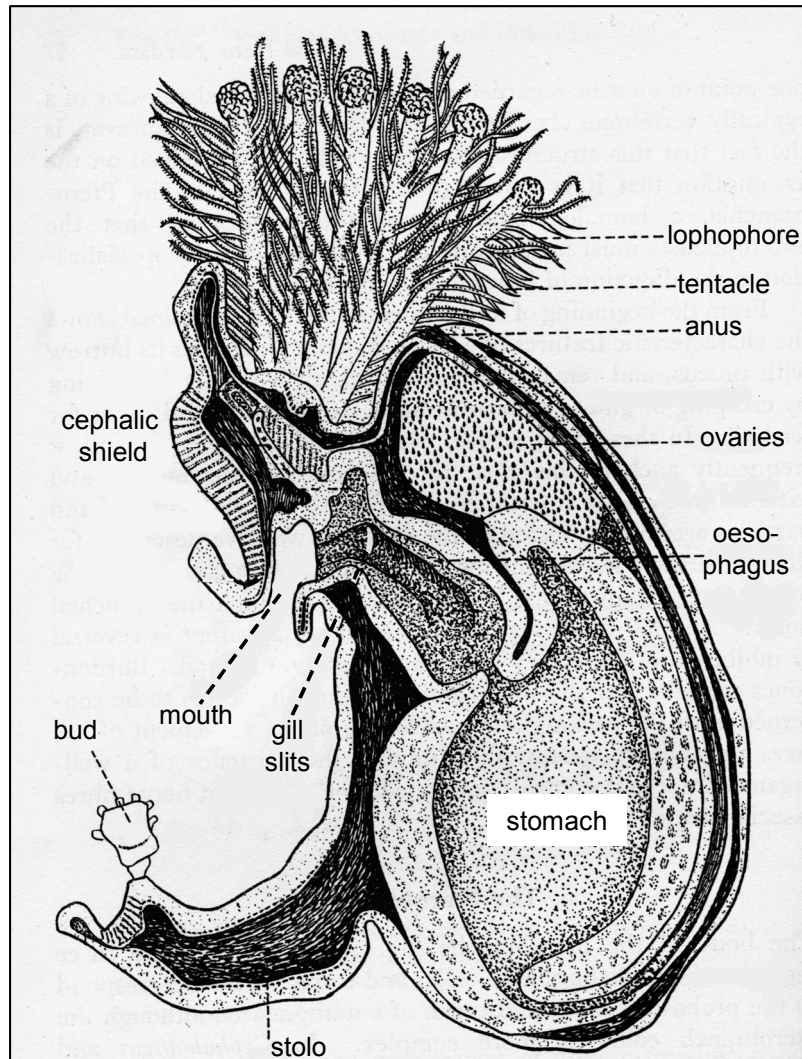


Figure 4: Illustration of *Cephalodiscus* sp. (adapted from [20])

The zoids possess a single blood vessel in which the heart located dorsally in the metasoma pumps the blood to the lower part of the body and draws it ventrally to the top. The nervous system lies intraepithelially in the epidermis and forms a ganglion below the lophophore.

## 2.2 BIOLOGICAL ACTIVITY OF CEPHALOSTATIN 1

Cephalostatin 1 was tested extensively by the National Cancer Institute in order to assess the growth inhibitory effects. The values obtained from the assays yielded a mean  $GI_{50}$  concentration of approximately 1 nM in the 2-day NCI-60

screen [23]. Beyond the *in vitro* tests, cephalostatin 1 was tested on several xenografts such as melanoma, sarcoma, leukaemia and even on a human mammary carcinoma model. All these tumours were inhibited *in vivo* [24].

### **3. AIM OF THE WORK**

The marine compound cephalostatin 1 displays a unique cytotoxicity profile in the NCI-60 screen demonstrating its potent cytostatic effect. However, the mode of action of cephalostatin 1 as cytotoxic agent has not been investigated yet. Therefore, the present study focuses on the signalling pathway involved in the apoptotic cell death induced by cephalostatin 1 in Jurkat leukaemia T cells.

### **4. APOPTOSIS / PROGRAMMED CELL DEATH AND NECROSIS**

Apoptosis or programmed cell death is an essential physiological process governing development and homeostasis of multicellular organisms. The term “apoptosis” was first coined by Kerr *et al.* in 1972 when he described a distinct form of cell death characterised by cell shrinkage, internucleosomal cleavage of chromatin, blebbing of the plasma membrane and finally fragmentation of the cell into apoptotic bodies. The apoptotic bodies are enclosed by an intact plasma membrane. On this way, leakage of cellular material into the surrounding tissue and subsequent inflammation is prevented [25]. The vesicles shed by apoptotic cells are phagocytosed by adjoining cells and macrophages. Apoptotic bodies are recognised, among others, by phosphatidylserine molecules present on the surface after their externalisation in the course of the apoptotic process [26;27]. The biochemical features of apoptosis follow a genetically controlled program that is evolutionarily conserved in almost all multicellular organisms. Studies of the molecular mechanisms in *Caenorhabditis elegans* provided an excellent background for the elucidation of the mammalian apoptosis pathways (see 5) [28].

In contrast to apoptosis, another cell death termed necrosis occurs after injuries or excessive contact with cytotoxic agents and typically induces inflammation [25]. Necrosis does not follow a designated molecular pathway but is defined by cellular swelling followed by a burst of the plasma membrane spilling the cellular content into the surrounding tissue. Thus, apoptosis and necrosis were initially regarded as two distinct forms of cell death.

However, not all apoptotic cells are engulfed by phagocytes. These unrecognised apoptotic particles may undergo a secondary necrosis [29] (see Figure 5). This finding led to the recent perception that necrosis is not so much a death pathway *per se*, distinguishable from apoptosis, but the process occurring after the cell has died [30;31]. Beyond that, recent studies in knockout mice revealed the potential conversion of an apoptotic process to necrotic cell death by silencing the mediators of the apoptotic cascade [32]. This suggests that a clear separation between the two forms of cell death might not be justified since an obvious crosstalk between the apoptotic and necrotic pathway exists.

During the entire course of embryogenesis, apoptotic processes govern the correct formation and development of tissues and organs. Tissue homeostasis is reached by a delicate balance between cell proliferation and apoptosis. Thereby, especially old, mutated or otherwise damaged cells are removed [33]. Furthermore, homeostasis of the immune system is a field where apoptosis plays a particularly important role. The proliferation of T and B lymphocytes is regulated by means of positive selection in order to ensure that only those cells with correctly rearranged antigen receptors stay alive [34]. Negative selection achieves the apoptotic death of self-reactive immune cells [35].

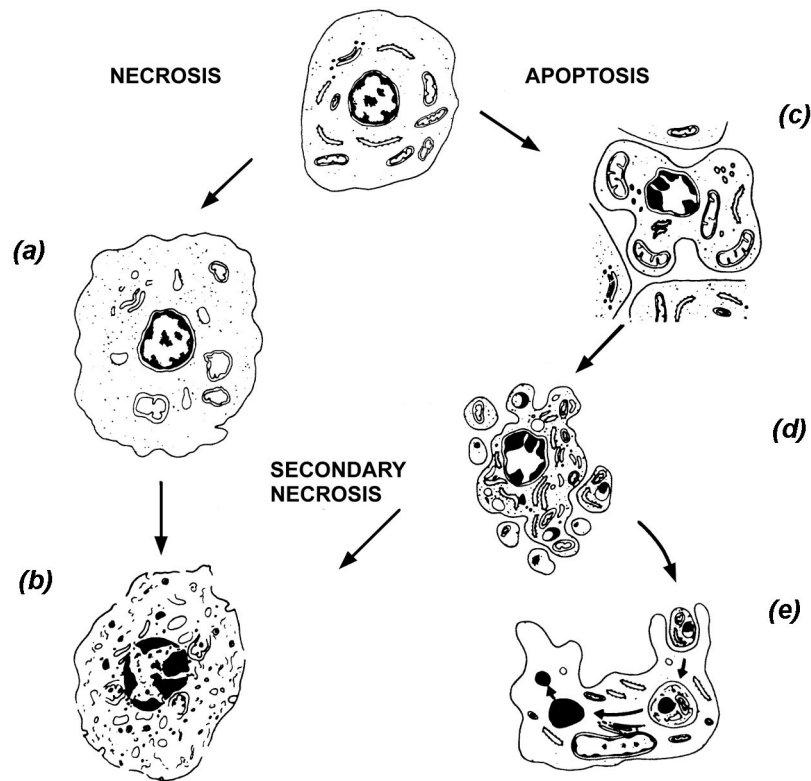


**Figure 5: Distinction between apoptosis and necrosis (adapted from [36]).**

Apoptosis denotes the organised fragmentation of the cell into apoptotic bodies without spillage of cellular contents into the surrounding tissue (c, condensation and blebbing; d, fragmentation into apoptotic bodies with intact membranes; e, phagocytosis of apoptotic bodies by phagocytes). In contrast, in necrosis or accidental cell death, the cell is ruptured and leakage of cell material induces inflammation (a, cell swelling; b, disintegration of the cell). When apoptotic bodies are not phagocytosed by macrophages or adjacent cells, a secondary necrosis might develop.

## 5. SIGNAL TRANSDUCTION IN APOPTOSIS

In apoptosis, the cell is subject to biochemical alterations such as degradation of a variety of proteins, condensation of chromatin, internucleosomal cleavage of DNA and finally fragmentation of the cell into apoptotic bodies. These processes are executed and mediated by a complex molecular machinery including death-specific enzymes and regulatory molecules. Most prominent in this array are the caspases – a family of proteases which is divided into initiator and effector caspases (see under 5.1). Once the cell receives an apoptosis-

inducing signal, the caspases are activated in a cascade leading eventually to the demise of the cell. Currently, three different apoptotic pathways have been proposed depending on the death signal: the extrinsic or receptor-mediated pathway (5.2), the intrinsic or mitochondrial pathway (5.3) and the ER-mediated pathway (5.4). Of course, these signalling pathways do not always proceed independently of each other since interaction at diverse stages has become obvious in numerous models.

## 5.1 CASPASES

The family of cysteine-dependent caspases plays a pivotal role in the regulation of apoptosis. To date, the family comprises 14 members which all display the unique specificity for substrate cleavage after an aspartate residue. Only one other mammalian protease, the T lymphocyte serine protease granzyme B, shares this feature [37]. Apart from the function of caspases in apoptosis, some members of the family are involved in inflammation by their cytokine processing ability.

Caspases are synthesised as inactive zymogens which share a similar structure (Figure 6). The pro-caspases are composed of a N-terminal prodomain followed by a large (~ 20 kDa) and a small subunit (~ 10 kDa). The large subunit contains the catalytic cysteine residue within a conserved QACXG motif. For processing, the zymogen is first cleaved between the large and the small subunit. Subsequently, the prodomain is removed. An active heterotetrameric caspase is formed by self-association of two processed zymogens and consists of two large and two small subunits. Each heterodimer contains an active site formed by residues of both the large and small subunit [38;39].

Caspases are classified as either initiator caspases which are activated first in the cascade (caspase-1, -2, -4, -5, -8, -9, -10 and -12) or executor caspases which are activated by initiator caspases (-3, -6, -7 and -14) [40]. Initiator caspases are characterised by a long prodomain which contains special

structural motifs such as DED (death effector domain; caspase-8 and -10) or CARD (caspase recruitment domain; caspase-4, -5 and -9). These motifs serve as binding sites to adaptor molecules such as FADD (see 5.2) or Apaf-1 (see 5.3) which are crucial for the activation of initiator caspases in that they connect the pro-caspase to apoptotic sensors (death receptors or mitochondria) and bring the two zymogens into close proximity enabling transactivation [41].

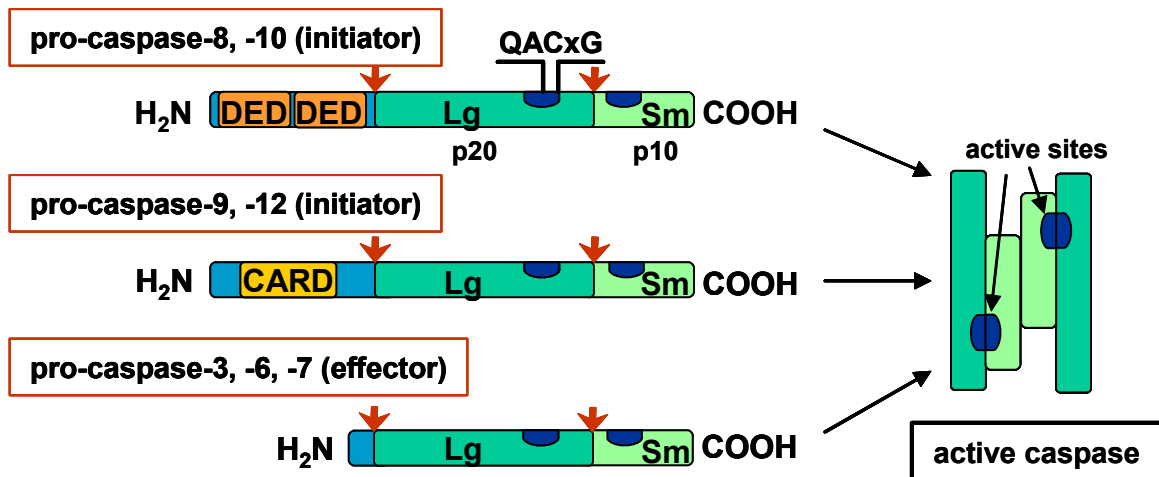


**Figure 6: Schematic illustration of the structure of zymogens and active caspases.**

Pro-caspase-8 and -10 carry two repeats of the DED in their long prodomain (blue) whereas a CARD domain is present in the prodomain of caspase-9 and -12. All effector caspases have short prodomains. The active caspase is composed of two small (Sm) and two large subunits (Lg) and contains two active sites. The caspase cleavage motif including the catalytic cysteine (QACxG) is located in the large subunit.

Active effector caspases are responsible for the regulated disassembly of the apoptotic cell by cleaving the so-called death substrates. The range of these substrates is vast and includes inactivation of survival mechanisms as well as degradation of structural proteins. The latter is evident e.g. in an extensive actin, fodrin and lamin cleavage provoking dissolution of the nucleus and cell shrinkage [42]. Cleavage of the DNA repair enzyme PARP (poly (ADP-ribose) polymerase) as well as the destruction of ICAD (inhibitor of caspase-activated DNase) leading to functional CAD / DFF (caspase-activated DNase / DNA fragmentation factor) aids in DNA fragmentation [39]. Beyond the repair enzymes, cleavage of proteins involved in cell cycle regulation results in a halt of proliferative activity [43]. An amplification of the apoptotic process is achieved

by activation of further caspases. This area also implies the inactivation of anti-apoptotic proteins such as Bcl-2 and Bcl-x<sub>L</sub> [44;45].

Given the destructive potential of active caspases for cellular fate, various mechanisms have developed for tightly controlling activation of the cell death mediators. These regulations include mechanisms that prevent caspase activation as well as the inhibition of active caspases. The former is obtained by anti-apoptotic proteins of the Bcl-2 family (see 5.3.1). Caspase inhibitors were first identified in cowpox viruses and baculoviruses which encode three classes of inhibitor proteins: CrmA (cytokine responsive modifier A), p35 and IAPs (inhibitor of apoptosis proteins) [46]. CrmA belongs to the serpin family and inhibits caspase-1 and -8 while p35 is a broad spectrum caspase inhibitor [47]. Both proteins are pseudosubstrate inhibitors acting by stably binding to the active site of their target caspase [48]. No mammalian homologues of CrmA or p35 have yet been identified. In contrast, several homologues of IAPs inhibit caspase-3, -7 and -9 in mammalian cells. Two mechanisms are described for IAP inhibition. First, they bind directly to the active site of caspase-3 and caspase-7. In addition to blocking of the active site, further inhibition of caspase-9 is achieved by direct interaction of IAPs with pro-caspase-9 and competing for Apaf-1 binding sites thereby preventing the processing of the zymogen form [49;50] (see also 5.3.2).

## **5.2 EXTRINSIC PATHWAY / DEATH RECEPTOR PATHWAY**

The extrinsic pathway integrates death signals via cell surface receptors. Death receptors belong to the TNF (tumor necrosis factor) receptor superfamily characterised by 2 – 5 extracellular cysteine-rich domains. In addition, death receptors contain a homologous cytoplasmic sequence referred to as death domain (DD). In mammals, several members of the superfamily are known such as TNF-R1, DR3, DR6, TRAIL-R1, TRAIL-R2 and the most extensively studied CD95 which plays a fundamental role in maintenance of a functional immune system [51]. Among these, some receptors, the so-called decoy receptors,

display truncated DDs suggesting an inhibition of transmission of the death signal to the apoptotic machinery [52].

Ligands specific for the death receptors are members of the TNF gene superfamily. By binding of the homotrimeric molecules to their receptor, three death receptors are brought close allowing a clustering of the intracellular DD. Since the receptor has no enzymatic activity, the activation of pro-caspases requires cytoplasmic adaptor molecules. In the case of CD95, this role is appointed to FADD (Fas-associated death domain) which is recruited *via* its own DD to the receptor triad. FADD contains another domain termed DED (death effector domain) that binds to the DED repeated in tandem in the

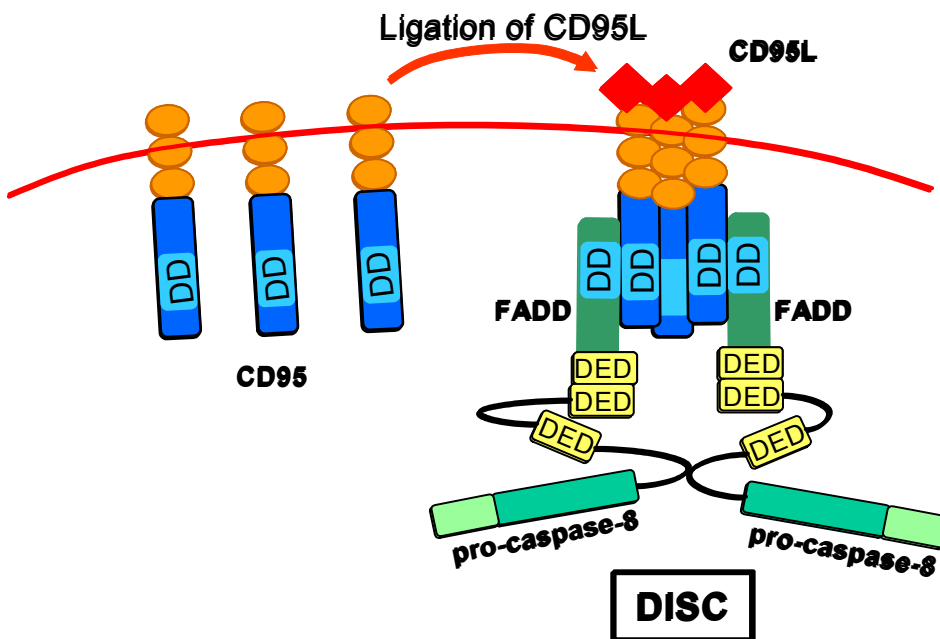


**Figure 7: Components of the receptor-mediated apoptotic pathway.**

On binding of CD95 ligand, CD95 trimerises and recruits FADD on its cytosolic domains via interaction with the death domain (DD). FADD binds pro-caspase-8 to its death effector domain (DED) completing the death-inducing signalling complex (DISC). Pro-caspase-8 is activated in the DISC through autolytic cleavage.

prodomain of caspase-8 (Figure 6). The complex composed of DD, FADD and two pro-caspase-8 molecules is referred to as DISC (death inducing signalling complex). In the DISC, pro-caspase-8 is autolytically cleaved and activated to

induce downstream effector caspases like caspase-3 and caspase-7. Other receptors employ mainly the same mode of caspase activation but include additional adaptor molecules in the signal transduction (e.g. TRADD – TNF receptor-associated death domain) [53;54].

### 5.3 INTRINSIC PATHWAY / MITOCHONDRIAL PATHWAY

Awareness of the importance of mitochondrial signals in apoptosis has increased tremendously in the past years. Once the basic principles were elucidated, increasing numbers of regulating mechanisms have been revealed.

Being the “powerhouse” of the cell, mitochondria fulfil vital functions in metabolism. Two membranes surround the two compartments of mitochondria: the matrix separated from the outside by the inner mitochondrial membrane (IMM) and the intermembrane space between the IMM and the outer mitochondrial membrane (OMM). The IMM contains the protein complexes of the electron transport chain which are important for the formation and maintenance of the mitochondrial membrane potential. Some proteins involved in the transport of electrons across the respiratory chain such as cytochrome c are located in the intermembrane space. The electrochemical gradient is required for ATP synthesis by the ATP synthase also present in the IMM. The transport of ADP molecules across the IMM into the matrix is performed by the ANT (adenine nucleotide transporter). The OMM also comprises a transport protein involved in respiration, the so-called VDAC (voltage-dependent anion channel) [55].

Beyond the function in cell metabolism, mitochondria play an essential role in stress-induced apoptosis. Often, chemotherapeutic agents, UV radiation or free radicals induce mitochondrial apoptosis characterised by a dissipation of the electrochemical gradient and the release of apoptogenic factors. The latter are harboured in the intermembrane space and include cytochrome c, AIF (apoptosis-inducing factor), EndoG (endonuclease G) and Smac / DIABLO

(second mitochondria-derived activator of caspases / direkt IAP binding protein with a low isoelectric point) [56]. Once an apoptotic signal has been transduced to the mitochondria, the apoptogenic factors are released into the cytosol. AIF and EndoG translocate into the nucleus inducing chromatin condensation and DNA fragmentation. These processes proceed independently of ATP and caspase activity. The function of Smac consists in the inhibition of IAPs (see 5.3.2).

Unlike the other factors that are not or only indirectly involved in caspase activation, cytochrome c is of utmost importance for the activation of caspase-9, the initiator caspase in the mitochondrial pathway. In the presence of cytochrome c, a cytosolic factor referred to as Apaf-1 (apoptosis protein-activating factor 1) undergoes a conformational change upon hydrolysis of dATP / ATP to dADP / ADP resulting in oligomerisation of Apaf-1. Apaf-1 carries a CARD domain by which a pro-caspase-9 can be recruited in a 1 : 1 ratio leading to the assembly of an apoptosome. In this complex, pro-caspase-9 is able to perform self-cleavage analogue to the activation of caspase-8 in the DISC. After activation, caspase-9 is able to initiate the caspase cascade [57].

The mode of release of the apoptogenic factors from the intermembrane space is still subject of investigations. It was proposed to occur through a pore complex called the permeability transition pore (PTP) at the contact sites between the two mitochondrial membranes. The PTP is mainly composed of the ANT in the inner and the VDAC in the outer membrane. Opening of the PTP results in dissipation of the membrane potential leading to the observed swelling of the mitochondrial matrix. Beyond the PTP, pro-apoptotic members of the Bcl-2 family such as Bax and Bak (see 5.3.1) have the ability to directly form pores in the OMM thus inducing release of the apoptogenic proteins. Anti-apoptotic Bcl-2 family proteins play important roles in maintaining the integrity of the mitochondrial membranes by several mechanisms (see 5.3.1) [58].

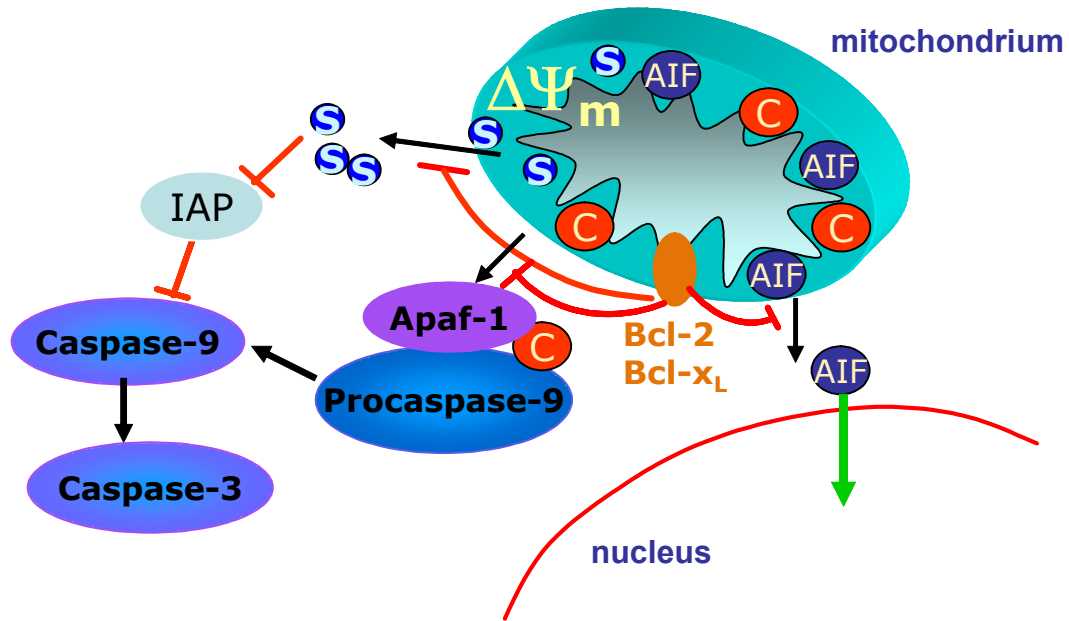


**Figure 8: Schematic illustration of the mitochondria-mediated apoptotic pathway.**

Cytochrome c (C) is released into the cytosol where it interacts with Apaf-1, ATP and pro-caspase-9 resulting in apoptosome formation. Hence, caspase-9 is activated. IAP (inhibitor of apoptosis protein) is able to bind to the active site of active caspase-9 leading to inhibition of apoptosis. Smac (S) acts as inhibitor of IAPs in that it competes with caspase-9 for the IAP binding site. AIF, once released, translocates into the nucleus and mediates DNA fragmentation. The anti-apoptotic proteins Bcl-2 and Bcl-x<sub>L</sub> inhibit the release of apoptogenic factors from the intermembrane space.

### 5.3.1 The Bcl-2 Family

Members of the Bcl-2 family, an evolutionarily conserved group of proteins, are important regulators of the apoptotic processes converging on the mitochondria as well as the endoplasmic reticulum (ER). Bcl-2, the first recognised member of the family, was found in B-cell lymphoma hence the name Bcl. The proteins are divided into three subgroups determined by their structure and function:

1. the anti-apoptotic fraction including Bcl-2, Bcl-x<sub>L</sub>, Bcl-w, A1, Mcl-1 and Boo
2. the pro-apoptotic Bax / Bak-like group encompassing Bax, Bok, Bcl-x<sub>s</sub>, Bak and Bcl-G<sub>L</sub>
3. the pro-apoptotic BH3-only proteins comprising Bad, Bik, Bid, Hrk, Bim, Bmf, Noxa and Puma

The structure of the Bcl-2 family proteins exhibits certain regions of homology referred to as BH1 – 4 (Bcl-2 homology) (Figure 9). Depending on the group, the proteins share either the BH domains 1 – 4 (anti-apoptotic), domains B1 – B3 (Bax / Bak-like) or only the BH3 domain (BH3-only). Most Bcl-2 proteins contain an N-terminal transmembrane region mediating their localisation to membranes of mitochondria, ER and nucleus [59].

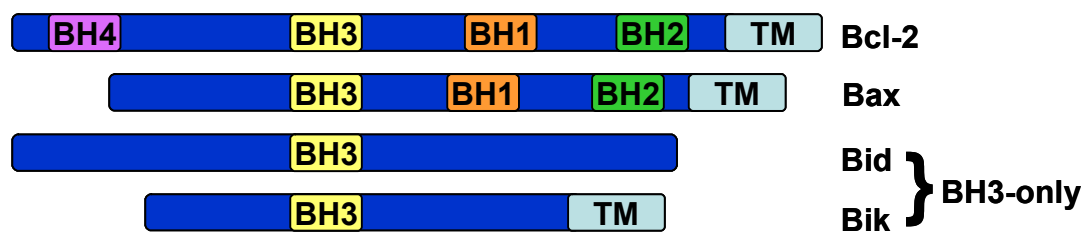


**Figure 9: Schematic illustration of representative members of the Bcl-2 family subgroups.**

Anti-apoptotic proteins such as Bcl-2 contain four Bcl-2 homology (BH) domains and an N-terminal transmembrane region (TM) while most Bax-like proteins lack the BH4 domain. Some BH3-only proteins may contain the TM (adapted from [60]).

The BH3-only proteins seem to act upstream in the apoptotic cascade and promote apoptosis by interaction with Bax / Bak-like proteins thereby inducing cytochrome c release (only Bid) or with anti-apoptotic Bcl-2 proteins thus inhibiting their protective role (all BH3-only members). Interaction between the different proteins occurs via docking of the amphiphatic  $\alpha$ -helical BH3 domain of the BH3-only molecules into the hydrophobic groove composed of the BH1 – BH3 regions of the target protein. The BH3-only proteins are expressed in a cell-type specific manner and serve as sensors to diverse kinds of cellular stress.

Due to the fundamental role of BH3-only proteins in apoptosis promotion, several mechanisms have emerged to tightly control the action of these mediators. Many are sequestered to cellular compartments other than the mitochondria and released only on apoptotic signaling (Bim, Bmf). Beyond that, dephosphorylation (Bad) as well as cleavage (Bid) is required for activation. Bid

is cleaved by active caspase-8 to a truncated form, tBid. tBid then translocates to the mitochondria and interacts with Bax and Bak resulting in conformational changes. The altered conformation of Bax / Bak allows insertion into the mitochondrial membrane and heterodimerisation provoking formation of pores and release of apoptogenic factors from the intermembrane space. Activation of Bax / Bak by tBid allows an amplification of the receptor-mediated apoptosis and indicates the intense crosstalk between the two pathways [56]. Another model for the induction of membrane permeability by Bax / Bak mentions the protein-protein interaction with ANT as well as VDAC in the mitochondrial membranes. On this way, Bax / Bak are suggested to induce formation of the PTP [61;62].

The mechanism by which anti-apoptotic proteins confer protection from mitochondrial damage includes two interaction sites. First, they bind to Bax / Bak-like proteins thus inhibiting conformational changes and insertion into the membrane. Second, they have been proposed to interact with pore-forming proteins in the membrane such as VDAC preventing channel formation [63]. Negative regulation of the anti-apoptotic proteins results from cleavage, hyperphosphorylation and interaction with BH3-only proteins [64].

### 5.3.2 Smac / DIABLO

Smac is a constitutively expressed 21 kDa protein located in the mitochondrial intermembrane space and composed of  $\alpha$ -helical bundles. The structure of the active form is an arch-shaped dimer with the C-terminus located at the respective ends of the arch. The protein is nucleus encoded and carries a mitochondrial location sequence on the N-terminus. On entry into the mitochondrial intermembrane space, this sequence is removed. Like cytochrome c and AIF, Smac is released upon apoptotic signals into the cytosol where it prevents the inhibition of caspases by IAPs [65].

Smac can interact with all mammalian IAPs, but its highest affinity was determined for human XIAP (X-linked inhibitor of apoptosis). IAPs bear 1 – 3 BIR domains (baculovirus IAP repeats) which are essential for their binding ability of caspase-3, -7 and -9. Caspase-3 and -7 are sequestered by the linker region between BIR1 and BIR2 while caspase-9 is bound by BIR3. Smac, however, is able to bind to BIR2 and BIR3 via its four N-terminal amino acids (Ala-Val-Pro-Ile) that became accessible after processing for mitochondrial entry thus competing for the caspase-9 binding site. The binding of caspase-3 and caspase-7 is most probably hindered by steric reasons once Smac has bound to BIR2 [66].

The IAP-inhibitory function of Smac is well established in *in vitro* models. *In vivo*, though, it has been shown that Smac<sup>-/-</sup> mice develop normally without any apparent phenotypes [67]. In addition, a splice variant referred to as Smac-β lacking the mitochondrial localisation sequence and the IAP binding region exerts pro-apoptotic effects although the mechanism has not been elucidated yet [68]. Most likely, the IAP inhibition pathway contains redundant effectors and one of the four known XIAP binding proteins is probably able to compensate for the loss of Smac [69].

#### 5.4 ER-MEDIATED PATHWAY

The endoplasmic reticulum (ER) serves many vital functions as intracellular Ca<sup>2+</sup> store and as site for protein folding and modification (e.g. glycosylation). Folding is carried out by chaperones such as BiP (binding protein). When the load of unfolded proteins rises above the capacity of the ER, a stress response named UPR (unfolded protein response) is triggered resulting in an upregulation of regulatory factors (e. g. chaperones) and a downregulation of protein synthesis. If these repair measures do not take hold, apoptosis is induced as final response [70;71]. Apoptosis induction triggered by ER signals involves several mechanisms beyond the caspase activation described below. Mechanisms include enhanced expression of the transcription factor CHOP /

GADD153 (C/EBP-homologous protein / growth arrest and DNA damage inducible protein 153) which triggers the transcription of apoptosis-relevant genes and JNK activation.

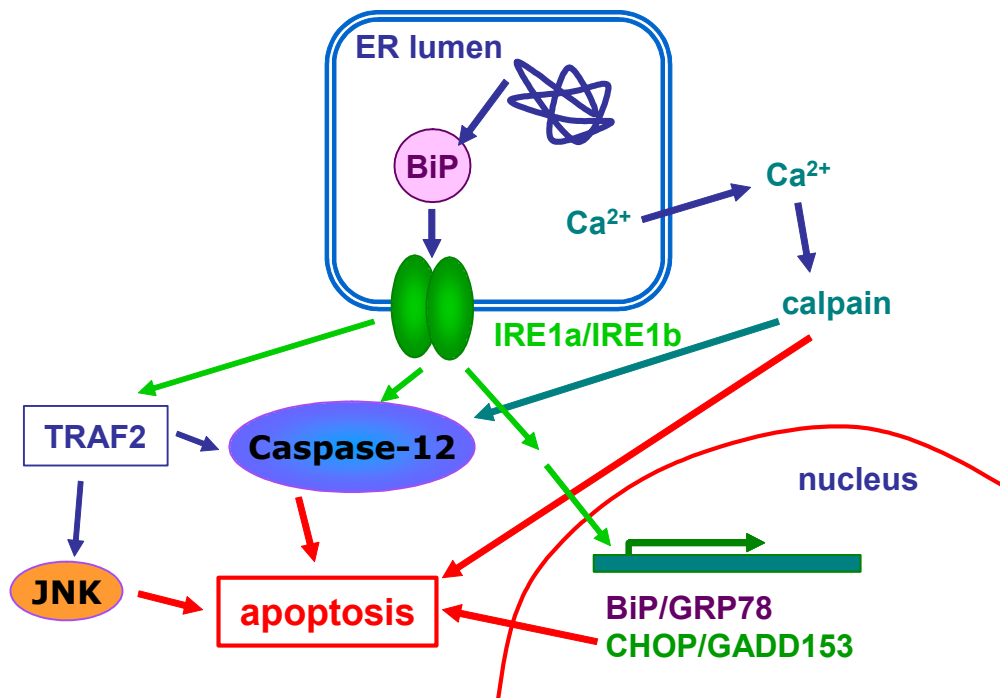


**Figure 10: Schematic representation of the ER-mediated pathway (adapted from [72]).**

The unfolded protein response (UPR) triggers the dimerisation of IRE1 *via* BiP signalling. Subsequently, IRE1 is able to activate JNK through TRAF2 (TNF-receptor associated factor 2), caspase-12 or to initiate transcription of BiP and CHOP. In ER stress, the Ca<sup>2+</sup> stores in the ER lumen is emptied into the cytosol resulting in activation of the Ca<sup>2+</sup>-dependent protease calpain.

The regulation of ER-mediated apoptosis is very complex and involves several members of the Bcl-2 family as well as Ca<sup>2+</sup> as major constituent of the signal transduction. When, upon an apoptotic signal or mediated by the UPR, the Ca<sup>2+</sup> store is emptied into the cytosol it induces activation of calpains [73], Ca<sup>2+</sup>-dependent proteases which are implicated either in activation of Bax (see 5.3.1) or of caspases. Also, it mediates Bad dephosphorylation and activation by induction of Ca<sup>2+</sup>-dependent calcineurin. In addition, through transport of Ca<sup>2+</sup> from the ER into the mitochondria *via* close contacts of the membranes, the mitochondria are sensitised to the action of pro-apoptotic proteins thus leading to an enhanced release of cytochrome c. The Ca<sup>2+</sup> concentration of the ER

lumen is very important in cellular sensitivity to apoptotic stimuli since a decreased  $[Ca^{2+}]_{ER}$  leads to resistance to ER-related apoptosis [74].

The ER-related apoptotic pathway employs two initiator caspases depending on the cell type. Caspase-12 was first detected in murine fibroblasts [75]. It is located exclusively on the cytoplasmic side of the ER membrane. Activation of caspase-12 is still not completely explained but seems to involve diverse mechanisms such as cleavage by calpain [76] or autolytic activation after recruitment to IRE1 / TRAF-2 (TNF receptor associated factor) [77]. In addition, caspase-7 was shown to translocate to the ER and activate caspase-12 [78]. Downstream of caspase-12, besides activation of effector caspases, a direct activation of caspase-9 by caspase-12 independently of cytochrome-c was shown by recent studies [79].

Another initiator caspase is an isoform of caspase-8, caspase-8L [80], which is peripherally associated with the ER membrane and is recruited to another ER surface protein called BAP31 (B-cell antigen receptor-associated protein) allowing self-activation. Apart from unleashing active caspases, ER stress signals attract Bax and Bak to the ER membrane which also induce  $Ca^{2+}$  release.

Regulation proceeds by members of the Bcl-2 family. Beyond its localisation in the mitochondrial membrane, the anti-apoptotic protein Bcl-2 is also present at the ER. ER-based Bcl-2 maintains  $Ca^{2+}$  homeostasis and prevents caspase activation by interaction with BAP31 and pro-apoptotic Bax / Bak and Bik [81]. The latter is a BH3-only protein located mainly on the ER. It has been shown that the Bik : Bcl-2 ratio plays a crucial role in the induction of ER-related apoptosis. In addition to the crosstalk through  $Ca^{2+}$  transfer, a high Bik : Bcl-2 ratio allows Bik to initiate crosstalk between ER and mitochondria by inducing Bax-dependent release of cytochrome c [82]. Furthermore, Bcl-x<sub>L</sub> is also present at ER membranes and serves anti-apoptotic functions.

### III. MATERIALS AND METHODS

#### 1. MATERIALS AND SOLUTIONS

All chemicals were purchased at Sigma-Aldrich (München, Germany) or Roth (Karlsruhe, Germany) unless stated otherwise.

<u>PBS</u>		<u>TBS-T</u>	
NaCl	7.20 g	Tris-base	3.0 g
Na <sub>2</sub> HPO <sub>4</sub>	1.48 g	NaCl	11.1 g
KH <sub>2</sub> PO <sub>4</sub>	0.43 g	Tween-20	2 ml
H <sub>2</sub> O	ad 1000 ml	H <sub>2</sub> O	ad 1000 ml

#### 2. CEPHALOSTATIN 1

Cephalostatin 1, isolated as described in the following protocol, was kindly provided by Dr. G. R. Pettit (Cancer Research Institute, Arizona State University, Tempe, USA) [10].

##### 2.1 ISOLATION

The *Cephalodiscus gilchristi* Ridewood specimens used for isolation of cephalostatin 1 were collected by scuba at a depth of 20 m in the Indian Ocean south-east of Africa. Extraction and isolation of cephalostatin 1 were performed as described by Pettit et al. [10].

### 3. CELL CULTURE

#### 3.1 CELL LINES

The subclone J16 of the Jurkat cell line, derived from an acute lymphatic leukemia, was graciously provided by Dr. S. Eichhorst (Klinikum Großhadern, Munich, Germany). This subclone is particularly sensitive to CD95-induced apoptosis. Jurkat T cells transfected with vector control, *bcl-2* or *bcl-x<sub>L</sub>* [83] as well as CD95 deficient cells [84] were kindly provided by Drs. P. Krammer and H. Walczak (DKFZ, Heidelberg, Germany). Jurkat cells carrying a vector control, wildtype *bcl-2* or a *bcl-2* mutant in which Ser<sup>69</sup>, Thr<sup>70</sup> and Ser<sup>87</sup> were changed to Ala were made available by Prof. S. Korsmeyer (Dana Farber Cancer Institute, Boston, USA [85]).

All cells were cultured in RPMI 1640 (PAN Biotech, Aidenbach, Germany), supplemented with FCS gold (PAA Laboratories, Cölbe, Germany) and pyruvate, in a humidified atmosphere at 5 % CO<sub>2</sub> and 37° C. For experiments, no passage higher than 20 was used. For transfected cells, in order to remove any cells having lost their plasmids, the selection antibiotic geneticin (G418, PAA Laboratories, Cölbe, Germany) at a final concentration of 1 mg/ml was added every fifth passage. Cells exposed to G418 were not used for experiments.

#### 3.2 CELL CULTURE TECHNIQUES

##### 3.2.1 Freezing and thawing

For long-term storage, passages 1-10 were stored in liquid nitrogen while higher passages were kept at -80° C. Since ice crystals forming during the freezing process could rupture the cells, a special freezing medium was used.

Cells were centrifuged at 360 x g, resuspended in freezing medium at a concentration of 5 x 10<sup>5</sup> (1.5 ml per cryovial) and frozen at -20° C for one day.

Afterwards, they were transferred to  $-80^{\circ}\text{C}$  and, if desired, after another day to liquid nitrogen.

#### Freezing medium

RPMI 1640	70 %
FCS gold	20 %
DMSO	10 %

The content of a cryovial was defrosted by gently dissolving in 30 ml prewarmed complete medium. The culture was left to grow for at least five days before any experiments.

### **3.2.2 Determination of cell concentration**

Due to the fact that the genome of Jurkat cells is quite unstable and mutations occur frequently when cell density is too high, cultures must not be grown over  $1.5 \times 10^6$  cells / ml. For the determination of the cell concentration 1 ml of cell suspension was transferred to an Eppendorf tube, vortexed and analysed in a Coulter Counter (Coulter, Krefeld, Germany). The concentration required was achieved by dilution with prewarmed medium.

### **3.2.3 Splitting and seeding**

Cells were split every two to three days and diluted to  $1 \times 10^5$  / ml respectively  $8 \times 10^4$  / ml before weekends.

For experiments, cells were seeded a day before stimulation. The cell suspension was centrifuged at  $360 \times g$  and resuspended in prewarmed medium. After determining the cell density, the appropriate concentration was adjusted by dilution in prewarmed medium. Table 3 shows the concentrations used in the following experiments.

Table 3: Experimental conditions.

Experiment	Concentration	Plate	Volume
Cytotoxicity test (MTT assay) (4.1)	$9 \times 10^5$ / ml	96 well	100 $\mu$ l
Propidium iodide exclusion assay / quantification of apoptosis according to Nicoletti <i>et al.</i> [86] (4.2, 5.2)	$7 \times 10^5$ / ml	24 well	500 $\mu$ l
Staining by Annexin V (5.3)	$7 \times 10^5$ / ml	24 well	1 ml
Staining by JC-1 (5.4) / staining with Hoechst 33342 (6.2.1)	$7 \times 10^5$ / ml	24 well	1 ml
Immunocytochemistry / transmission electron microscopy (6.3, 6.4)	$7 \times 10^5$ / ml	24 well	1 ml
Caspase activity assay (7)	$5 \times 10^5$ / ml	24 well	500 $\mu$ l
Western Blot analysis (8)	$7 \times 10^5$ / ml	24 well	1 ml
Comet assay (10)	$6 \times 10^5$ / ml	24 well	1 ml

## 4. CYTOTOXICITY ASSAYS

### 4.1 MTT ASSAY

The degree of cytotoxicity of a substance can be measured with a colorimetric assay using the tetrazolium salt MTT (3-(4,5-dimethylthiazol-2-yl)-2,5-diphenyl tetrazolium bromide). The assay is based on the reduction of MTT by enzymes of the mitochondrial electron transport assembly, which produces blue formazans. The reduction is proportional to the activity of the assembly and thus to the vitality of the cell. The absorption of the formazans can be measured at 550 nm in a spectrophotometer [87].

#### Protocol:

Cells were seeded at a concentration of  $9 \times 10^5$  / ml in a 96-well plate (100  $\mu$ l per well) the day before stimulation. Stimulation was carried out with different concentrations of cephalostatin 1 (0.1 nM – 100  $\mu$ M) for 24 h. 1  $\mu$ l of DMSO was

used as control for zero inhibition and etoposide was applied as positive control at a concentration of 25  $\mu\text{g} / \text{ml}$ . After 24 h, 10  $\mu\text{l}$  of MTT solution (stock solution: 5 mg/ml in PBS, sterile filtered and kept in aliquots at  $-20^{\circ}\text{C}$ ) were added to each well and incubated at  $37^{\circ}\text{C}$  for 60 minutes. After that, cells were lysed by adding 190  $\mu\text{l}$  DMSO to each well and shaking the plates in the dark for another hour. Finally, the absorption of the solubilised formazan crystals was measured at 550 nm in an ELISA plate reader (SLT spectra, SLT Labinstruments, Crailsheim, Germany).

## 4.2 PROPIDIUM IODIDE EXCLUSION ASSAY

Propidium iodide (PI) is a fluorochrome which intercalates into the DNA. It absorbs light at 488 nm (maximum) and emits light with a maximum at 620 nm. Healthy cells with an intact membrane do not take up the dye while the dye permeates membranes of late-apoptotic or dead cells. Thus, living cells can be distinguished from dead cells which show an increased fluorescence signal.

### Protocol:

$7 \times 10^5$  cells per ml (24-well plate, 500  $\mu\text{l}$  per well) were either left untreated or stimulated with cephalostatin 1. After incubation, cells were harvested by centrifugation (600 x g, 10 min) and washed once with PBS. Staining was carried out by resuspending the pellets each in 500  $\mu\text{l}$  PI solution (2.5  $\mu\text{g}$  PI in PBS). The probes were incubated for 5 min at room temperature and subsequently stored on ice. Measurement was performed in a flow cytometer (FACS Calibur, Becton Dickinson, Heidelberg, Germany) with the fluorescence channel 2 (FL-2,  $\lambda_{\text{em}}$  585 nm) (for a more detailed description of flow cytometry see 5.1). Cells from 0 to  $10^1$  (arbitrary fluorescence units, logarithmic scale) in a histogram were regarded living while cells appearing in a peak around  $10^3$  were regarded apoptotic or dead.

## 5. QUANTIFICATION OF APOPTOSIS BY FLOW CYTOMETRY

Apoptotic cells show several morphologic alterations. Among these are condensation and fragmentation of DNA and breakdown of the nucleus. Early in the apoptotic progress, phosphatidylserine is exposed on the outside of the plasma membrane. Provided that mitochondria are involved in the signal transduction, the dissipation of mitochondrial membrane potential is often observed in the intrinsic apoptotic pathway. Quantitative detection of these events can be accomplished by flow cytometry.

### 5.1 INTRODUCTION TO FLOW CYTOMETRY

Flow cytometry is a useful method for the measurement of cell size and granularity as well as the detection of fluorescent stains. Since apoptotic cells shrink and become more granulated, their light scatter pattern changes characteristically. DNA alterations or changes in the distribution of diverse proteins can be quantified by staining with appropriate fluorochromes.

#### Principle:

##### FACS buffer

NaCl	8.12 g
KH <sub>2</sub> PO <sub>4</sub>	0.26 g
Na <sub>2</sub> HPO <sub>4</sub>	2.35 g
KCl	0.28 g
Na <sub>2</sub> EDTA	0.36 g
LiCl	0.43 g
Na-azide	0.20 g
H <sub>2</sub> O	ad 1000 ml, pH 7.37

In a flow cytometer, cells travel in a laminar fluid stream past a focused laser beam. The morphologic features of a cell are measured by changes in the beam of laser light that are caused by a cell passing through this beam. Some of the incident light is scattered in the forward direction (forward scatter = FSC) and denotes the cell size as smaller particles scatter less light. Light scattered at right angles is a characteristic of the internal complexity of a cell (side scatter = SSC). These two parameters give rise to the dot plot. The relative intensity of fluorescent stains is measured with detectors appropriate to the specific emission spectrum of the fluorochrome and is represented in a histogram plot.

## 5.2 QUANTIFICATION BY STAINING WITH PROPIDIUM IODIDE

The DNA content of growing cells changes according to the cell cycle phase. In  $G_0/G_1$ , cells possess a DNA content of  $2n$  (diploid). During S phase, the DNA is doubled and thus, the DNA content lies between  $2n$  and the final  $4n$  of the  $G_2/M$  phase (mitosis). This particular distribution of cells in a growing culture can be made visible in a histogram plot by staining the cells with PI [86]. Since the dye intercalates into the DNA after permeabilisation, cells in  $G_0/G_1$  emit a lower fluorescence intensity than cells in  $G_2/M$  phase while cells in S phase appear between them. The intensity of the fluorescent light of a cell is directly proportional to its DNA content. In apoptosis, the DNA becomes fragmented. When the low molecular weight fragments are eluted from the cells by a hypotonic buffer, the cells take up less stain than cells with uncompromised DNA. These apoptotic cells appear at an intensity range lower than the  $G_0/G_1$  peak and are characterised as sub $G_1$  peak.

### Protocol:

Cells were seeded at a concentration of  $7 \times 10^5$  / ml in a 24-well plate (500  $\mu$ l per well) and either left untreated or stimulated with cephalostatin 1. Stimulation concentrations, times and used inhibitors are listed in Table 4. After the appropriate period of time, cells were harvested by centrifugation (600 x g, 10 min) and washed once with cold PBS. The pellets were resuspended in 500  $\mu$ l

**Table 4: Assay settings for quantitative detection of apoptosis.**

Experiment	Concentration of cephalostatin 1	Stimulation period	Preincubation
Concentration-dependent induction of apoptosis (IV.2.2)	0.001 – 10 $\mu$ M	24 h	
Time-dependent induction of apoptosis (IV.2.2)	1 $\mu$ M	0 – 24 h	
Caspase involvement in cephalostatin 1-induced apoptosis (IV.3.1.1)	1 $\mu$ M	24 h	zVADfmk (1 h)
Apoptosis induction in CD95 deficient cells (IV.3.2.2)	1 $\mu$ M	0 – 24 h	
Apoptosis induction in caspase-8 deficient cells (IV.3.2.2)	1 $\mu$ M	0 – 24 h	
Dependence of cephalostatin 1-triggered apoptosis on caspase-9 (IV.3.3.6)	1 $\mu$ M	16 h	zLEHDfmk (1 h)
Inhibition of apoptosis by Bcl-2 or Bcl-x <sub>L</sub> overexpression (IV.3.3.7)	1 $\mu$ M	0 – 24 h	
Inactivation of Bcl-2 (IV.3.3.8)	1 $\mu$ M	0 – 24 h	

hypotonic fluorochrome solution (HFS) and left overnight at 4°C in the dark. Untreated cells were used for adjustment of instrument settings. The fluorescence intensity (FL-2) as well as scatter parameters were acquired. The percentage of apoptotic cells was determined from the region of the subG<sub>1</sub> peak.

HFS (light protection!)

Propidium iodide	50 µg
Sodium citrate	0.1% (w/v)
Triton X-100	0.1% (v/v)
PBS	ad 1 ml

**5.3 QUANTIFICATION BY STAINING WITH ANNEXIN V**

Early in apoptosis, the cell membrane loses its normal asymmetry. The membrane phospholipid phosphatidylserine (PS) that is located almost exclusively on the cytoplasmic side of the membrane of living cells is translocated to the outside of the membrane by a phospholipid specific scramblase [27]. These exposed molecules are supposed to constitute the “eat-me” signal to macrophages nearby which recognise the PS molecules on the surface and phagocytose the apoptotic cells [26].

The annexin V assay makes use of this exposure of PS for the detection of cells in early or immediate apoptosis, even before events like DNA fragmentation can be measured. Annexin V is a small  $\text{Ca}^{2+}$  dependent protein with a high and selective affinity for PS. It can be tagged with FITC without compromising its binding properties to PS thus enabling the marked cells to be analysed by flow cytometry [88]. An additional staining with PI opens the opportunity to distinguish between live cells (no staining), apoptotic cells (Annexin V labeling, but no PI uptake) and dead cells (double staining).

Protocol:

The evaluation of phosphatidylserine exposure was carried out using an Annexin V-FITC Apoptosis Detection Kit from Calbiochem (Schwalbach, Germany) according to the manufacturer’s instructions.

Cells ( $7 \times 10^5$  / ml, 1 ml, 24-well plate) were either left untreated or stimulated with cephalostatin 1 (1 µM) for different periods of time (0 – 24 h) and collected by centrifugation (600 x g, 4° C, 10 min). They were washed once with cold

PBS, resuspended in 500  $\mu$ l cold 1 x binding buffer and incubated with 1.25  $\mu$ l Annexin V-FITC solution for 15 min at room temperature. After another centrifugation step (600 x g, 4° C, 10 min), the pellet was resuspended in a volume of 500  $\mu$ l cold 1 x binding buffer and 10  $\mu$ l PI solution was added. The probes were set on ice in the dark and immediately analysed by FACS. The instrument settings were adjusted with apoptotic cells stained with Annexin-FITC only (FL-1;  $\lambda_{em}$ : 530 nm) or with PI only (FL-2,  $\lambda_{em}$ : 585 nm).

#### 5.4 MEASUREMENT OF MITOCHONDRIAL POTENTIAL DISSIPATION

The mitochondria are the site of energy production in a living cell. This production of ATP is driven by an electrochemical gradient consisting of a proton gradient and a transmembrane electrical potential ( $\Delta\psi_m$ ) built across the inner membrane (180 - 220 mV, negative inside). The dissipation of this potential is often observed in apoptosis. Measurement of this event is made possible by the lipophilic fluorescent cation 5,5',6,6'-tetrachloro-1,1',3,3'-tetraethylbenzimidazol-carbocyanine iodide (JC-1) which selectively targets the mitochondria and localises to the inner membrane [89].

In living cells, the monomers form aggregates due to the potential of the membrane which emit light at approx. 590 nm when excited at 490 nm. The orange fluorescence can be analysed in the FL-2 channel of the flow cytometer. When the mitochondrial membrane is permeabilised, the potential-sensitive aggregates resolve into the monomers which causes a shift in emitted light from 590 to 530 nm (green). This shift can be detected in the flow cytometer by an increase of cells being measured by the FL-1 (green) channel [90].

##### Protocol:

JC-1 (Molecular Probes, Eugene, USA) was solubilised in DMSO at a stock concentration of 5 mM. Solutions were stored at -20° C.

Untreated or cephalostatin 1-treated cells ( $7 \times 10^5$  / ml, 1 ml, 24-well plate; stimulation with 1  $\mu$ M cephalostatin 1 for 0 – 24 h) were incubated with 1.25  $\mu$ M JC-1 (final concentration) for 10 min at 37° C in the dark. Following staining, the probes were collected into polypropylene tubes and kept at 37° C in a water bath until measurement.

Since the spectra of the fluorescent emissions of JC-1 aggregates and monomers overlap to a certain extent, a correction of the FACS measurement was necessary. Compensation of FL1 – FL2 was adjusted at 4 % and FL2 – FL1 was set at 12 %.

The shift in fluorescent emission was also examined using fluorescence microscopy (see 6.2.2).

## **6. MICROSCOPY**

### **6.1 LIGHT MICROSCOPY**

Morphologic changes of apoptotic cells such as shrinking, blebbing and formation of apoptotic bodies can be detected by visualisation in a light microscope.

Cells at a concentration of  $7 \times 10^5$  (24-well plate) were either left untreated or stimulated with 1  $\mu$ M cephalostatin 1 for 24 h. After incubation, probes were viewed with a Zeiss Axiovert 25 microscope (Zeiss, Jena, Germany) at a 200 x magnification and pictures were taken with the connected reflex camera.

### **6.2 FLUORESCENCE MICROSCOPY**

#### **6.2.1 Hoechst staining**

A characteristic feature of an apoptotic cell is condensation of DNA followed by its fragmentation. Vital staining of DNA with Hoechst 33342 allows for

visualisation of DNA changes in a fluorescence microscope. After being taken up by an active transport mechanism, the dye binds AT pairs in the DNA and can be detected without any requirement for fixation [91]. Healthy cells emit only weak blue fluorescence since the DNA is distributed evenly in the nucleus. The nucleus in apoptotic cells is smaller in size and due to the condensed DNA shows a strong blue signal. Apoptotic bodies are visible as small clumped dots.

Protocol:

$7 \times 10^5$  cells / ml (24-well plate, 1 ml) were either left untreated or stimulated with cephalostatin 1 (1  $\mu$ M) for various periods of time. 10  $\mu$ l of Hoechst solution were added (0.1 mg/ml stock concentration in distilled water) to each well and the plate was incubated at 37° C for 5-7 min. Subsequently, the plate was kept on ice until analysis. Pictures were taken with a Zeiss Axiovert 25 microscope (Zeiss, Jena, Germany) and connected camera using filter 02 ( $\lambda_{\text{ex}}$ : 365 nm,  $\lambda_{\text{em}}$ : 420 nm).

### **6.2.2 JC-1 staining**

Samples were prepared as described under 5.4. Cells were viewed at 200 x magnification with a Zeiss Axiovert 25 microscope (Zeiss, Jena, Germany) using filter 09 ( $\lambda_{\text{ex}}$ : 450-490 nm,  $\lambda_{\text{em}}$ : 520 nm).

### **6.3 CONFOCAL LASER SCANNING MICROSCOPY (CLSM)**

CLSM differs from conventional microscopy in that it offers a higher optical resolution. This is accomplished by two conjugated pinholes, one illumination pinhole through which only a disk-shaped area is lighted and one in front of the detector which is focused on the same focal plane as the illumination pinhole and allows light solely from there to pass. Thus, out of focus blurs are cut off and image definition is enhanced. For the analysis of protein release from the intermembrane space of mitochondria an LSM 510 Meta (Zeiss, Jena, Germany) was used. It is equipped with different lasers which enable co-localisations using different fluorochromes.

Protocol:

Cells were seeded at  $7 \times 10^5$  per ml and stimulated with cephalostatin 1 ( $1 \mu\text{M}$ ) or etoposide ( $25 \mu\text{g/ml}$ ) for 8 h.  $4 \times 10^4$  cells were centrifuged onto glass slides in a cytospin funnel and dried at RT overnight. Samples were fixed and permeabilised with 4 % *para*-formaldehyde containing 0.05 % saponin in PBS for 15 minutes at room temperature. After washing with 0.03 % saponin in PBS, probes were blocked with 1 % BSA, 1 % FCS, 0.1 % Tween-20 in PBS for 1 h and washed twice in PBS. Anti-cytochrome c antibody and anti-Smac antibody were applied together (1 : 100 dilution in blocking buffer) for co-staining. The anti-AIF antibody was used in the same concentration. The antibody solutions (15  $\mu\text{l}$  per sample) were brought up carefully after drying the glass slide in order to avoid spreading. After incubation for 1 h at RT, the samples were washed twice in PBS. Subsequently, the probes were incubated with the respective secondary antibodies, coupled to the fluorophores Alexa488 or Alexa633 (see Table 7) at a dilution of 1 : 200 in PBS for another 1 h. Finally, the slides were washed twice in PBS and a cover slip was fixed with mounting medium (DakoCytomation GmbH, Hamburg, Germany) which was allowed to solidify for at least 2 h.

Instrument settings for the laser-scanning microscope were applied as listed in Table 5. For co-staining, pictures were taken in multi-track mode.

**Table 5: Instrument settings for confocal laser scanning microscopy.**

Fluorophore	Excitation wavelength	Detection filter
Alexa488	480 nm (Argon laser)	505-530 nm BP
Alexa633	633 nm (HeNe2 laser)	650 nm LP

#### 6.4 TRANSMISSION ELECTRON MICROSCOPY

Electron microscopy offers the opportunity to examine samples on a very fine scale. Morphological details of cell structure and alterations of diverse cell organelles can be shown in high resolution. The “illumination” of the probe is

achieved by a beam of electrons. Where the sample is thicker or denser, fewer electrons are transmitted to the phosphor image screen behind and thus less light is generated.

Preparation and electron microscopic analyses of the probes were performed by Prof. Dr. G. Wanner and Ms. Cornelia Niemann at the Botanical Institute, LMU Munich, Germany.

Protocol:

$7 \times 10^5$  cells per ml (24-well plate; 1 ml) were either left untreated or stimulated with cephalostatin 1 (1  $\mu$ M) for 0 – 16 h. Following stimulation, cells were harvested at 360 x g at 4°C for 10 min and washed with cold PBS. Again, probes were centrifuged, resuspended in fixative solution and stored at 4°C.

Fixing buffer

75 mM cacodylate, pH 7,0  
75 mM NaCl  
2 mM MgCl<sub>2</sub>

Fixative solution

2.5 % glutaraldehyde in fixing buffer

For primary fixation, probes were kept for at least 1 h in fixative solution. Subsequently, they were washed with fixing buffer for increasing lengths of time (5, 15, 30 and 60 min). Secondary fixation was accomplished by incubation with 1 % OsO<sub>4</sub> in fixing buffer. Finally, another washing step in fixing buffer for 15 min was succeeded by a series of washings with distilled water (5, 30 and 60 min). After fixation, the samples were dehydrated with a mixture of water and acetone of increasing acetone concentration.

Dehydration procedure:

<b>Duration</b>	<b>Acetone concentration</b>	<b>Additional stains</b>
15 min	10 %	
30 min	20 %	1 % uranyl acetate
15 min	40 %	
15 min	60 %	
15 min	80 %	
15 min, 30 min, 60 min	100 %	

Once the probes had been transferred to the final dehydration fluid, they were embedded in Spurr low-viscosity epoxy resin. The infiltration process was carried out by increasing concentrations of epoxy resin in acetone:

<b>Duration</b>	<b>Epoxy resin concentration</b>
1 h	50 %
2 – 5 h	66 %
4 h	100 %

Finally, probes were polymerised by heating to 65 – 70°C for 16 h.

Pictures were taken at a LEO EM 912 with an integrated  $\Omega$  energy filter in zero-loss mode (LEO – Zeiss AG, Jena, Germany).

## 7. CASPASE ACTIVITY ASSAY

Caspase activity can be detected by appearance of the active cleavage products which are generated from the caspase zymogens by western blot analysis (see 8). Another approach utilises the specificity of caspases for cleavage after aspartate residues in a particular peptide sequence. For caspase-3, this sequence is DEVD. The peptide is labelled with the fluorophore 7-amino-4-trifluoromethyl coumarin (AFC) whose blue fluorescence shifts to green upon release from the substrate by active caspase-3. Caspase activity is directly proportional to the fluorescence signal.

### Protocol:

Cells were seeded at  $5 \times 10^5$  / ml in a 24-well plate and stimulated with cephalostatin 1 (1  $\mu$ M) for different periods of time. For some experiments, a preincubation with 50  $\mu$ M zLEHDfmk preceded stimulation. After treatment, cells were harvested by centrifugation (370 x g, 4° C, 10 min) and washed twice with ice-cold PBS. Pellets were resuspended in 100  $\mu$ l lysis buffer and frozen at  $-80^\circ$  C until next day. After defrosting, cell lysates were collected by centrifugation (14,000 x g, 4° C, 10 min). 10  $\mu$ l of each supernatant (triplicates) were transferred to two 96-well flat bottom plates – one for caspase activity assay, one for protein determination.

<u>Lysis buffer</u>	<u>Buffer B</u>
5 mM MgCl <sub>2</sub>	50 mM HEPES, pH 7.5
1 mM EGTA	1 % Sucrose
0.1 % Triton X-100	0.1 % CHAPS
25 mM HEPES, pH 7.5	

### Substrate solution (prepare immediately before experiment)

Buffer B	9 ml
10 mM DEVD-AFC in DMSO	45 $\mu$ l
16 % DTT	100 $\mu$ l

For caspase activity assay, 190  $\mu$ l of substrate solution were added to each well. At once, the first reading was performed in a Tecan SPECTRAFluor Plus plate reader ( $\lambda_{\text{ex}}$ : 390 nm,  $\lambda_{\text{em}}$ : 535 nm; Tecan, Crailsheim, Germany) using Xfluo4 software. The following measurements were carried out in 30 minute intervals up to 2.5 h.

Protein determination was carried out as described under 8.2.

For interpretation of results, the readings were normalised by the protein concentration. The actual activity was calculated by evaluating the difference between the 1.5 h interval and the 2 h interval.

## 8. WESTERN BLOT ANALYSIS

### 8.1 PREPARATION OF SAMPLES

#### 8.1.1 Whole cell lysates

Lysis buffer	Lysis buffer for phosphorylated proteins (prepare immediately before experiment)
30 mM Tris-HCl, pH 7.5	2 mM EDTA
150 mM NaCl	137 mM NaCl
2 mM EDTA	10 % Glycerol
1 % Triton X-100	2 mM $\text{Na}_4\text{P}_2\text{O}_7$
Complete <sup>TM</sup>	20 mM Tris-base
	1 % Triton-X 100
	20 mM $\text{C}_3\text{H}_7\text{Na}_2\text{O}_6\text{P}$
	10 mM NaF
	2 mM $\text{Na}_3\text{VO}_4$
	1 mM PMSF
	Complete <sup>TM</sup>

Cells were seeded in 24-well plates ( $8 \times 10^5$  per ml; 1 ml) and either left untreated or stimulated with cephalostatin 1 (1  $\mu$ M) for 0 – 24 h. For harvest, three wells were pooled and centrifuged at  $360 \times g$ ,  $4^\circ \text{C}$  for 10 min. The pellet was washed in cold PBS. After another centrifugation, the pellet was resuspended in 100  $\mu$ l lysis buffer and stored on ice for 30 min. The solution was cleared by centrifugation ( $10,000 \times g$ ,  $4^\circ \text{C}$ , 10 min) and the protein solution transferred to fresh tubes. Protein determination was performed following the protocol of Bradford (see 8.2). The protein solution was diluted 1 : 5 with 5 x sample buffer, boiled at  $95^\circ \text{C}$  for 5 min and stored at  $-20^\circ \text{C}$  or used directly for electrophoresis.

#### Sample buffer (5 x)

3.125 M Tris-HCl, pH 6.8	100 $\mu$ l
Glycerol	500 $\mu$ l
20 % SDS	250 $\mu$ l
16 % DTT	125 $\mu$ l
5 % Pyronin Y	5 $\mu$ l
H <sub>2</sub> O	20 $\mu$ l

#### **8.1.2 Cytosolic and particulate fractions**

In apoptosis, factors from the intermembrane space of mitochondria are released into the cytosol where they form part of activation complexes for caspases (e. g. cytochrome c, Smac) or they translocate into the nucleus where they participate in DNA fragmentation (Endonuclease G, AIF). For analysis of release of these factors, the cytosol has to be separated from the mitochondria. This is accomplished by a permeabilisation buffer containing a low concentration of digitonin which forms complexes with cholesterol in the cell membrane. Thus, small pores develop through which the cytosol is eluted into the iso-osmotic buffer while organelles are retained inside the cell. The protocol was carried out following the procedure of Leist *et al.* [92] in a modified version.

Permeabilisation buffer

210 mM Mannitol

70 mM Sucrose

10 mM Hepes pH 7.2

0.2 mM EGTA

5 mM Succinate

0.15 % (w/v) BSA

60 µg/ml Digitonin

Protocol:

Cells were seeded and stimulated as for whole cell lysate preparation. Three wells for each probe were pooled and centrifuged at 360 x g, 4° C for 10 min. The supernatant was discarded thoroughly. The pellets were resuspended carefully in 100 µl permeabilisation buffer and incubated on ice for 20 min. The cytosolic fraction was obtained by centrifugating the solution at 360 x g (4° C, 10 min) and the supernatant was cleared of any remaining cell fragments at 13,000 x g (4° C, 10 min). The pellet of the first centrifugation after permeabilisation containing the mitochondria, the other organelles and the membranes was resuspended in 0.1 % Triton-X 100 in PBS (100 µl) and lysed for 15 min on ice. The supernatant of a subsequent centrifugation step (13,000 x g; 4° C; 10 min) constitutes the mitochondria-enriched fraction. This fraction is referred to as mitochondrial fraction in the “Results” section.

Protein determination was carried out with the Bradford method (see 8.2). The probes were diluted with 5 x sample buffer and boiled at 95° C for 5 min. Afterwards, they were separated by SDS-PAGE immediately or stored at -20° C.

## 8.2 PROTEIN DETERMINATION

The method developed by Bradford [93] makes use of the feature of Coomassie Brilliant Blue G-250 to change its absorption maximum from 465 nm to 595 nm

on binding to proteins. The protein content of the lysates can thus be quantified by comparing the absorption with a calibration curve prepared with increasing concentrations of BSA in H<sub>2</sub>O.

Measurement was performed in ELISA plates in an SLT Spectra ELISA reader (SLT, Crailsheim, Germany). Cell lysates were diluted 1 : 10 in H<sub>2</sub>O. 190 µl of Bradford solution (BioRad, Hercules, USA; diluted 1 : 5 in H<sub>2</sub>O) were added to 10 µl lysate solution and 5 minutes were allowed for the colour shift to develop. Plates were measured at 592 nm.

### 8.3 SDS-PAGE

The protein samples described above are separated by denaturing SDS-polyacrylamide gel electrophoresis according to Laemmli [94]. Sodium dodecyl sulfate (SDS) is an anionic detergent which binds to the hydrophobic parts of the proteins and solubilises them. Thereby, proteins lose secondary and tertiary structures and only retain their primary structure. SDS confers a high negative charge to the proteins proportional to the length of the amino acid chain thus covering any charges the proteins displayed themselves. In an electric field, the negatively charged proteins are drawn towards the anode and they are separated solely on the basis of their size by the pores of the polyacrylamide gel. Further unfolding of the proteins is achieved by adding the reducing agent dithiothreitol (DTT) by which disulfide bonds inside the proteins are cleaved.

The molecular weight is determined by comparison with molecular weight standard mixtures (Rainbow marker RPN 755, Amersham, Freiburg, Germany) or prestained Precision Protein Standards, BioRad, München, Germany).

All protein separations were carried out in discontinuous gel electrophoresis where a stacking gel allows proteins to be concentrated in a line before they enter the separation gel. The concentration of the separation gel was adjusted depending on the size of the protein to be detected (see Table 6).

Table 6: Used gel concentrations for SDS-PAGE.

Analysed protein	Gel concentration
Apaf-1 / BiP / calpain / PARP	7.5 %
caspase-8 / caspase-9 / pJNK	10 %
Bcl-2 / pBcl-2 / Bcl-x <sub>L</sub> / caspase-3 / caspase-7 / caspase-12 / CHOP / XIAP	12 %
AIF / cytochrome c / Smac	15 %

Electrophoresis was carried out using a vertical apparatus Mini Protean II (BioRad, Hercules, USA) which allows two gels to be run in parallel.

For gel preparation an acrylamide 30 % / bis-acrylamide 0.8 % 37.5 : 1 (v/v) stock solution (Rotiphorese™ Gel 30, Roth, Karlsruhe, Germany) was used.

Samples with equal amount of protein and the molecular weight marker were loaded into the slots of the prepared polyacrylamide gels. Electrophoresis was run at 100 V for 21 min for stacking and at 200 V for separation of the protein mixture (power supply: Biometra, Göttingen, Germany).

Separation gel 12%		Stacking gel	
PAA solution 30 %	6.0 ml	PAA solution 30 %	1.7 ml
1.5 M Tris, pH 8.8	3.75 ml	1.5 M Tris, pH 8.8	1.0 ml
SDS 10 %	0.15 ml	SDS 10 %	0.1 ml
H <sub>2</sub> O	5.1 ml	H <sub>2</sub> O	7.0 ml
TEMED	15 µl	TEMED	20 µl
APS	75 µl	APS	100 µl

Electrophoresis buffer

Tris base	3 g
Glycine	14.4 g
SDS	1.0 g
H <sub>2</sub> O	ad 1000 ml

**8.4 WESTERN BLOTTING AND DETECTION OF PROTEINS**

For detection of the protein of interest, the protein bands are transferred after electrophoresis onto blotting membranes, incubated with specific antibodies and visualised by chemiluminescence reagents.

Anode buffer

5 x Tris-CAPS	20 ml
Methanol	15 ml
	ad 100 ml

Cathode buffer

5 x Tris-CAPS	20 ml
SDS 10 %	1 ml
	ad 100 ml

5 x Tris-CAPS

Tris	36.34 g
CAPS	44.26 g
	ad 1000 ml

The western blot was carried out by semi-dry blotting using a discontinuous buffer system. Polyvinylidene membranes (Immobilon-P; Millipore, Bedford, USA) were activated by soaking in methanol for 5 minutes followed by at least 30 minutes in anode buffer. The transfer stack consisted of a thick blotting paper (BioRad, Hercules, USA) wetted in anode buffer, followed by the membrane, the gel and finally a second thick blotting paper soaked in cathode buffer. The transfer was performed on a Transblot SD semidry transfer cell (BioRad, Hercules, USA) at 1.5 mA / cm<sup>2</sup> for 40-60 minutes depending on the size of the protein to be detected. After transfer, the membranes were blocked in 5 % non-fat dry milk in TBS-T for 1 h at RT. Subsequently, the membrane

was immersed in the respective antibody solution (see Table 7) diluted in 1 % non-fat dry milk in TBS-T overnight at 4° C. After three wash steps in TBS-T for 10 minutes each, the adequate secondary horseradish peroxidase-labeled antibody was applied for 1 h at RT.

**Table 7: Primary antibodies**

Antibody	Isotype	Dilution	Company
AIF	Rabbit IgG	1 : 1000	Chemicon, Hofheim, Germany
Apaf-1	Mouse IgG <sub>1</sub>	1 : 250	BD Transduction Laboratories, Heidelberg, Germany
Bcl-2	Mouse IgG <sub>1</sub>	1 : 250	Upstate, Lake Placid, USA
phospho-Bcl-2	Rabbit IgG	1 : 1000	Cell Signaling, Frankfurt, Germany
Bcl-x <sub>L</sub>	Rabbit IgG	1 : 1000	Cell Signaling, Frankfurt, Germany
BiP / GRP78	Mouse IgG <sub>2a</sub>	1 : 250	BD Transduction Laboratories, Heidelberg, Germany
Calpain	Mouse IgG <sub>1</sub>	1 : 1000	Chemicon, Hofheim, Germany
Caspase-3: HRPO	Mouse IgG <sub>2a</sub>	1 : 1000	BD Transduction Laboratories, Heidelberg, Germany
Caspase-7	Mouse IgG <sub>1</sub>	1 : 1000	BD Pharmingen, Heidelberg, Germany
Caspase-8	Mouse IgG <sub>2b</sub>	1 : 1000	Upstate, Lake Placid, USA
Caspase-9 (Western Blot)	Mouse IgG <sub>1</sub>	1 : 100	Calbiochem, Bad Soden, Germany
Caspase-9 (Immunoprecipitation)	Rabbit IgG		Sigma-Aldrich, München, Germany
Caspase-12	Rabbit IgG	1 : 1000	Cell Signaling, Frankfurt, Germany

Antibody	Isotype	Dilution	Company
GADD153 / CHOP10	Rabbit IgG	1 : 250	Sigma-Aldrich, München, Germany
PARP	Mouse IgG <sub>1</sub>	1 : 100	Calbiochem, Bad Soden, Germany
phospho-JNK	Mouse IgG <sub>1</sub>	1 : 2000	Cell Signaling, Frankfurt, Germany
Smac/DIABLO	Rabbit IgG	1 : 500	Biozol, Eching, Germany
XIAP	Mouse IgG <sub>1</sub>	1 : 250	BD Transduction Laboratories, Heidelberg, Germany

Development of the blot was carried out after three more washings (TBS-T, 10 minutes each) with the ECL Plus substrate solution (Amersham Biosciences, Freiburg, Germany). Thereafter, the membrane was exposed to X-ray film for the appropriate time period which was developed in a tabletop film processor (Curix 60, Agfa, Köln, Germany).

### 8.5 COOMASSIE STAINING OF GELS

After protein transfer, gels were stained with Coomassie blue (anazolene) to ensure equal protein loading and blotting efficiency. Proteins are fixed inside the gel by acetic acid which prevents diffusion of the bands.

<u>Staining solution (filtration before storage)</u>		<u>Destaining solution</u>	
Coomassie blue	0.3 %	Glacial acetic acid	10 %
Glacial acetic acid	10 %	Ethanol	30 %
Ethanol	45 %	H <sub>2</sub> O	
H <sub>2</sub> O			

Gels were stained for 30 minutes on a shaking platform and subsequently destained in several loads of destaining solution until the proteins appeared as clearly defined blue bands.

## 8.6 MEMBRANE STRIPPING

In order to detect different proteins successively on PVDF membranes, bound antibodies resulting from previous experiments have to be removed. For that purpose, membranes were immersed in stripping buffer (65.2 mM Tris-HCl, pH 6.8, 2 % SDS, 100 mM 2-Mercaptoethanol) and treated for 30 minutes at 50° C on a shaking platform. Subsequently, remnants of stripping buffer were washed away by three wash steps in TBS-T (10 minutes, RT). Stripping efficiency was confirmed by applying ECL Plus substrate solution (see 8.4). When no bands became apparent the membrane was blocked again to cover unspecific binding sites with 5 % non-fat dry milk in TBS-T for 1 h at RT. Afterwards, the next primary antibody was brought up.

## 9. IMMUNOPRECIPITATION

Immunoprecipitation is used for the enrichment of certain proteins from cell lysates. For that, antibodies specific for the protein of interest are added to the cell lysate. After formation of the antigen-antibody-complex, this complex is precipitated with Protein A, a bacterial protein with high affinity to the F<sub>c</sub> part of immunoglobulins. Once the protein is dissociated from the immune complex, the protein and any bound ligands can be analysed by Western blot.

### Protocol:

Cells were treated and harvested as described under 8.1. In the meantime, for each sample, 50 µl of a solution of protein A, immobilised on agarose beads, were centrifuged shortly and resuspended in lysis buffer. 2.5 µl of the respective antibody were added to 50 µl bead solution and mixed gently for 1 h at RT. After this time, the bead solutions were centrifuged (3,000 x g, 2 minutes, 4° C) and carefully washed three times with lysis buffer. Once the protein concentration of the cell lysates had been determined (see 8.2), 300 – 400 µg protein were filled up to a final volume of 250 µl with lysis buffer and added to the bead solution. In order to allow the immune complexes to form, the samples

were mixed overnight at 4° C by end-over-end rocking. Afterwards, the precipitates were harvested by centrifugation (3,000 x g, 4° C, 2 minutes). 40 µl of the supernatant were kept as binding control. The pellet was washed three times with lysis buffer. After the last wash solution had been removed completely, sample buffer containing 2-mercaptoethanol was added to the pellet and the probe is heated to 95° C for 5 minutes to dissolve the protein from the precipitate. The beads were removed by centrifugation. 30 µl of each supernatant were analysed by Western blot as described under 8.

## 10. COMET ASSAY / SINGLE CELL GEL ELECTROPHORESIS

The comet assay allows for rapid detection of DNA damage in single cells. Cells embedded in agarose are lysed and electrophoresed in alkaline conditions enabling the detection of DNA single and double strand breaks.

### Protocol:

The assay was carried out following the manufacturer's instructions (Trevigen Inc, Gaithersburg, MD, USA). All steps were performed under dimmed light to prevent DNA damage by UV light.

Cells were seeded at  $6 \times 10^5$  / ml in a 24-well plate and either left untreated or stimulated with cephalostatin 1 (1 µM) or etoposide (10 µM) for 4 h. Harvest was performed by centrifugation at 360 x g, 4° C for 10 min. Pellets were resuspended in ice cold PBS to give a final concentration of  $1 \times 10^5$  cells / ml. Meanwhile, the LMAgarose was molten and kept at 37° C. Cell suspension and agarose were carefully mixed at a ratio of 1 : 10 and 75 µl were immediately pipetted onto a microscope slide (CometSlide™). In order to allow solidification of the agarose, slides were placed at 4° C in the dark for 10 min. Successively, slides were immersed in Lysis Solution (2.5 M sodium chloride, 100 mM EDTA, pH 10, 10 mM Tris Base, 1 % sodium lauryl sarcosinate, 1 % Triton-X-100) for 40 min at 4° C and then in alkaline solution (300 mM NaOH, 200 mM EDTA) for 40 min at RT. Electrophoresis was carried out under alkaline conditions in 300

mM NaOH, 1 mM EDTA at 1 V / cm (distance between the electrodes) and 300 mA for 30 min at 4° C. Finally, slides were neutralised by dipping several times in H<sub>2</sub>O and air dried overnight. The samples were stained with 50 µl of diluted SYBR<sup>®</sup> Green solution per agarose circle. Pictures were taken at a Zeiss Axiovert 25 microscope (Zeiss, Jena, Germany) using filter 09 ( $\lambda_{\text{ex}}$ : 450-490 nm,  $\lambda_{\text{em}}$ : 520 nm).

## 11. STATISTICS

All experiments were performed at least three times. Results are expressed as mean  $\pm$  SEM. Statistical analysis was performed by ANOVA with Bonferroni multiple comparison post-test or by unpaired two-tailed Student t-test. P values < 0.05 were considered significant. Analysis was performed with GraphPad PRISM<sup>®</sup> software, Version 3.02 (GraphPad Software Inc., San Diego, USA).

## IV. RESULTS

### 1. CYTOTOXIC ACTIVITY OF CEPHALOSTATIN 1

Cephalostatin 1 shows a remarkable cytotoxicity profile in the NCI-60 panel (see II.2). For the Jurkat cells in use here, the cytotoxic effect was investigated with the MTT assay (see III.4.1). As depicted in Figure 20, cell viability is affected already at 0.1 nM cephalostatin 1 with the maximal effectivity being reached at 10  $\mu$ M. The  $IC_{50}$  calculated from these results is 1.25 nM.

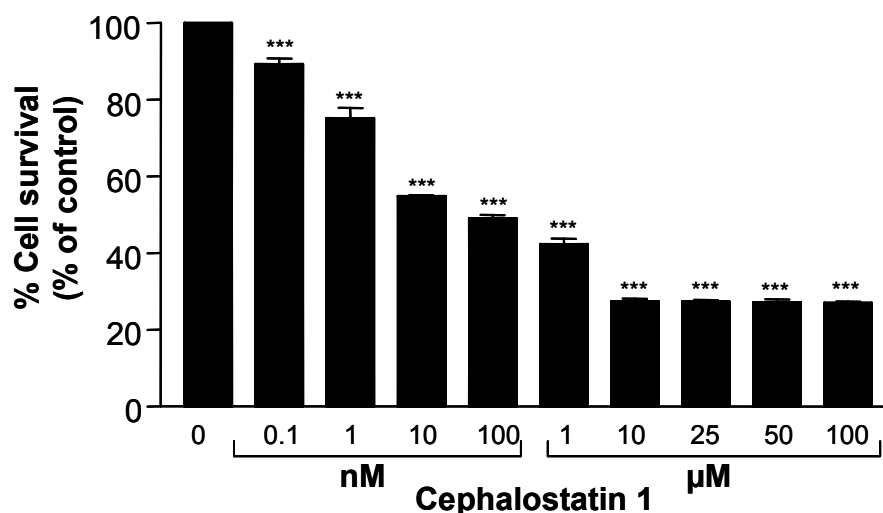


**Figure 11: Cytotoxic effects of cephalostatin 1 in Jurkat cells.**

Cells were stimulated with cephalostatin 1 (concentrations as indicated) for 24 h. Impairment of cell viability was analysed by an MTT assay as described in Materials & Methods. Bars represent the mean  $\pm$  SE of three independent experiments performed in triplicate. \*\*\*  $p < 0.001$  (ANOVA / Dunnett)

### 2. APOPTOSIS-INDUCTION BY CEPHALOSTATIN 1

The next step consisted in evaluation of the type of cell death induced by cephalostatin 1. Several methods were undertaken in order to deduce if cephalostatin 1 induces apoptosis.

## 2.1 MORPHOLOGIC ALTERATIONS

### 2.1.1 Light microscopic analysis of cephalostatin 1-treated cells

As described in II.4, during apoptosis, the cell undergoes distinct morphologic changes such as cell shrinkage and the formation of apoptotic bodies. Cephalostatin 1 treatment (1  $\mu$ M, 24 h) induces apoptotic body formation as indicated by the arrows in Figure 12.

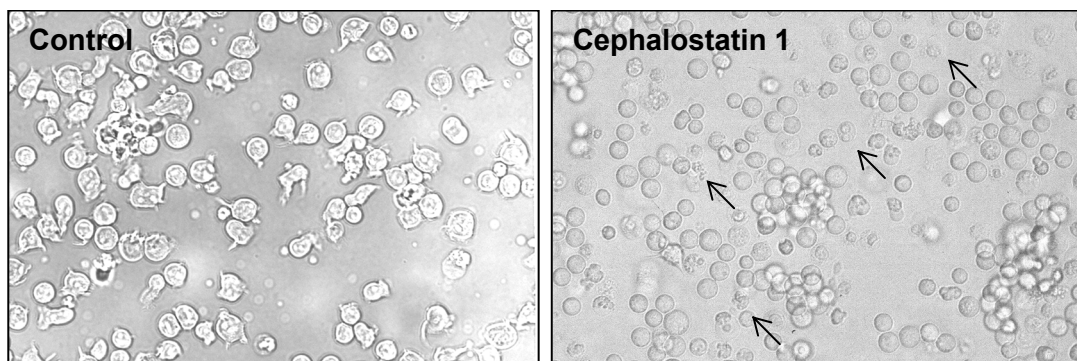


**Figure 12: Lightmicroscopic picture of Jurkat T cells.**

After incubation with cephalostatin 1 (1  $\mu$ M, 16 h), pictures were taken from untreated cells (control, *left panel*) or cephalostatin 1-stimulated cells (*right panel*). Arrows indicate apoptotic bodies.

### 2.1.2 Morphologic analysis per flow cytometry

Changes in size and granularity are detectable by flow cytometric measurement. The decrease in cell size observed in apoptosis leads to lower forward scatter values while an increase in granularity is visualised in the dot plot as higher sideward scatter values (see III.5.1). As demonstrated in Figure 13, cephalostatin 1 stimulation (1  $\mu$ M, 24 h) leads to cell shrinkage (shift of the cell cloud to the left) and an augmentation of cellular granularity (shift of the cell cloud towards the top).

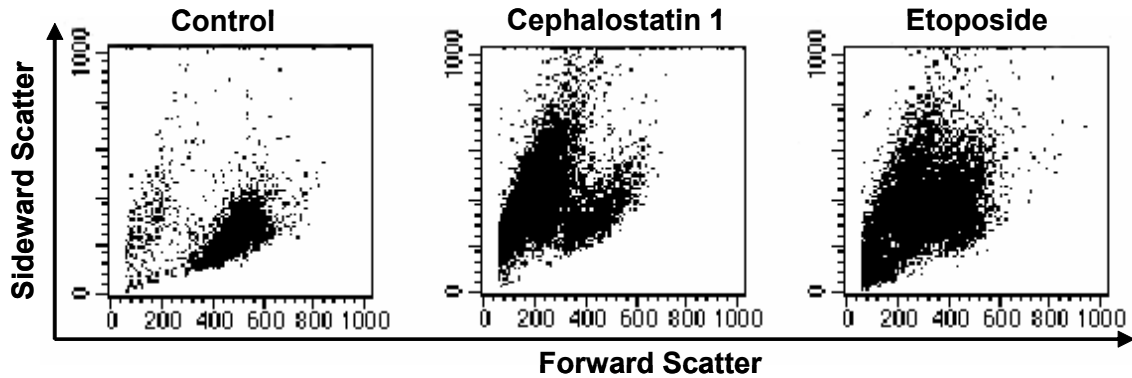


**Figure 13: Measurement of cell size and granularity by FACS.**

Untreated cells or cells incubated with cephalostatin 1 (1  $\mu$ M, 24 h) were analysed by flow cytometry as described under Materials & Methods. Etoposide (25 mg/ml, 24 h) served as positive control.

### 2.1.3 Morphologic changes of the nucleus

Apoptotic nuclei are a site of numerous biochemical processes. The chromatin is condensed by enzymatic action of EndoG and other enzymes and finally the DNA is fragmented by cleavage between the histones, e.g. by CAD (caspase-activated DNase), thus inducing evenly sized fragments of 192 bp and multiples thereof [95].

By staining with Hoechst 33342, condensation and fragmentation of DNA was shown clearly for cephalostatin 1-treated cells in Figure 14. The DNA of untreated cells (left panel) is dispersed evenly across the nucleus and visible as faint blue circles. In the middle panel (8 h of stimulation), the colour intensity is increased indicating condensed chromatin and some cells display DNA fragments. The right panel (16 h of stimulation) shows the majority of cells with fragmented DNA.

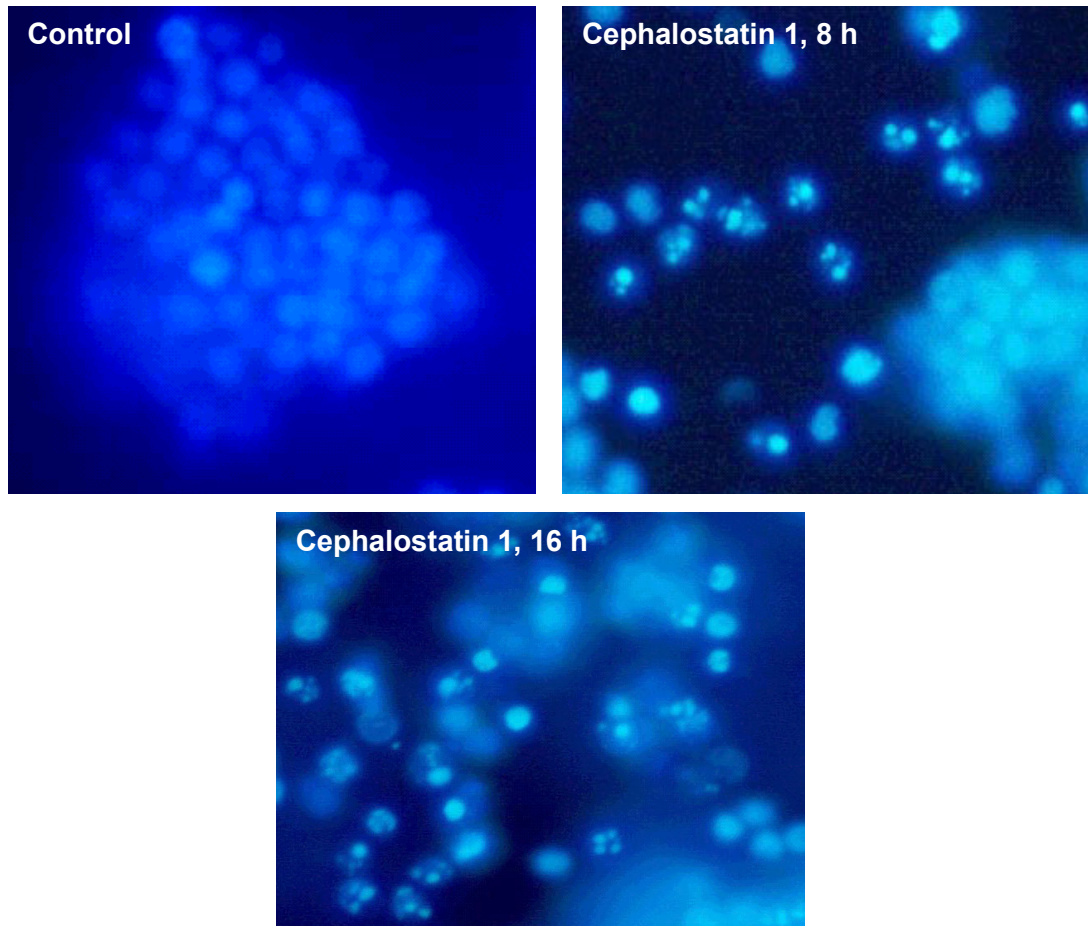


**Figure 14: Nuclear changes on cephalostatin 1 treatment.**

Cells were treated with cephalostatin 1 (1  $\mu\text{M}$ ) for 8 h and 16 h. After incubation, cells were stained with Hoechst 33342. Representative pictures of untreated (*Control*) and treated cells are shown.

#### **2.1.4 Phosphatidylserine exposure**

Phosphatidylserine (PS), an aminophospholipid normally located in the cytosolic layer of the plasma membrane, is translocated to the outside of the membrane by scramblases in apoptotic conditions. Once outside, it serves as signal for phagocytes and other neighbouring cells thus triggering removal of the apoptotic cells.

Cephalostatin 1 induces prominent PS exposure as indicated in Figure 15.

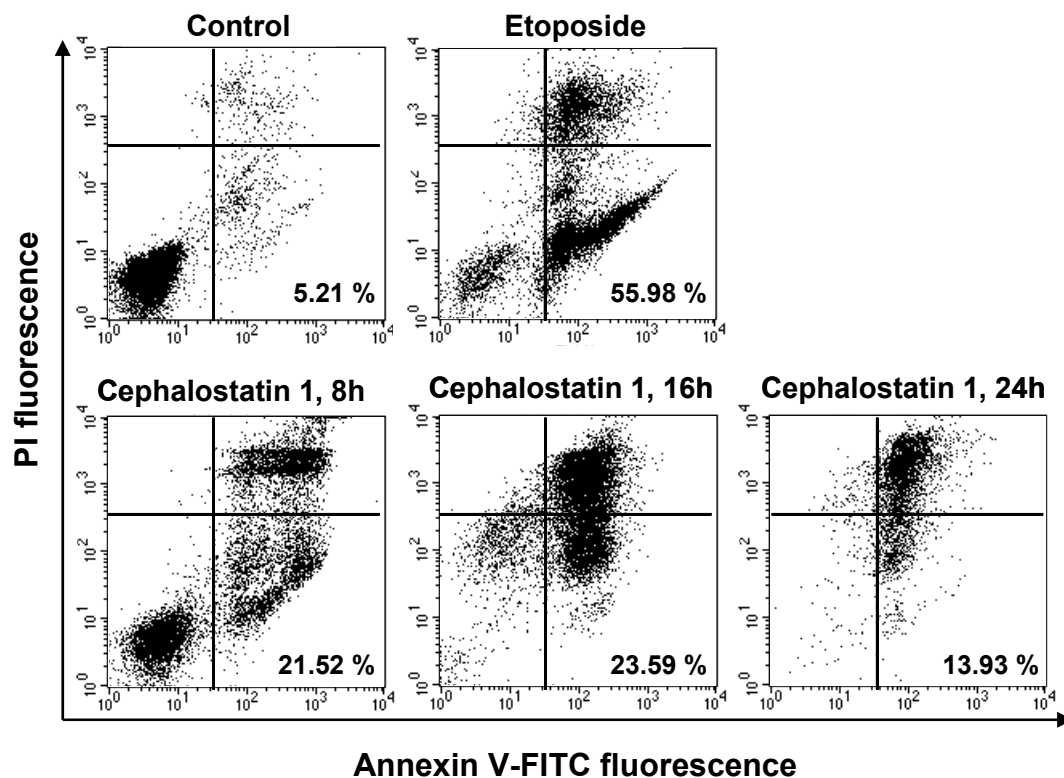


**Figure 15: Measurement of PS exposure by Annexin V staining.**

FACS analysis of annexin V-FITC and PI-stained cells, either left untreated, stimulated with cephalostatin 1 (1  $\mu$ M) for 8 – 24 h or with etoposide (25  $\mu$ g/ml, 8 h) as positive control. Cells appearing at the lower right quadrant show positive annexin V-FITC staining indicating phosphatidylserine exposure on the cell surface and no DNA staining with PI proving intact cell membranes.

## 2.2 QUANTITATIVE ANALYSIS OF CEPHALOSTATIN 1-INDUCED APOPTOSIS

The fragmentation of DNA followed by disintegration of the cell into the apoptotic bodies which may contain part of the DNA fractions results in reduced DNA content. DNA content changes during the four phases of the cell-division cycle. Somatic cells are diploid (2n) in the  $G_0/G_1$ -phase (gap phase 0/1) and double the DNA in the S-phase (synthesis phase) (4n). Finally, in mitosis (M-phase) after  $G_2$ -phase, cells divide and the resulting two daughter cells are again diploid. The amount of cellular DNA can be visualised by DNA staining and subsequent flow cytometry (see III.5.2). Untreated Jurkat cells display the normal cell cycle distribution (Figure 16, control). After cephalostatin 1 treatment (1  $\mu$ M, 24 h), peaks left of the  $G_0/G_1$  peak appear representing the apoptotic cells with a lower DNA content than cells in  $G_0/G_1$ -phase. These peaks are

referred to as sub- $G_0/G_1$  peaks. Etoposide (25  $\mu\text{g/ml}$ , 24 h) was used as positive control.

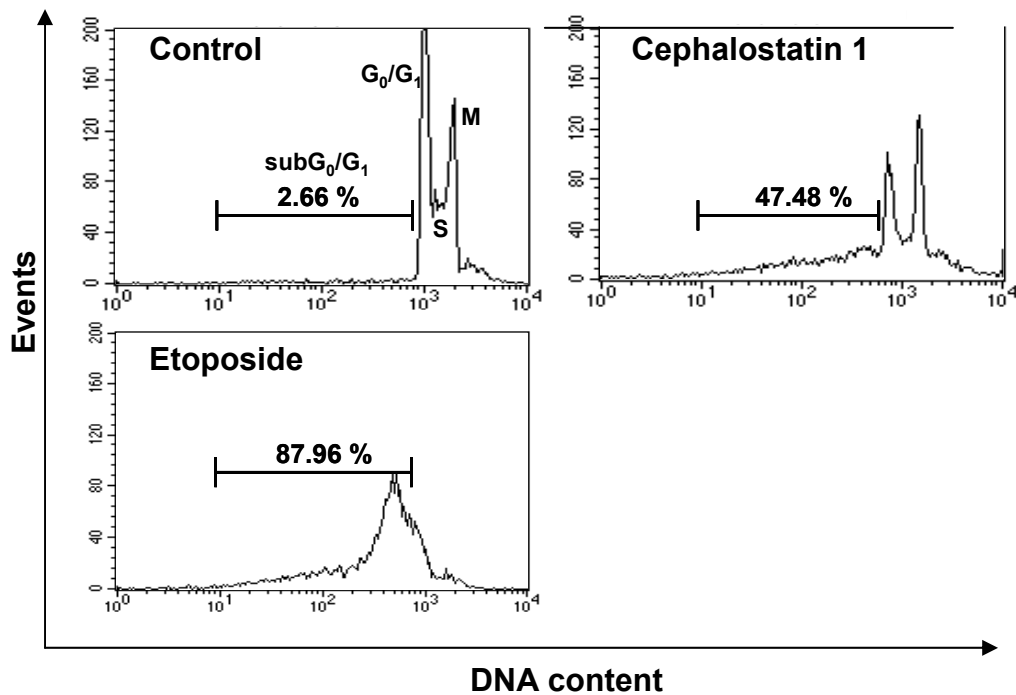


**Figure 16: Detection of cephalostatin 1-induced apoptosis by PI staining.**

FACS analysis of PI-stained nuclei of cells left untreated, stimulated with cephalostatin 1 (1  $\mu\text{M}$ ) or etoposide (25  $\mu\text{g/ml}$ ) for 24 h. Histograms demonstrate the distribution of nuclei according to their DNA content. Counts left of the  $G_1$ -peak (gated) indicate the appearance of nuclei with subdiploid DNA content.

Quantification of the sub- $G_0/G_1$  peak shows that cephalostatin 1 induces dose- and time-dependent apoptosis in Jurkat T cells.

Already concentrations of 1 nM cephalostatin 1 triggered a significant increase in apoptosis (Figure 17, 24 h). The highest percentage of apoptosis was reached at 1  $\mu\text{M}$  cephalostatin 1. Therefore, this concentration was chosen for further experiments. The response of the Jurkat cells to cephalostatin 1 proceeded time-dependently with the first significant apoptotic level reached at 6 h of stimulation (Figure 18).

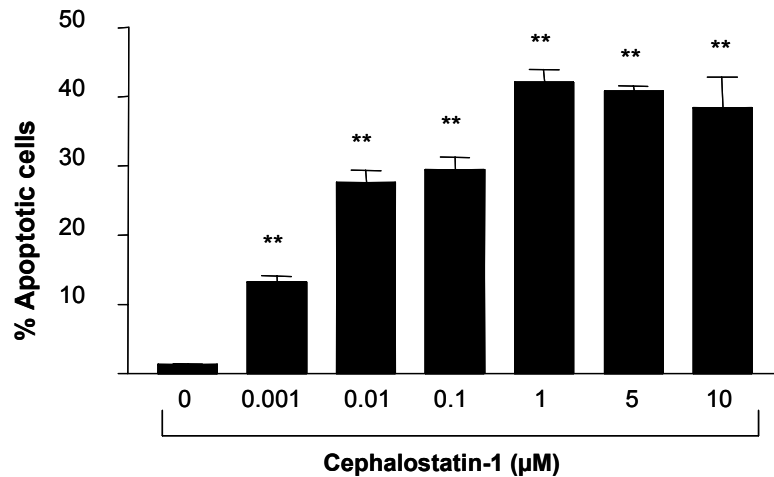


**Figure 17: Cephalostatin 1-induced apoptosis is dose-dependent.**

Cells were stimulated with increasing concentrations of cephalostatin 1 for 24 h. % *Apoptotic cells* denote the percentage of cells with subdiploid DNA content. Bars represent the mean  $\pm$  SE of three independent experiments performed in triplicate. \*\*  $p < 0.01$  (ANOVA / Dunnett).

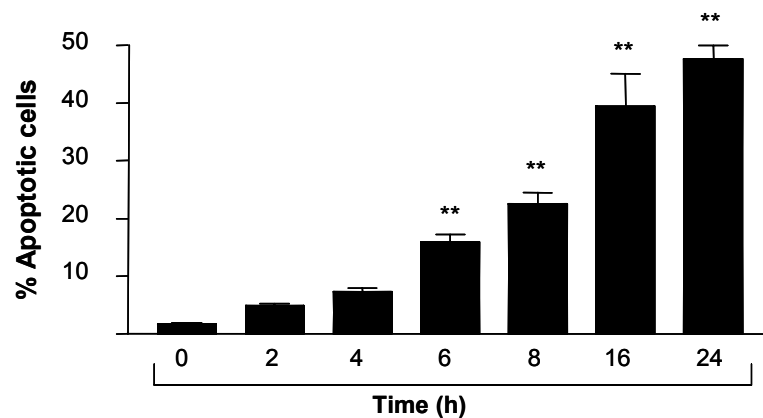


**Figure 18: Cephalostatin 1-induced apoptosis proceeds time-dependently.**

Cells were stimulated with cephalostatin 1 (1  $\mu$ M) for 0 – 24 h. % *Apoptotic cells* indicate the percentage of cells with subdiploid DNA content. Bars represent the mean  $\pm$  SE of three independent experiments performed in triplicate. \*\*  $p < 0.01$  (ANOVA / Dunnett).

### 3. SIGNAL TRANSDUCTION IN CEPHALOSTATIN 1-INDUCED APOPTOSIS

#### 3.1 CASPASES ARE ESSENTIAL FOR CEPHALOSTATIN 1-INDUCED APOPTOSIS

Caspases are the major executors of apoptosis induced by numerous stimuli. However, a growing body of evidence suggests that apoptotic cell death can

also be mediated by calpains [96], cathepsins [97] and AIF [98] to name but a few alternative enzymes.

### 3.1.1 Inhibition of apoptosis by zVADfmk

In order to prove if cephalostatin 1-induced apoptosis is dependent on caspase activity, cells were preincubated for 1 h with the broad spectrum caspase inhibitor zVADfmk (25  $\mu$ M). Caspase inhibition prevented cephalostatin 1-triggered apoptosis (1  $\mu$ M, 24 h) indicating that the signal pathway relies on caspases (Figure 19).

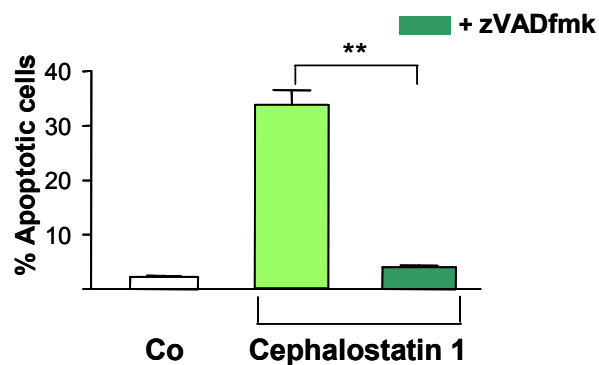


**Figure 19: The pan-caspase inhibitor zVADfmk prevents cephalostatin 1-triggered apoptosis.**

Cells were left untreated (Co), incubated with cephalostatin 1 (1  $\mu$ M, 24 h) or pretreated with zVADfmk (25  $\mu$ M, 1 h) and subsequently treated with cephalostatin 1 (1  $\mu$ M, 24 h). Apoptotic cells were quantified by flow cytometry. Bars represent the mean  $\pm$  SE of three independent experiments performed in triplicate. \*\*  $p < 0.01$  (ANOVA / Dunnett).

Caspase-3 belongs to the effector caspases downstream in the caspase cascade. Activated by the initiator caspases, it plays the most prominent role in the effector phase [99]. The substrates cleaved by caspase-3 include cytoplasmic and nuclear proteins, proteins involved in DNA repair, cell cycle and apoptosis regulation and several kinases [38]. The cleavage of PARP, a DNA repair enzyme, is regarded as proof of caspase-3 activity.

Cephalostatin 1 (1  $\mu$ M, time points indicated) induces caspase-3 activation after 8 h as shown in Figure 20 A. The appearance of the active fragment (p17) at 8 h correlates with cleavage of PARP (B) and also with the first significant increase in fluorescence intensity detected by the caspase activity assay (C).

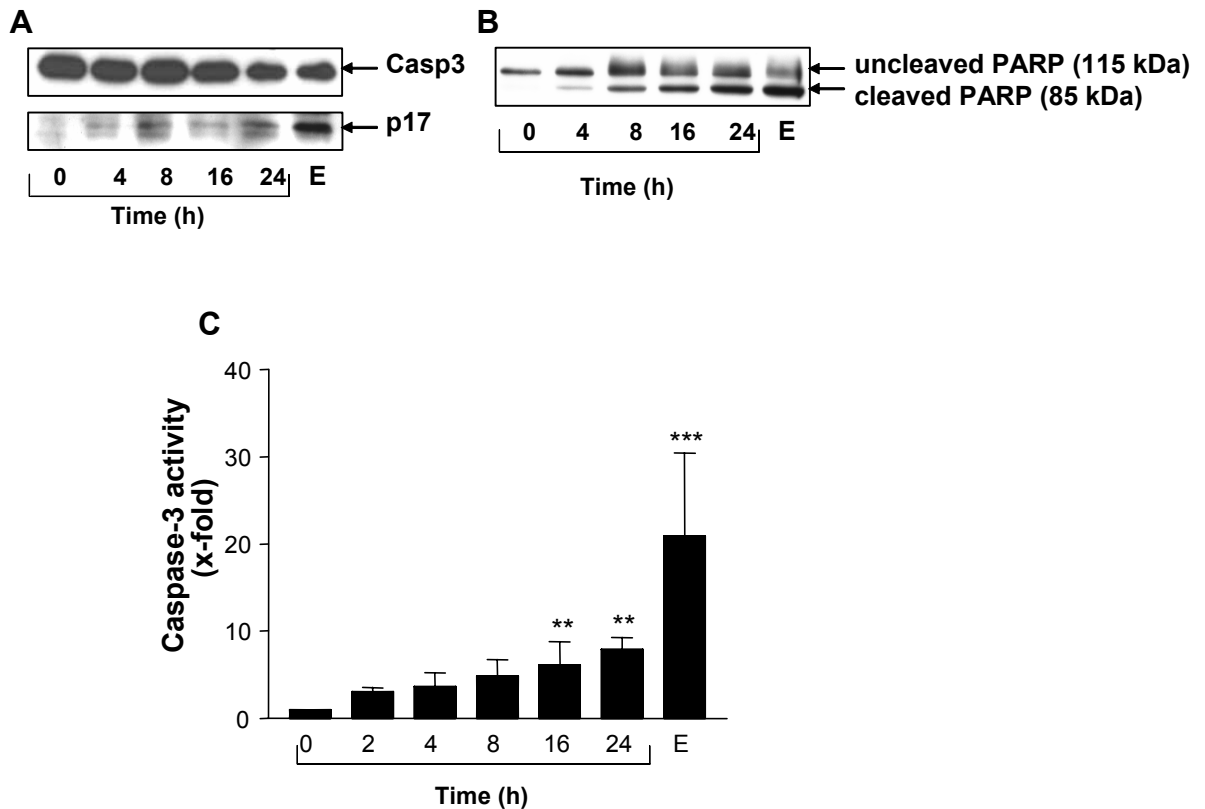


**Figure 20: Caspase-3 activation by cephalostatin 1 (1  $\mu$ M).**

Representative Western blots showing time-dependent (0 – 24 h) cleavage of caspase-3 to its active subunit (p17, **A**) and of PARP (**B**) after cephalostatin 1 treatment (1  $\mu$ M). Both experiments were performed three times with consistent results. **C**, caspase-3 activity in cephalostatin 1-stimulated cells. Bars represent the mean  $\pm$  SE of three independent experiments performed in triplicate. \*\*  $p < 0.01$ , \*\*\*  $p < 0.001$  (ANOVA / Dunnett).

## 3.2 INVOLVEMENT OF THE CD95 PATHWAY

As described in II.5.2, activation of death receptors by their ligands ensues activation of caspase-8 as initiator caspase. Subsequently, caspase-8 is able to induce caspase-3 cleavage.

### 3.2.1 Activation of caspase-8

In order to investigate the involvement of caspase-8 in signalling transduction, cleavage products of caspase-8 were detected by Western blotting. Cleavage of caspase-8 produces two intermediates (p42 and p44) which are further processed to the active 20 kDa fragment. Jurkat cells were treated with cephalostatin 1 (1  $\mu$ M) for the indicated times. Figure 21 demonstrates that

cephalostatin 1 led to an activation of caspase-8 at 16 h. Compared to the apoptosis induction reaching significant levels already after 6 h, the activation of an initiator caspase 10 h later suggests that caspase-8 only plays a subordinate role in cephalostatin 1-induced apoptosis.

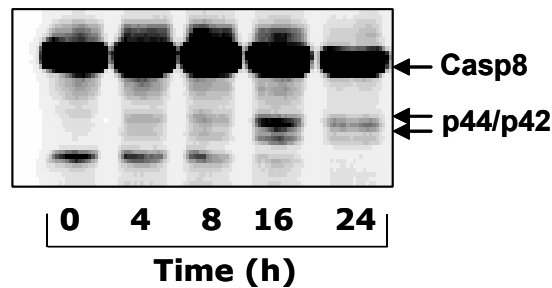


**Figure 21: Caspase-8 activation by cephalostatin 1.**

Caspase-8 cleavage after incubation with cephalostatin 1 (1  $\mu$ M, 0 – 24 h) to the p42 and p44 cleavage products. One representative Western blot out of three is shown.

### 3.2.2 Apoptosis induction in CD95 deficient cells

The question if cephalostatin 1 employs death receptors for apoptotic signaling was addressed using Jurkat cells deficient in the CD95 receptor (subclone Jurkat<sup>R</sup>) and Jurkat cells deficient in caspase-8. Effects were compared to S-Jurkat cells (especially sensitive to the CD95 ligand (CD95-L) and used as basis for the deletion of CD95) and to the subclone A3 (providing the basis cell line for the caspase-8 deletion). The Jurkat<sup>R</sup> cell line was stimulated for 24 h with the concentrations given in Figure 22 A. For the caspase-8 deficient cells, a time course was prepared with 1  $\mu$ M cephalostatin 1 (Figure 22 B).

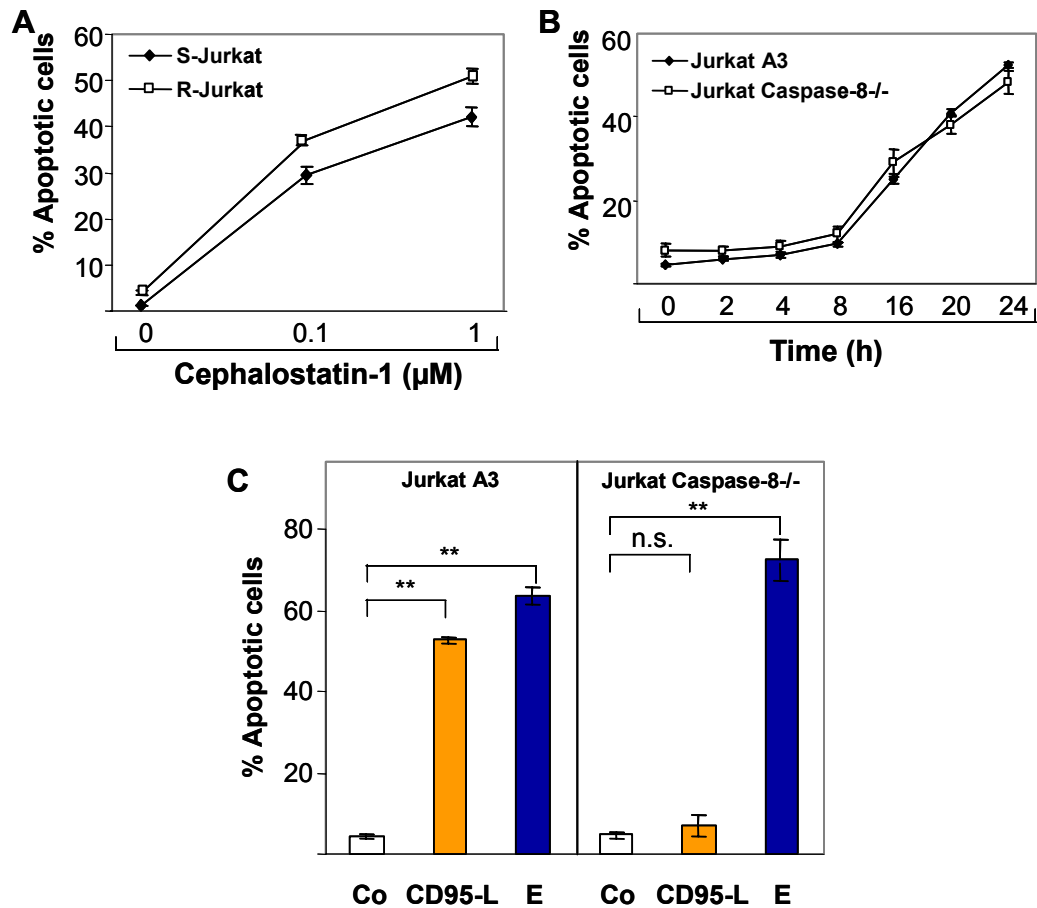


**Figure 22: Involvement of the CD95 receptor system in cephalostatin 1-induced apoptosis.**

**A**, Jurkat and Jurkat<sup>R</sup> cells were treated with the indicated concentrations of cephalostatin 1 for 24 h. **B**, Jurkat A3 and Jurkat caspase-8<sup>-/-</sup> cells were stimulated with cephalostatin 1 (1 μM) for different periods of time (0 – 24 h). **C**, Jurkat A3 (*left panel*) and Jurkat caspase-8<sup>-/-</sup> cells (*right panel*) were either left untreated (Co), treated with soluble CD95 ligand (CD95-L, 200 ng/ml) or etoposide (E, 25 μg/ml) for 24 h. Apoptotic cells were quantified by FACS analysis. All experiments were carried out three times in triplicate. Data points and bars represent the mean ± SE. \*\* p < 0.01 (ANOVA / Dunnett).

Compared to their controls, the Jurkat<sup>R</sup> cells responded equally to cephalostatin 1 treatment indicating that the CD95 receptor is not required for cephalostatin 1-induced apoptosis. Since other death receptors such as TNF receptor or TRAIL receptor also involve caspase-8 as initiator caspase, caspase-8<sup>-/-</sup> cells were incubated with cephalostatin 1. However, no reduction in apoptosis could be detected compared to control cells. In order to assure that no functional caspase-8 was expressed, A3 and caspase-8<sup>-/-</sup> cells were stimulated with soluble CD95-L (200 ng/ml) and etoposide (25 μg/ml). As expected, caspase-8 deficient cells were protected against CD95-L, but not against etoposide (C).

Thus, lack of CD95 receptor or caspase-8 does not interfere with apoptosis induction by cephalostatin 1 suggesting that the extrinsic pathway is not essential for cephalostatin 1-induced apoptosis. It is possible, though, that caspase-8 activation acts as amplification loop.

### 3.3 INVOLVEMENT OF THE MITOCHONDRIA

Mitochondria are part of the intrinsic apoptotic pathway and provide factors vital for the activation of initiator caspase-9, for DNA fragmentation and inhibitors for proteins which may prevent caspase activity (see II.5.3). In many apoptotic models, the dissipation of the mitochondrial inner membrane potential ( $\Delta\Psi_m$ ) that is essential for ATP production in physiological conditions is one of the first events in the mitochondrial pathway. Permeabilisation of the outer membrane is involved in the release of apoptogenic factors from the intermembrane space.

#### 3.3.1 Morphological alterations of cephalostatin 1-activated mitochondria

Mitochondrial swelling and subsequent rupture of the outer mitochondrial membrane are considered one mechanism mediating the release of apoptogenic factors [100]. These changes are detectable on the ultrastructural level by transmission electron microscopy.

As depicted in Figure 23, the mitochondria of untreated cells have only little contrast relative to the cytoplasm (A, B, black arrows). The membrane system of the endoplasmic reticulum (ER) appears normal (B, red arrow). Upon stimulation with cephalostatin (1  $\mu$ M) for 16 h, immense changes occur in the cells. The nuclei are condensed and fragmented and the nuclear membranes are dilated (D, blue arrows). Similarly, the ER membranes are enlarged and vesicles which are presumably ER-derived accumulate in the cytoplasm (E, asterisks). Most surprisingly, the mitochondria in cephalostatin 1-treated cells

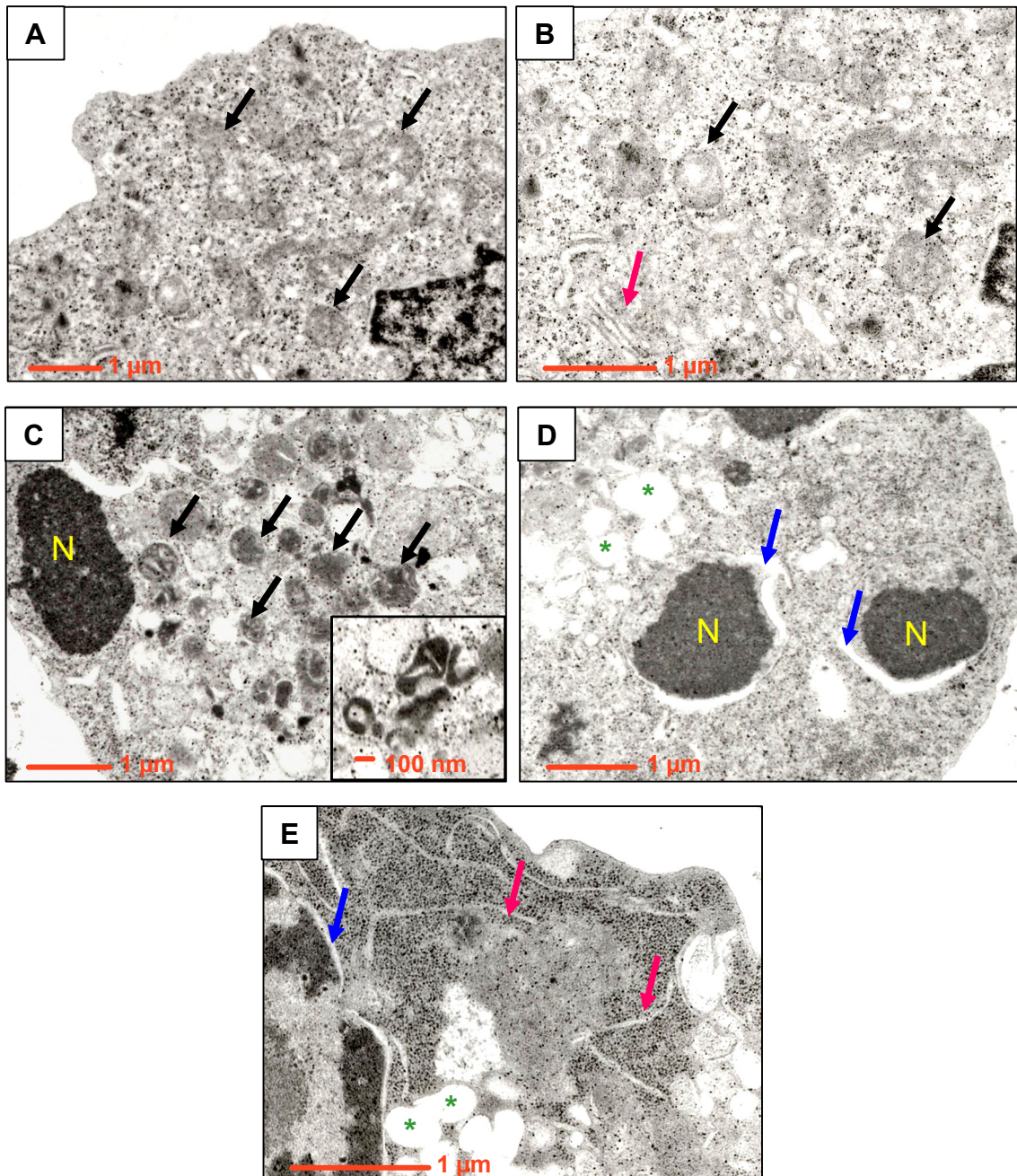


**Figure 23: Electron microscopic analysis of cephalostatin 1-mediated mitochondrial changes.**

Cells were left untreated (**A**, **B**) or stimulated with cephalostatin 1 (1  $\mu$ M, 16 h) (**C**, **D**, **E**). Electron micrographs were prepared as described under Materials & Methods. **A**, **C**, 1 : 5,000 fold magnification; **B**, **D**, **E** 1 : 10,000 fold magnification. Black arrows indicate mitochondria, blue arrows point to enlarged nuclear membranes and red arrows denote ER membranes. Asterisks demonstrate the vesicles that accumulate in the cytoplasm upon cephalostatin 1 treatment. N, nucleus.

appear smaller with increased electron density compared to the untreated cells suggesting a condensation of the mitochondrial matrix. In contrast, the cristae appear blurred and swollen (C, insert).

### 3.3.2 Alterations of the mitochondrial membrane potential

The dissipation of the mitochondrial membrane potential was visualised by staining with the mitochondria-targeted dye JC-1 (see III.5.4). Mitochondria of Jurkat control cells display mainly an orange fluorescence from the JC-1 aggregates indicating unchallenged membrane function (Figure 24, A). During the time course of cephalostatin 1 treatment (1  $\mu\text{M}$ ), the fluorescence increasingly shifts to a green colour as the JC-1 aggregates dissolve into monomers due to dissipation of the membrane potential. Etoposide (25  $\mu\text{g/ml}$ ) was used as positive control.

A quantification of membrane permeabilisation was carried out by flow cytometry (Figure 24 B). Cells with green fluorescence indicating a disturbed gradient were counted at each time point. The first significant increase was detected after 8 h and cells with dissipated  $\Delta\psi_m$  made up more than 70 % after 24 h. This suggests that the mitochondria are affected by cephalostatin 1 treatment and might play a role in the signal transduction.

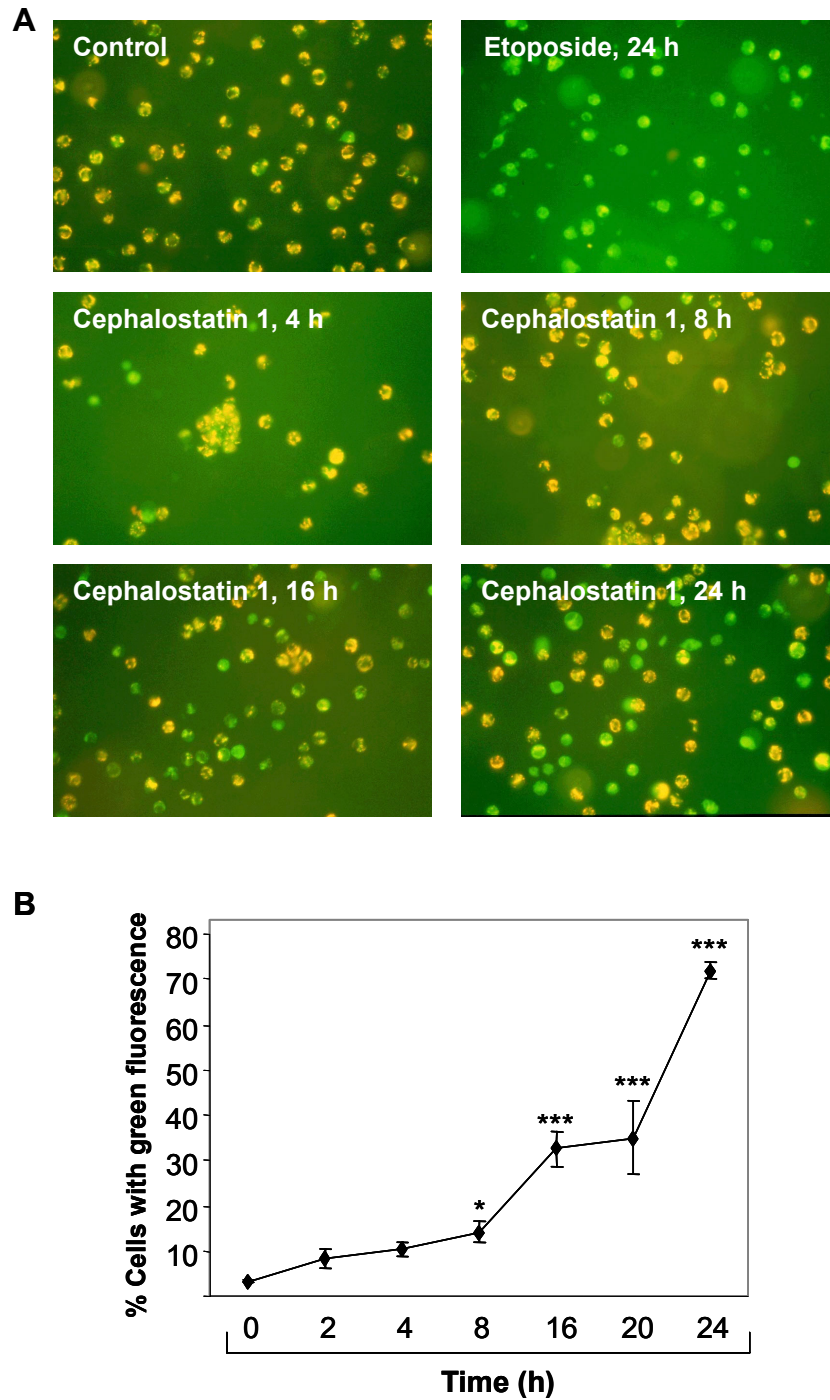


**Figure 24: JC-1 staining of cephalostatin 1-treated cells.**

Cells were incubated with cephalostatin 1 (1  $\mu$ M) or etoposide (25  $\mu$ g/ml) for the indicated time periods and subsequently loaded with the fluorochrome JC-1 (0.25  $\mu$ g/ml). **A**, representative microscopic pictures of a cephalostatin 1 time course experiment. **B**, cells showing predominantly green fluorescence were quantified by FACS analysis as described under Materials & Methods. All experiments were performed three times with consistent results. Data points indicate mean  $\pm$  SE. \*  $p < 0.05$ , \*\*\*  $p < 0.001$  (ANOVA / Dunnett).

### 3.3.3 Activation of caspase-9

The initiator caspase activated by the mitochondrial pathway is caspase-9. Since cephalostatin 1 leads to a breakdown of the electrochemical gradient across the inner membrane it is likely that caspase-9 is activated in the course of cephalostatin 1-induced apoptosis. Indeed, cephalostatin 1 (1  $\mu$ M) induces caspase-9 activation after 4 h as shown in Figure 25. Compared to the activation of caspase-8, caspase-9 cleavage is triggered earlier suggesting that it might act upstream of caspase-8.

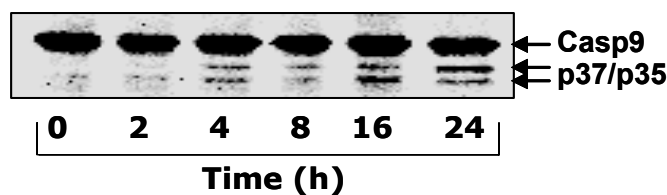


**Figure 25: Activation of caspase-9 by cephalostatin 1.**

Caspase-9 cleavage after incubation with cephalostatin 1 (1  $\mu$ M, 0 – 24 h) to the p35 and p37 cleavage products. One representative Western blot out of three is shown.

### 3.3.4 Release of apoptogenic factors from the intermembrane space

Mitochondria harbour several factors contributing either to DNA fragmentation or activation of caspases which are released into the cytosol upon diverse stimuli. Among the latter, in most models, cytochrome c is essential for the formation of the apoptosome resulting in caspase-9 activation. In Figure 26, Western blots of the cytosolic and mitochondrial fractions of cell lysates after cephalostatin 1 stimulation (1  $\mu$ M, time points as indicated) are displayed. Surprisingly, cephalostatin 1 does not induce the release of cytochrome c in contrast to the positive control etoposide (25  $\mu$ g/ml, 8 h). Thus, caspase-9 is activated by a cytochrome c-independent mechanism. Similarly to cytochrome c, AIF cannot be detected in the cytosolic fraction of cephalostatin 1-treated Jurkat cells. In contrast, cephalostatin 1 induces a rapid and strong release of Smac that precedes caspase-9 activation and is not abrogated by the pan-caspase inhibitor zVADfmk. These results suggest that the release of Smac proceeds independently of caspases.

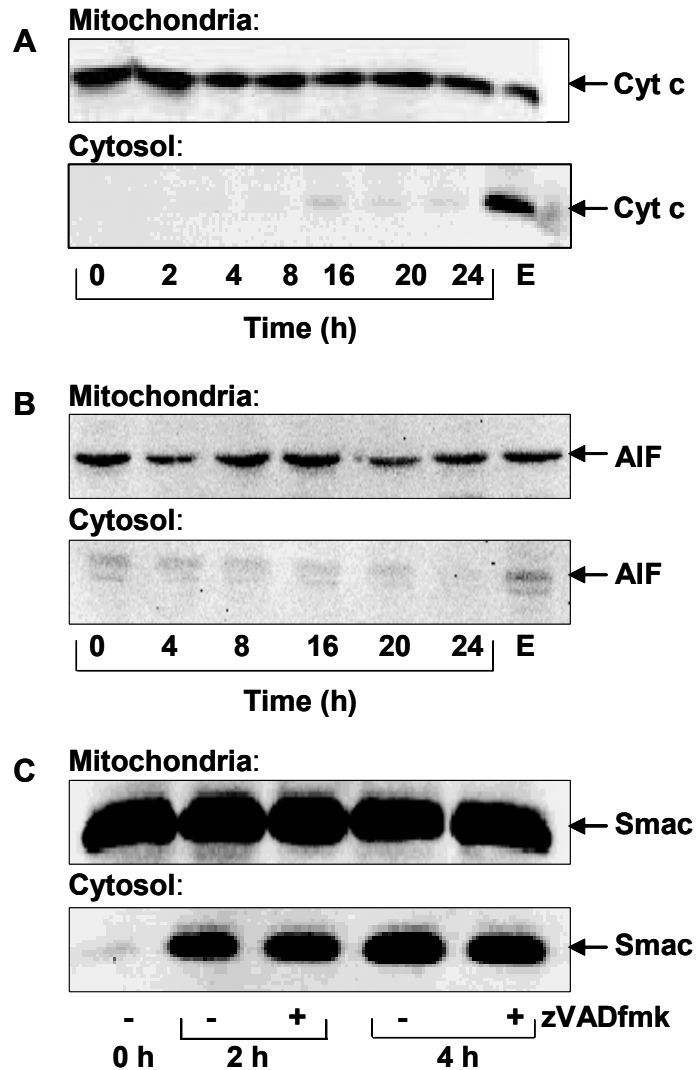


**Figure 26: Release of apoptogenic factors from the intermembrane space.**

Cells were treated with cephalostatin 1 (1  $\mu$ M) for the indicated times or with etoposide (25  $\mu$ g/ml) as positive control. Cytosolic and mitochondrial fractions were prepared as described under Materials & Methods. **A**, **B**, neither cytochrome c nor AIF were released upon cephalostatin 1 treatment. **C**, cells were pretreated with zVADfmk (25  $\mu$ M, 1 h) where indicated. Smac release is not inhibited by the pretreatment. Representative Western blots of three independent experiments are shown.

In order to corroborate the Western blot results, the release of cytochrome c, AIF and Smac was investigated by confocal laser scanning microscopy (see III.6.3). In untreated cells, all three proteins co-localise in a punctuated pattern representing the mitochondria (Figure 27). After stimulation with cephalostatin 1 (1  $\mu$ M, 8 h), the release of Smac is visible as diffuse staining while cytochrome c is distinctly detected only in the mitochondria. Etoposide (25  $\mu$ g/ml, 8 h), in contrast, induces the transfer of both cytochrome c and Smac into the cytosol.

AIF, however, was not released upon cephalostatin 1 treatment and only to a small extent in response to etoposide.

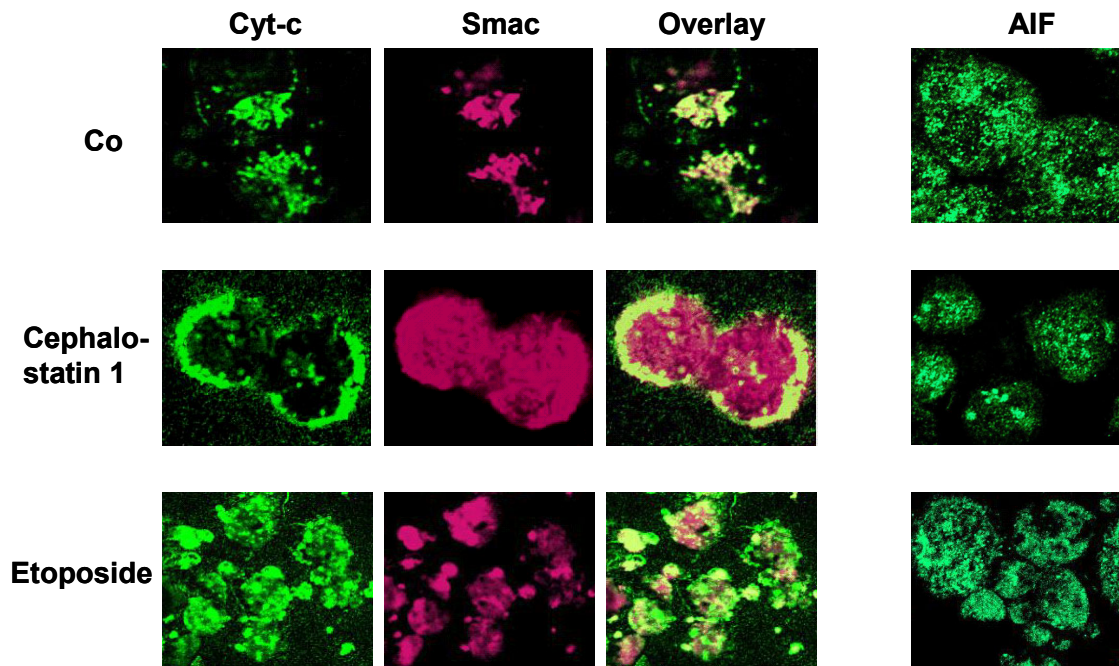


**Figure 27: Detection of released mitochondrial factors by confocal laser scanning microscopy.**

Cells were either left untreated or stimulated with cephalostatin 1 (1  $\mu\text{M}$ ) or etoposide (25  $\mu\text{g/ml}$ ) for 8 h and prepared for confocal laser scanning microscopy as described under Materials & Methods. Representative figures are shown. Cyt-c, cytochrome c.

Smac acts by sequestering inhibitors of active caspases (see II.5.3.2). In order to clarify whether Smac fulfils this function in cephalostatin 1-triggered apoptosis, immunoprecipitation experiments were performed. After treatment with cephalostatin 1 (1  $\mu\text{M}$ ) or etoposide (25  $\mu\text{g/ml}$ ) for 4 h, Smac and caspase-9 were immunoprecipitated and the resulting complexes were analysed for the presence of XIAP (x-linked inhibitor of apoptosis) for which Smac displays the highest affinity among the IAP family. In untreated cells, XIAP is bound to caspase-9 thus inhibiting its activity (Figure 28 A). On stimulation with cephalostatin 1, however, XIAP is displaced from caspase-9 and becomes associated with Smac (Figure 28 B). This suggests that Smac released by cephalostatin 1 aids in the activation of caspase-9.

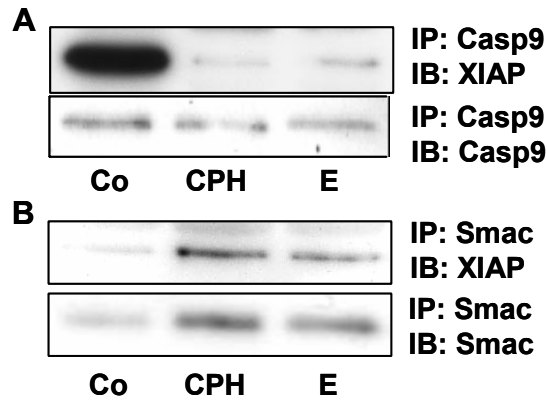


**Figure 28: Immunoprecipitation of Smac and caspase-9.**

Cells were stimulated with cephalostatin 1 (1 $\mu$ M) or etoposide (E, 25 $\mu$ g/ml) for 4 h. **A**, lysates were immunoprecipitated (IP) with anti-caspase-9 antibody and analysed by immunoblotting (IB) with anti-XIAP antibody (*upper panel*) or anti-caspase-9 antibody (*bottom panel*). **B**, lysates were immunoprecipitated (IP) with anti-Smac antibody, followed by immunoblotting (IB) with anti-XIAP (*top panel*) or anti-Smac antibody (*lower panel*). All experiments were performed three times with analogous results. Representative Western blots are shown.

### 3.3.5 Formation of an apoptosome

Formation of the apoptosome usually requires cytochrome c derived from the mitochondria, the cytosolic factor Apaf-1, ATP and pro-caspase-9 (see II.5.3). However, some studies have shown that caspase-9 can be activated independently of cytochrome c [101-103] although in part of these cases, it is not clear whether an alternative form of apoptosome is required, whether the assembly of the apoptosome parts is possible without cytochrome c at all or if caspase-9 is activated completely without apoptosome formation. Therefore, it was tested, if caspase-9 activation by cephalostatin 1 treatment involves an association of caspase-9 with Apaf-1.

Jurkat cells were incubated with cephalostatin 1 (1 h) or etoposide (25  $\mu$ g/ml) for 4 h. Immunoprecipitates of caspase-9 were analysed for association of Apaf-1 which would indicate that caspase-9 is recruited into an apoptosome. Figure 29 demonstrates that cephalostatin 1 does not induce a binding between caspase-9 and Apaf-1 whereas in cells treated with the positive control etoposide, as expected, Apaf-1 associates with caspase-9. This finding together with the fact that cytochrome c is not released affirms the conclusion that

caspase-9 is not activated by an apoptosome in cephalostatin 1-induced apoptosis.

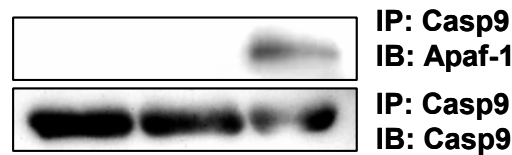


**Figure 29: Immunoprecipitation of caspase-9: detection of Apaf-1 binding.**

Cells were stimulated with cephalostatin 1 (1 $\mu$ M) or etoposide (E, 25 $\mu$ g/ml) for the indicated time, and lysates were immunoprecipitated (IP) with anti-caspase-9 antibody, followed by immunoblotting (IB) with anti-Apaf-1 (*top panel*) or anti-caspase-9 antibody (*lower panel*). A representative western blot out of three is shown.

### 3.3.6 Necessity of caspase-9 for cephalostatin 1-induced apoptosis

The results suggesting that no apoptosome formation occurs upon cephalostatin 1 treatment brings forth the question how caspase-9 is activated. It has been shown that caspase-9 can be activated by other initiator caspases such as caspase-8 and caspase-12 [79;102]. Thus, caspase-9 might not act as primary initiator caspase in cephalostatin 1-induced apoptosis and merely provide an enhancement to the apoptotic signalling.

In order to prove whether caspase-9 is activated as topmost caspase in the cascade, cells were pretreated with the caspase-9 inhibitor zLEHDfmk (50  $\mu$ M) followed by cephalostatin 1 (1  $\mu$ M, 16 h) or etoposide (25  $\mu$ g/ml) stimulation and subsequently analysed apoptosis induction. In addition, caspase-3 activity was measured to investigate if caspase-9 acts upstream of caspase-3. As depicted in Figure 30, the caspase-3 activity induced by both drugs was abrogated by the caspase-9 inhibitor indicating that caspase-3 is indeed activated by caspase-9. In contrast, pretreatment with the inhibitor led to an inhibition of etoposide-induced apoptosis but only to a slight decrease in apoptosis mediated by cephalostatin 1. This indicates that caspase-9 contributes to but is not essential for cephalostatin 1-triggered apoptosis.

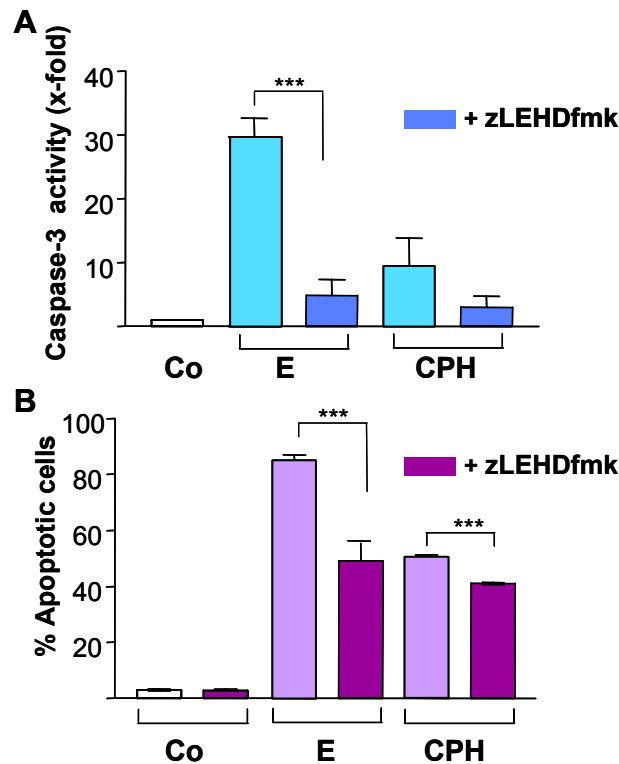


**Figure 30: Necessity of caspase-9.**

Cells were either left untreated (CO) or activated with cephalostatin (CPH, 1  $\mu$ M) or etoposide (ETO, 25  $\mu$ g/ml) in the absence or presence of the caspase-9 inhibitor zLEHDfmk (50  $\mu$ M, 1 h pretreatment) for 16 h. Then caspase-3 activity (A) or apoptosis (B) was quantified as indicated in Materials & Methods. Bars represent the mean  $\pm$  SE of three independent experiments performed in triplicate. \*\*\*  $p < 0.001$  (ANOVA/Dunnett).

### 3.3.7 Overexpression of anti-apoptotic proteins Bcl-2 and Bcl-x<sub>L</sub>

The anti-apoptotic Bcl-2 family members Bcl-2 and Bcl-x<sub>L</sub> are potent inhibitors of the mitochondrial apoptotic pathway (see II.5.3.1). In addition, both are localised to the ER membranes where they are also able to exert their anti-apoptotic function.

In order to investigate if the two anti-apoptotic proteins have an impact on cephalostatin 1-mediated apoptosis, Jurkat cells overexpressing Bcl-2 (Jurkat/*bcl-2*) or Bcl-x<sub>L</sub> (Jurkat/*bcl-x<sub>L</sub>*) and their control cells (Jurkat/*2neo* or Jurkat/*x<sub>L</sub>neo* respectively) were stimulated with cephalostatin 1 (1  $\mu$ M) for different periods of time. A Western blot analysis was carried out to verify that

the expression levels of Bcl-2 or Bcl-x<sub>L</sub> respectively indeed differ from control cells (Figure 31).

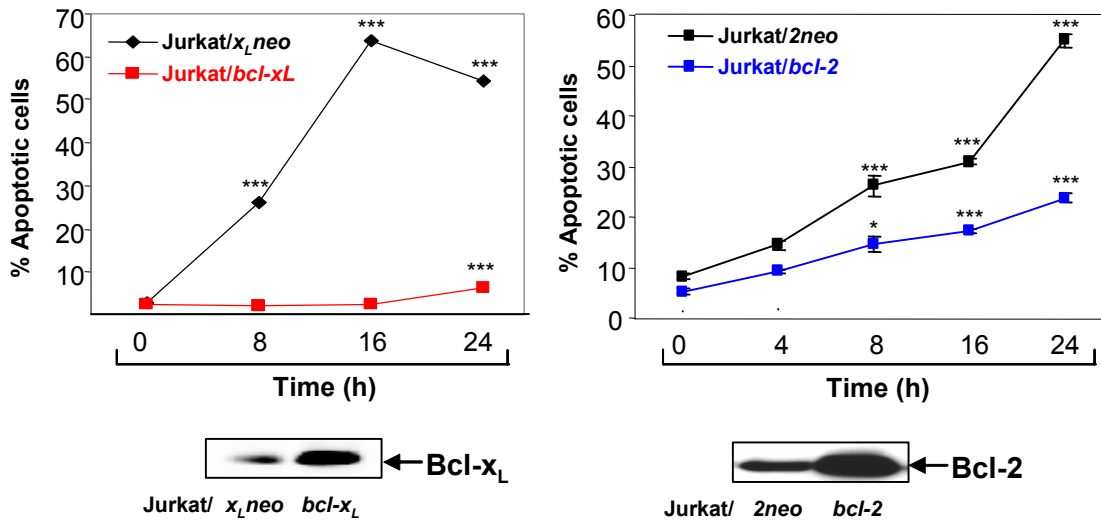


**Figure 31: Influence of overexpression of Bcl-2 and Bcl-x<sub>L</sub> on cephalostatin 1-mediated apoptosis.**

**A**, Control cells (Jurkat/*2neo*) and cells overexpressing Bcl-2 (Jurkat/*bcl-2*) were stimulated with cephalostatin 1 (1  $\mu$ M) for the indicated periods of time, stained with PI and analysed by flow cytometry for apoptosis (*upper panel*). Cell lysates of Jurkat/*neo* and Jurkat/*bcl-2* were analysed for Bcl-2 expression by Western blot analysis (*lower panel*). **B**, Control cells (Jurkat/*x<sub>L</sub>neo*) and cells overexpressing Bcl-x<sub>L</sub> (Jurkat/*bcl-x<sub>L</sub>*) were treated and analysed as described in **A**. **A – B**, Data are the mean  $\pm$  SE of three independent experiments performed in triplicate. \*,  $p < 0.05$ , \*\*\*  $p < 0.001$  (ANOVA/Dunnett), compared to untreated cells.

As shown in Figure 31 A, overexpression of Bcl-x<sub>L</sub> delayed the onset of cephalostatin 1-induced apoptosis. The first significant apoptosis in Jurkat/*bcl-x<sub>L</sub>* cells was not detected until 24 h after treatment whereas Jurkat/*x<sub>L</sub>neo* cells already showed considerable apoptosis levels 8 h after stimulation with cephalostatin 1.

Bcl-2, however, was not as effective in counteracting the apoptotic signalling of cephalostatin 1 (Figure 31 B). Jurkat/*bcl-2* cells were affected to a lower extent compared to their control cells but the protection was incomplete. As in Jurkat/*2neo* cells, cephalostatin 1 induced significant apoptosis levels after 8 h. These results suggest that cephalostatin 1 disposes is able to attenuate Bcl-2 anti-apoptotic function. Experiments concerning the signalling leading to Bcl-2 inactivation are presented in 3.3.8.

In order to elucidate if Bcl-x<sub>L</sub> inhibits cephalostatin 1-triggered apoptosis on the mitochondrial level, Jurkat/x<sub>L</sub>neo and Jurkat/bcl-x<sub>L</sub> cells were incubated with cephalostatin 1 (1 μM, 0 – 24 h). Subsequently, the release of Smac and dissipation of  $\Delta\psi_m$  were determined. As depicted in Figure 32 A, corresponding to the delayed onset of apoptosis, Smac is released later in the time course of cephalostatin 1 treatment in Jurkat/Bcl-x<sub>L</sub> cells compared to Jurkat/x<sub>L</sub>neo (16 h versus 2 h). Thus, Bcl-x<sub>L</sub> exerts its protective role at least partially on the mitochondrial membranes. Of note, mitochondrial membrane permeabilisation occurred indifferent from Bcl-x<sub>L</sub> expression levels (Figure 32 B) suggesting that dissipation of  $\Delta\psi_m$  is only a consecutive event in cephalostatin 1-induced apoptosis.

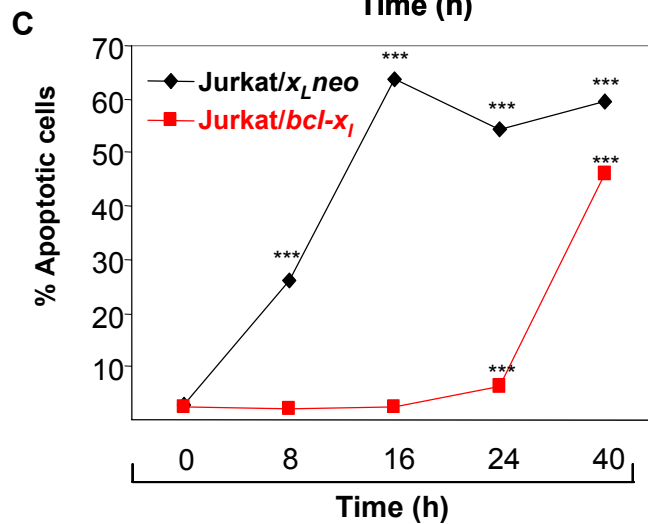
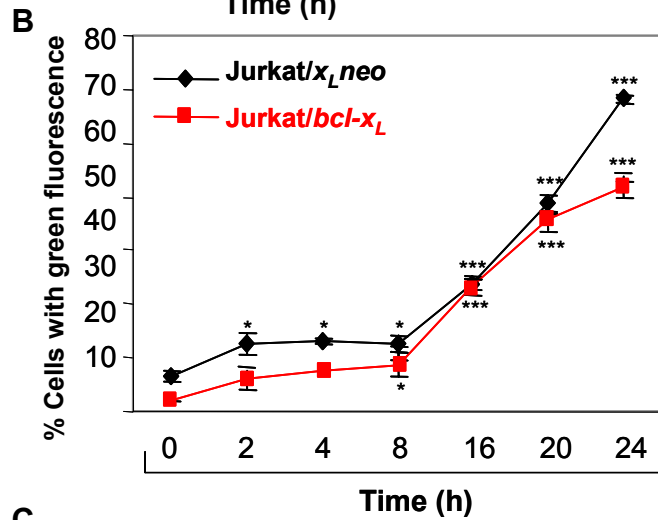
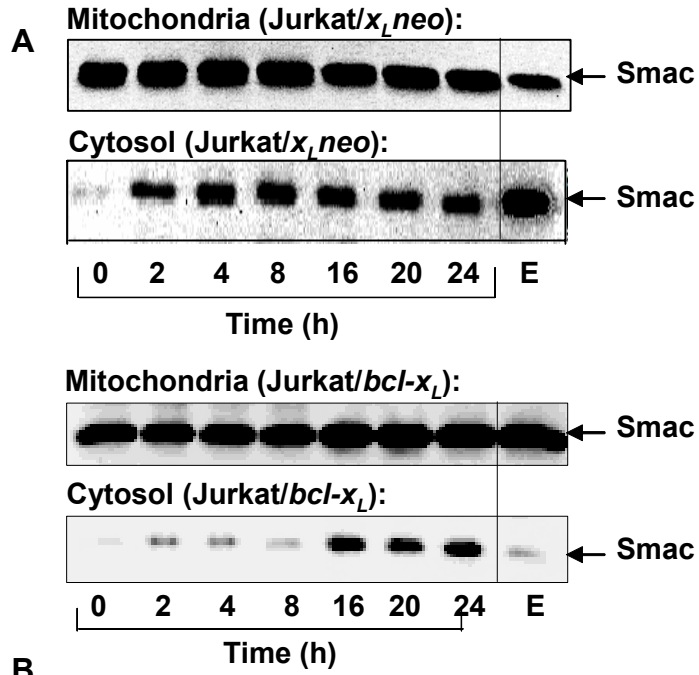


**Figure 32: Impact of Bcl-x<sub>L</sub> overexpression on cephalostatin 1-induced Smac release and membrane permeabilisation.**

**A**, Jurkat/x<sub>L</sub>neo (upper panel) and Jurkat/bcl-x<sub>L</sub>, (lower panel) were treated with cephalostatin 1 (1 µM) for the indicated time or as positive control with etoposide (*E*, 25 µg/ml, 16 h). Cytosolic and mitochondrial protein was prepared as described under Materials & Methods and Smac/DIABLO detected by a specific antibody using western blot analysis. A representative western blot is shown. **B**, Jurkat/neo and Jurkat/bcl-x<sub>L</sub> cells were incubated with cephalostatin 1 (1 µM) for the indicated time. Apoptosis was quantified by flow cytometry. **C**, Cells treated as in B were loaded with the fluorochrome JC-1 (0.25 µg/ml). Cells showing predominantly green fluorescence were quantified by FACS analysis. Data points and bars represent the mean ± SE of three independent experiments performed in triplicate. \*  $p < 0.05$ , \*\*\*  $p < 0.001$  (ANOVA/Dunnett).

### 3.3.8 Inactivation of Bcl-2

#### Mechanism of Bcl-2 inactivation

Since Jurkat cells overexpressing Bcl-2 are only partially protected against cephalostatin 1, the next focus lay on the signalling pathway leading to a decreased anti-apoptotic effect of Bcl-2. Several mechanisms for Bcl-2 inactivation have been proposed including cleavage of Bcl-2 mRNA or protein and hyperphosphorylation at Thr<sup>69</sup> and Ser<sup>87</sup>.

To elucidate which mechanism applies for cephalostatin 1, Jurkat/bcl-2 cells were left untreated or stimulated with cephalostatin 1 (1 µM) for different time periods and analysed for Bcl-2 hyperphosphorylation *via* Western blot analysis.

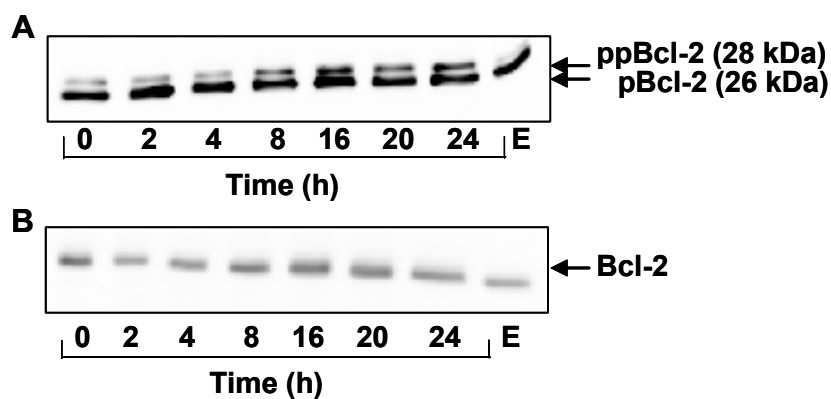


**Figure 33: Time course of hyperphosphorylation of Bcl-2.**

Jurkat/bcl-2 cells were incubated with 1 µM cephalostatin 1 for 2 – 24 h or as positive control with etoposide (*E*, 25 µg/ml, 16 h). Cell lysates were analysed by Western blotting for hyperphosphorylated Bcl-2 (ppBcl-2) (**A**) and total unphosphorylated Bcl-2 (**B**).

As depicted in Figure 33 A, Bcl-2 is indeed hyperphosphorylated 8 h after cephalostatin 1 treatment indicated by the appearance of an additional band at 28 kDa. Etoposide (E; 10  $\mu$ M, 16 h) used as control showed no effect. To exclude that Bcl-2 levels are changed by cephalostatin 1, cell lysates were tested for the total Bcl-2 levels. Figure 33 B demonstrates that the overall amount of Bcl-2 remained unchanged during the time course of cephalostatin 1 treatment. The data suggest that cephalostatin 1 disables Bcl-2 solely by hyperphosphorylation.

In order to confirm the theory that the observed Bcl-2 hyperphosphorylation is indeed the mechanism of Bcl-2 inactivation Jurkat cells overexpressing a mutant form of Bcl-2 were employed. In this mutant Bcl-2 protein, all three phosphorylation sites (Thr<sup>69</sup>, Ser<sup>70</sup>, Ser<sup>87</sup>) are substituted by alanine to prevent phosphorylation and thus inactivation of Bcl-2. In comparison to cells carrying the vector alone (Jurkat/*2neo*) and cells overexpressing the wildtype Bcl-2 protein (Jurkat/*bcl-2*), the mutant cell line (Jurkat/*mbcl-2*) was completely protected against cephalostatin 1 (Figure 34 A). To prove that all three cell lines responded as they are reported to, they were exposed to taxol (1  $\mu$ M, 24 h). Figure 34 B shows that the Jurkat/*mbcl-2* cells were better protected against taxol-induced apoptosis than cells overexpressing the wild-type Bcl-2 protein while Jurkat/*neo* cells succumbed freely to apoptosis.

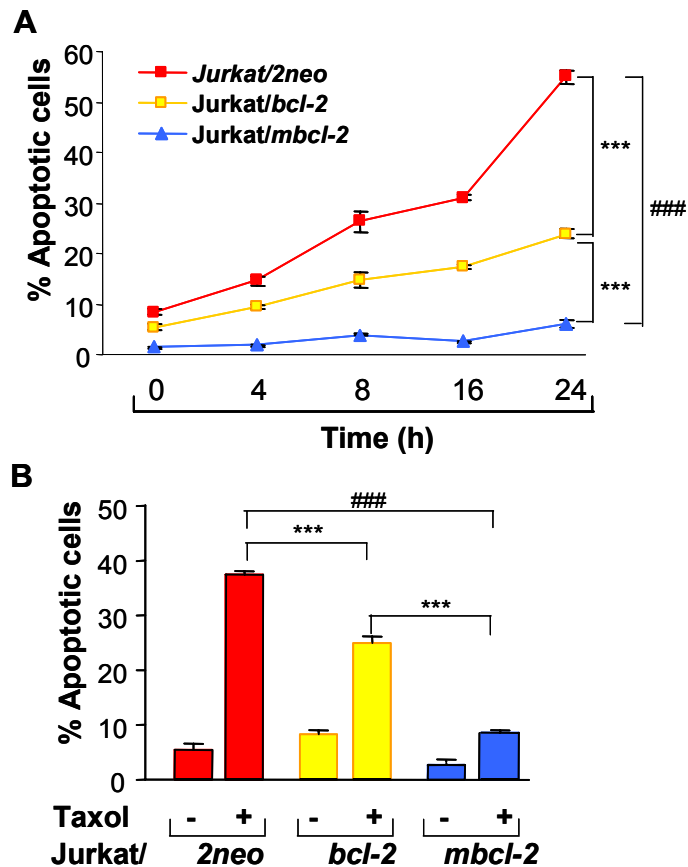


**Figure 34: Apoptosis induction by cephalostatin 1 in cells overexpressing wildtype or mutated Bcl-2.**

Control cells (Jurkat/2neo), cells overexpressing wildtype Bcl-2 (Jurkat/bcl-2) or Bcl-2 with alanine-substituted phosphorylation sites (Thr69, Ser70, Ser87) (Jurkat/mbcl-2) were stimulated with cephalostatin 1 (1  $\mu$ M) for the indicated periods of time (**A**) or with taxol (1  $\mu$ M, 24 h) (**B**). Apoptotic cells were quantified by flow cytometry. Data are the mean  $\pm$  SE of three independent experiments performed in triplicate. \*\*\*  $p < 0.001$  (ANOVA/Dunnett).

### Mediator of Bcl-2 hyperphosphorylation

Of interest was further which kinase may be responsible for the cephalostatin 1-induced Bcl-2 hyperphosphorylation. *Via* Western blot analysis, the activation of JNK upon cephalostatin 1 stimulation was investigated in Jurkat cells. As depicted in Figure 35 A, both JNK1 and JNK2 were phosphorylated and thus activated already 2 h after cephalostatin 1 treatment and phosphorylation increased up to 8 h after stimulation. In order to establish a link between JNK activation and Bcl-2 hyperphosphorylation, Jurkat cells were pre-treated with the specific JNK inhibitor SP600125. Figure 35 B reveals that the inhibitor

abolishes Bcl-2 hyperphosphorylation after treatment with cephalostatin 1 as well as with taxol.

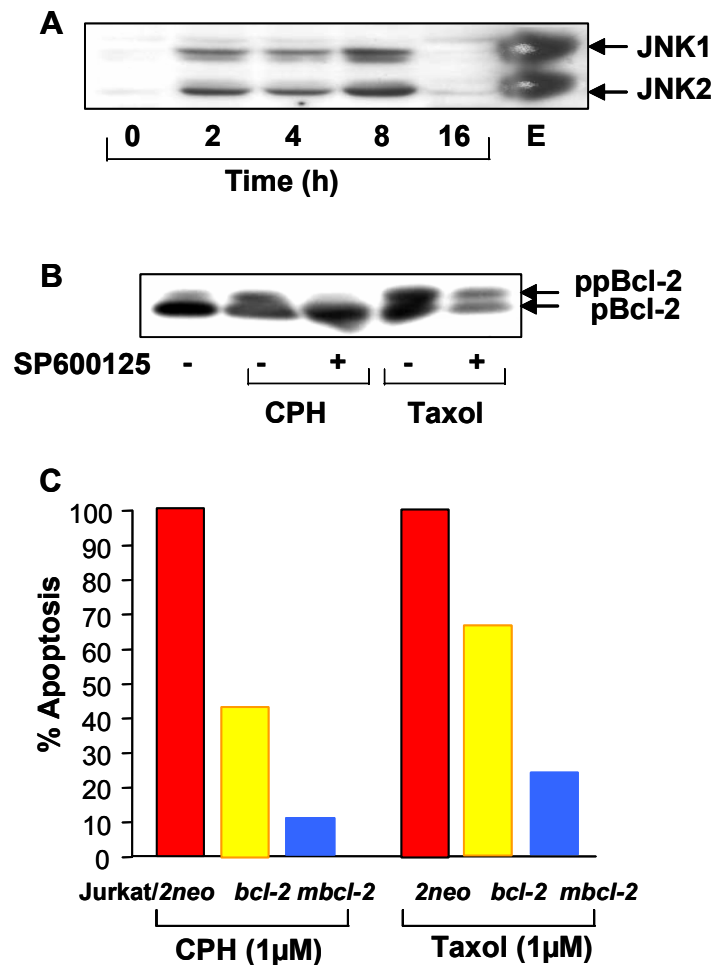


**Figure 35: Involvement of JNK in cephalostatin 1-induced Bcl-2 hyperphosphorylation.**

**A**, Jurkat/bcl-2 cells were stimulated with cephalostatin 1 (1  $\mu$ M) for the indicated periods of time. Etoposide (E, 25  $\mu$ g/ml, 8 h) was used as positive control. Cell lysates were analysed with anti-phospho-JNK antibody for the activated forms of JNK1 (p46) and JNK2 (p54). **B**, Cells were incubated with (+) or without (-) SP600125 (10  $\mu$ M) for 1 h and further stimulated with cephalostatin 1 (1  $\mu$ M) or taxol (1  $\mu$ M) for 16 h. Lysates were immunoblotted with anti-phospho-Bcl-2 antibody. **C**, Jurkat/neo, Jurkat/bcl-2 and Jurkat/mbcl-2 were left untreated, treated with cephalostatin 1 (1  $\mu$ M) or taxol (1  $\mu$ M) for 24 h (as described in Figure 34 A and B). The diagram shows the percentage of apoptotic cells at 24 h of Jurkat/bcl-2 and Jurkat/mbcl-2 compared to Jurkat/neo cells (= 100%).

Of note, taxol seems to lead to a stronger hyperphosphorylation than cephalostatin 1. To clarify whether this difference in Bcl-2 hyperphosphorylation has an impact on Bcl-2 inactivation, the levels of apoptosis induced by these two drugs in Jurkat/neo, Jurkat/bcl-2 and Jurkat/mbcl-2 cells were compared as shown in Figure 35 C. As expected, Bcl-2 overexpressing cells are more

sensitive to taxol than to cephalostatin 1 suggesting that the stronger hyperphosphorylation induced by taxol leads indeed to a stronger inactivation of Bcl-2. However, Jurkat/*mbcl-2* cells also showed a higher sensitivity towards taxol compared to cephalostatin 1 which implies an additional mechanism to inactivate Bcl-2.

### **Signalling upstream of JNK activation and Bcl-2 hyperphosphorylation**

It is widely accepted that JNK is an important player in the cellular stress response to a wide variety of stimuli. The majority of compounds reported to induce Bcl-2 hyperphosphorylation activate JNK and induce a cell cycle arrest in M-phase, as e.g. microtubule-damaging agents [104].

In order to investigate whether cephalostatin 1-induced JNK activation and successive Bcl-2 hyperphosphorylation depend on an M-phase arrest, the cell cycle distribution of untreated Jurkat cells and cells incubated with cephalostatin 1 (1  $\mu$ M) or taxol (1  $\mu$ M) for 8 h was investigated. The time point was chosen due to evident JNK activation (see Figure 35 A). As demonstrated by Figure 36, taxol induces a potent M-phase block whereas cephalostatin 1 did not interfere with cell cycle progression. Interestingly, cells in G<sub>1</sub> and S-phase seem to be more susceptible to cephalostatin 1 since the overall percentage of cells in G<sub>1</sub>- and S-phase decreased after cephalostatin 1 stimulation. The appearance of a sub-G<sub>1</sub> peak, (Figure 36, *middle panel*) reveals that cells formerly present in G<sub>1</sub> and S underwent apoptosis. The percentage of cells in the G<sub>2</sub>/M-phase was not altered after cephalostatin 1 treatment compared to control. These results indicate that both JNK activation and Bcl-2 phosphorylation induced by cephalostatin 1 occur independent of M-phase blockade.

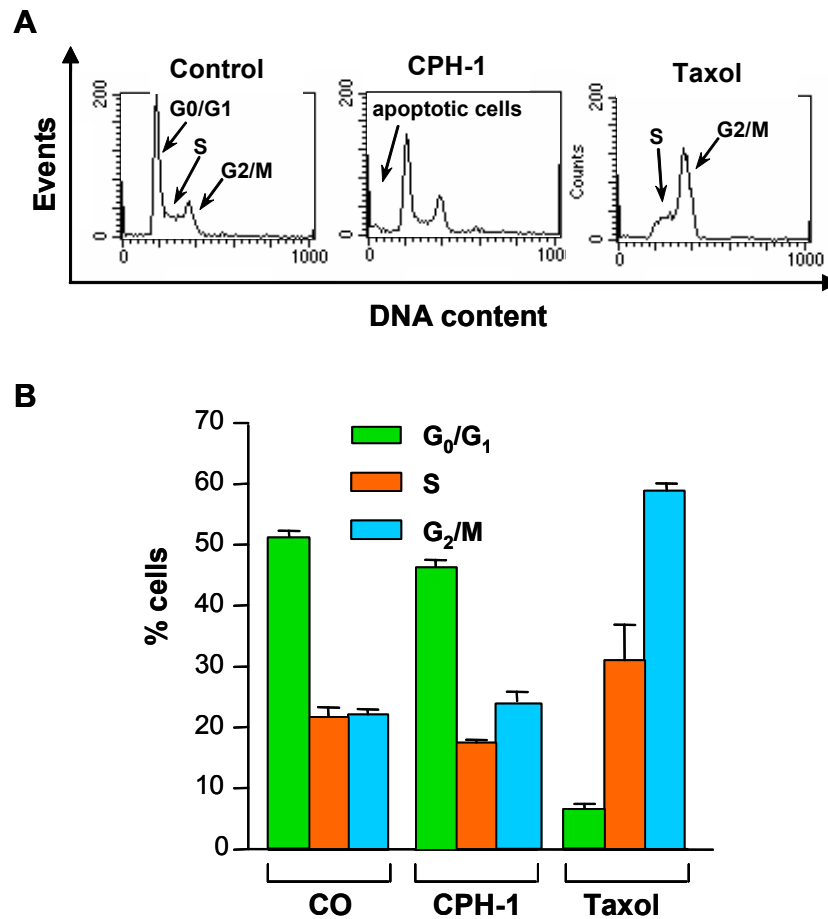


**Figure 36: Cell cycle analysis of cephalostatin 1 and taxol-treated cells.**

**A**, Jurkat cells were incubated with cephalostatin 1 (1  $\mu$ M) or taxol (1  $\mu$ M) for 8 h, stained with PI and analysed by FACS. The histograms show the distribution of cells according to their DNA content. Cell cycle phases are marked by arrows. **B**, Quantification of cells in G<sub>0</sub>/G<sub>1</sub>, S and G<sub>2</sub>/M-phase. The data shown are the mean  $\pm$  SE of three independent experiments performed in triplicate.

Many genotoxic agents mediate JNK activation [105] and some have been described to phosphorylate Bcl-2 [106]. To elucidate whether cephalostatin 1 leads to DNA lesions, Jurkat cells treated with cephalostatin 1 (1  $\mu$ M) or etoposide (10  $\mu$ M) for 4 h were subjected to a comet assay (see III.10). Both drugs induced comparable levels of apoptosis at these concentrations (data not shown). Figure 37 provides clear evidence that etoposide induces DNA damage visible as the typical comet tail whereas cephalostatin 1 does not. This experiment suggests that DNA damage is not the type of cell stress leading to cephalostatin 1-induced JNK activation.

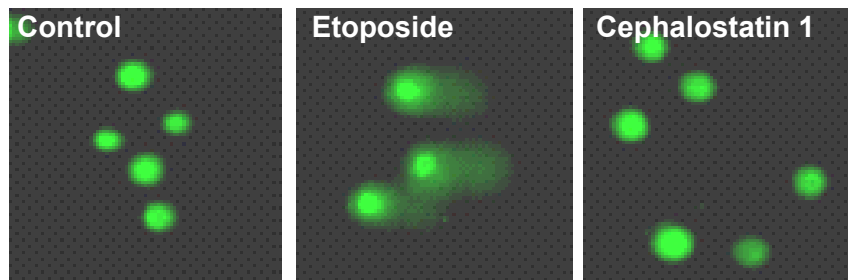


**Figure 37: Comet assay of cells stimulated with etoposide and cephalostatin 1.**

Jurkat cells were either left untreated (CO), stimulated with cephalostatin 1 (CPH-1; 1  $\mu$ M) or etoposide (10  $\mu$ M) for 4 h. DNA damage analysis was performed by comet assay as described under Materials & Methods. Representative pictures of three independent experiments are shown.

### 3.4 INVOLVEMENT OF THE ENDOPLASMIC RETICULUM

Endoplasmic reticulum stress (ER stress) provides another model for the activation of caspase-9.

#### 3.4.1 Cephalostatin 1 elicits ER stress

As illustrated in II.5.4, the UPR induces upregulation of the chaperone BiP and the transcription factor CHOP which may serve as marker for the induction of ER stress. Cephalostatin 1 induces rapid upregulation of BiP after 2 h (Figure 38, A) which is enhanced persistently throughout the stimulation period. In accordance, CHOP transcription is also increased after 2 h (Figure 38, B). CHOP levels, however, fall below control level after 8 h of stimulation. As positive control, cells were stimulated with tunicamycin (T, 1  $\mu$ g/ml), an established inducer of ER stress which inhibits protein glycosylation inside the ER lumen [107].

These results show clearly that cephalostatin 1 induces ER stress. The process precedes activation of caspase-9 indicating that ER stress is triggered upstream of caspase-9. Compared to the time course of Smac release which is released after 2 h, upregulation of ER stress markers happens in parallel. This suggests that cephalostatin 1 targets different cellular organelles equivalently.

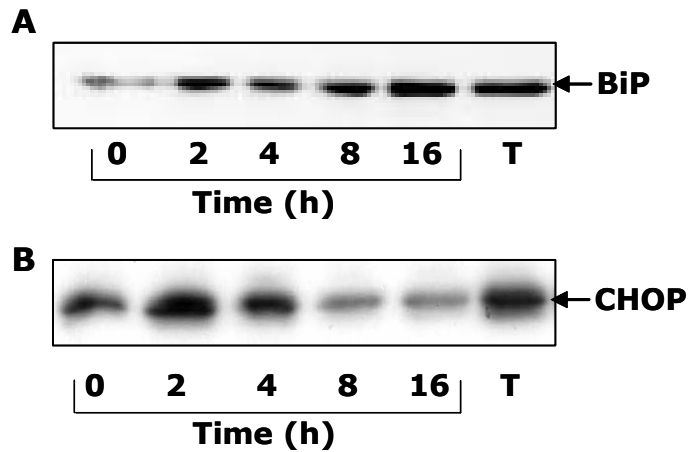


**Figure 38: Induction of ER stress marker proteins by cephalostatin 1.**

Cells were incubated with 1  $\mu$ M cephalostatin 1 for 0 – 24 h or tunicamycin (1  $\mu$ g/ml) for 16 h (A) / 3 h (B) and analysed by Western blotting for the chaperone BiP (A) and the transcription factor CHOP (B). One representative Western blot out of three is shown.

### 3.4.2 Activation of caspase-12

Since cephalostatin 1 induces ER stress, it is conceivable that it also induces caspase-12 activation. To date, an antibody against the active fragments of caspase-12 is not available but the decrease of the zymogen form after 2 h which continues until 16 h when virtually no pro-caspase-12 is detectable indicates that cephalostatin 1 potentially induces the activation of caspase-12.

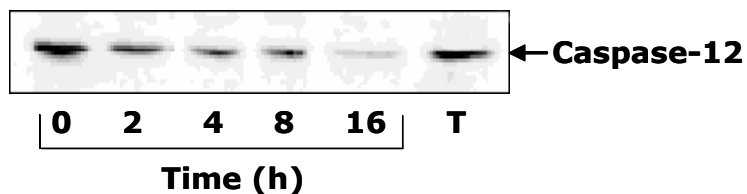


**Figure 39: Activation of caspase-12 by cephalostatin 1 treatment.**

Caspase-12 cleavage indicating activation after incubation with cephalostatin 1 (1  $\mu$ M, 0 – 24 h) or tunicamycin (1  $\mu$ g/ml, 8 h). One representative Western blot out of three is shown.

The early cleavage of the caspase-12 zymogen is correlated with the time course of ER stress (cf. Figure 38). As mentioned above, ER stress as well as activation of caspase-12 are detectable before caspase-9 activation. This suggests that caspase-12 might be the primary initiator caspase in cephalostatin 1-induced apoptosis. In addition, caspase-9 is obviously activated

downstream of caspase-12 and might act in the amplification of apoptosis induction.

Activation of caspase-12 is mediated by diverse mechanisms depending on the cell model (see II.5.4). For cephalostatin 1-induced apoptosis, the activation of caspase-7 and calpain, two potential triggers for caspase-12, was investigated.

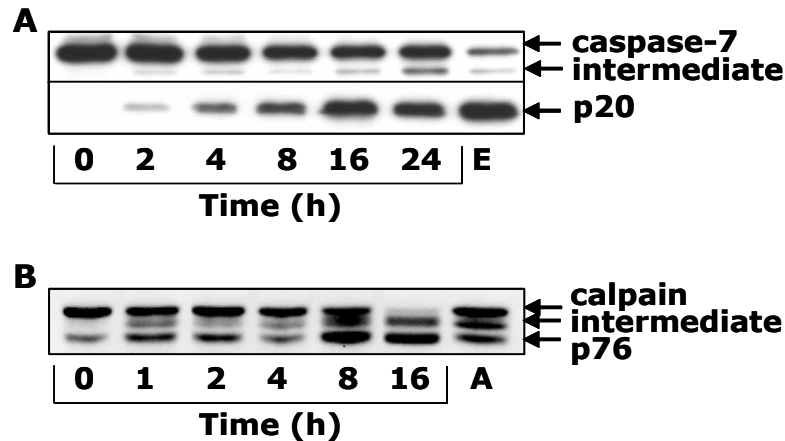


**Figure 40: Activation of caspase-7 and calpain by cephalostatin 1.**

Cells were stimulated with cephalostatin 1 (1  $\mu$ M) for the indicated times and subsequently analysed by Western blotting for cleavage of caspase-7 to the cleavage product p20 (**A**) and for cleavage of calpain to the active form (p76, **B**). Etoposide (E, 10  $\mu$ M, 16 h) or A23187 (A, 1  $\mu$ M, 16 h) were used as positive controls. All experiments were performed three times with consistent results. One representative Western blot is shown.

Removal of the prodomain of pro-caspase-7 (35 kDa) produces a 32 kDa intermediate which is further cleaved into the active subunits. The large subunit of active caspase-7 (Figure 40, A, p20) appeared at 2 h of treatment with further increase over the course of stimulation. Calpain which is autolytically activated in the presence of free Ca is notably activated after 1 h. Etoposide (E, 10  $\mu$ M) and A23187 (A, a calcium ionophore shown to activate calpain [108], 1  $\mu$ M) were used as positive controls. Both enzymes are activated early in the time course. However, at 2 h, when a clear activation of caspase-12 was determined, activation of caspase-7 appears modest in comparison to the levels of active calpain.

## V. DISCUSSION

Cancer is the second leading cause of death in the western countries. Although great improvements in cancer treatment have been achieved over the last decades, in many cases patients still lose the fight against this dreaded disease. Due to the vast diversity in marine life offering opportunities for the search for new remedies, intense interest in bioactive marine compounds has evolved. These substances might prove as invaluable new chemotherapeutics.

This work provides insight into the remarkable cytotoxic activity of cephalostatin 1, a compound isolated from the marine worm *Cephalodiscus gilchristi* Ridewood by the team of Dr. G.R. Pettit [1].

### **CHARACTERISATION OF THE CELL DEATH INDUCED BY CEPHALOSTATIN 1**

Cephalostatin 1 exhibits a cytotoxic activity at remarkably low concentrations in the MTT assay (significance reached at 0.1 nM) against Jurkat T cells. The  $IC_{50}$  was calculated as 1.25 nM which correlates well with the  $GI_{50}$  obtained from the NCI-60 panel (1 nM) [2].

Apoptotic cell death includes several defined biochemical alterations which can be employed for defining the type of cell death triggered by cephalostatin 1. Light microscopic analyses revealed the formation of apoptotic bodies. Usually, shedding of apoptotic fragments is accompanied by a condensation of the cell. A flow cytometry measurement of cell size and granularity clearly demonstrates that cephalostatin 1 leads to cell shrinkage and increased granularity. Evidence for apoptosis induction by cephalostatin 1 is also provided by DNA staining displaying the appearance of condensed chromatin and DNA fragments over the course of stimulation. Quantitative analysis of DNA fragmentation *via* FACS showed a time- and dose-dependent induction of apoptosis. In addition, flow cytometry was used for the detection of phosphatidylserine exposure which occurred after 8 h of stimulation with cephalostatin 1.

## **SIGNAL TRANSDUCTION PATHWAYS IN CEPHALOSTATIN 1-INDUCED APOPTOSIS**

Apoptotic changes resulting finally in the demise of the cell are commonly mediated by the caspase family that act as initiators as well as executors of the apoptotic cascade. Increasing numbers of recent studies, however, present models for caspase-independent apoptosis. These pathways are mediated by calpains [3;4], cathepsins [5-7], AIF [8-13] or Bax [14-16]. In this study, caspase activation was evidenced by Western blot analysis of cleavage products of caspase-3, -7, -8, -9 and -12. Indeed, cephalostatin 1-induced apoptosis is dependent on caspases as shown by abrogation of apoptosis after inhibition with the pan-caspase inhibitor zVADfmk. In spite of the prevention of cephalostatin 1-triggered apoptosis by zVADfmk, the initiation of the signal pathway may be performed by a mechanism different from the common caspase activation pathways.

So far, three pathways of apoptosis induction have been proposed: one employing death receptors on the cell membrane, another involving mitochondrial activation and the third emanating from the endoplasmic reticulum. In the following will be discussed which pathways are involved in cephalostatin 1-triggered apoptosis.

### **1.1 INVOLVEMENT OF CD95 PATHWAY**

The extrinsic pathway induced by activation of death receptors implies activation of caspase-8 as initiator caspase after assembly of the DISC.

Initially, upregulation of death receptor ligands observed upon treatment with anticancer drugs was regarded as crucial apoptosis-inducing mechanism of chemotherapeutic drugs. Thereafter, numerous studies have provided evidence against this theory and currently it is accepted that anticancer drugs primarily utilize mitochondrial signals, i.e. caspase-9 activated in the apoptosome

although a contribution of the death receptor system can not be completely excluded in some cases [17].

In this regard, cephalostatin 1 acts like a typical chemotherapeutic agent in that apoptosis induced by cephalostatin 1 does not require death receptor signalling. This was shown by CD95 deficient Jurkat cells which were killed equally to their controls. The possibility that another death receptor might be involved in the pathway was ruled out with caspase-8<sup>-/-</sup> cells which also underwent apoptosis indiscriminately from control cells. In addition, although caspase-8 was activated by cephalostatin 1 it occurred at a very late time point (16 h) indicating that caspase-8 is not activated as initiator caspase. More likely, cleavage of caspase-8 occurs by caspase-3 in the wake of the caspase cascade as shown for several anticancer drugs [18;19] leading to an amplification loop for apoptosis.

## **1.2 INVOLVEMENT OF MITOCHONDRIA IN CEPHALOSTATIN 1-INDUCED APOPTOSIS**

As mentioned above, the mitochondria are key mediators for the apoptotic process triggered by anticancer agents. Apoptogenic factors released from the intermembrane space (IMS) account for the activation of caspase-9 (cytochrome c and Smac) while others mediate caspase-independent apoptosis (AIF, EndoG).

The release mechanism of proteins present in the IMS has been the focus of intense studies and there is still much controversy on how the pore is composed and regulated. The oldest model implies the ANT on the IMM and the VDAC on the OMM (see Figure 41). Opening would be accompanied by loss of membrane potential, swelling of the matrix and finally rupture of the OMM releasing the intermembrane proteins into the cytosol [20]. The pro-apoptotic Bcl-2 family members Bax and Bak were shown to internalise into the OMM and form tetrameric channels enabling proteins to leak out of the IMS [21;22]. Recent studies provide evidence that the transition pore consists of more than the two components mentioned before. In addition, distinct opening modes have

been discussed depending on the  $\text{Ca}^{2+}$  concentration in the mitochondrial matrix [23]. In spite of the prevailing disaccord on the pore assembly, most agree that mitochondrial matrix swelling and dissipation of  $\Delta\psi_m$  occur in accordance with mitochondrial dysfunction resulting ultimately in apoptosis.

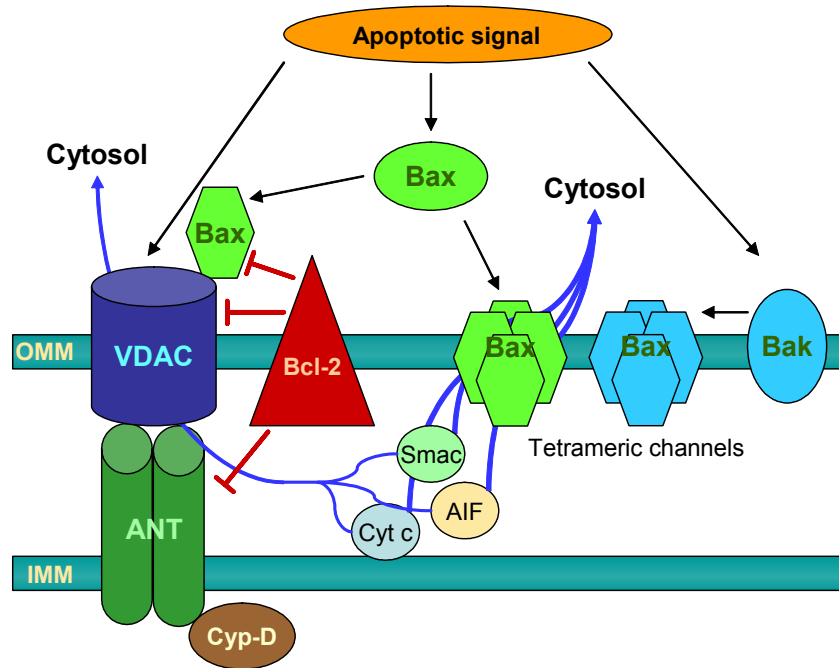


**Figure 41: Proposed models of the release of proteins from the mitochondrial IMS.**

An apoptotic signal induces opening of the permeability transition pore (PTP) consisting, among others, of VDAC (voltage-dependent anion channel), ANT (adenine nucleotide translocator) and Cyp-D (cytochrome c haptophyllin D) on the matrix side. Another model suggests the involvement of Bax which undergoes a conformational change upon an apoptotic signal and interacts with components of the PTP inducing an opening of the PTP. In addition, Bax and Bak were shown to form tetrameric channels in the OMM.

Cephalostatin 1-induced loss of mitochondrial membrane potential was detected by JC-1 staining. Analysis of the ultrastructural alterations of Jurkat cells upon stimulation with cephalostatin 1 revealed obvious dilatations of nuclear and ER membranes and fragmented nuclei. Most strikingly, the mitochondria were not enlarged as would be expected. Mitochondrial size was markedly reduced and the matrix seemed to be condensed. In contrast, the cristae appeared swollen. A recent publication also describes the condensation of mitochondrial matrix and cristal unfolding in an early phase of growth factor withdrawal which is supposed to facilitate the release of cytochrome c thus

triggering the caspase cascade [24]. This could apply for cephalostatin 1-induced apoptosis as well but the effect was observed at a late time point (16 h) contradicting the function of matrix condensation in apoptosis initiation. In addition, no cytochrome c release from the mitochondria was detected after cephalostatin 1 treatment. Thus, mitochondrial dysfunction initiated by cephalostatin 1 seems to occur in a previously unknown manner.

The observed mitochondrial dysfunction indicates an involvement of mitochondria in cephalostatin 1-mediated apoptosis. The common execution pathway emanating from the mitochondria involves the formation of the apoptosome consisting of cytochrome c from the IMS, the cytosolic protein Apaf-1 and pro-caspase-9. Indeed, caspase-9, the initiator caspase of the intrinsic pathway, was activated after 4 h. Activation occurred previous to caspase-8 cleavage suggesting that caspase-9 acts upstream in the initiation cascade.

Analysis of the release of apoptogenic factors into the cytosol, though, demonstrated that only Smac escaped from the IMS in contrast to cytochrome c and AIF which could not be detected in the cytosolic fraction. Therefore, activation of caspase-9 proceeds in a cytochrome c-independent mechanism. Cytochrome c-independent activation of caspase-9 has been shown for a TNF $\alpha$  model and several ER stress models [25-27]. In classical apoptosis, apoptosome formation involves cytochrome c thus, most probably, cytochrome c-independent activation of caspase-9 does not require Apaf-1 or a functional apoptosome. In line with this theory, cephalostatin 1-induced caspase-9 activation does not imply association of caspase-9 with Apaf-1.

In stress-induced apoptosis, Smac is released from mitochondria where it interacts predominantly with the caspase inhibitor XIAP in a manner that displaces caspases from XIAP [28]. Smac released by cephalostatin 1 fulfils this function by sequestering XIAP previously bound to caspase-9 thus fostering caspase-9 activation. Since Smac is selectively released from the mitochondria it obviously acts as main mitochondrial signalling molecule. This emphasizes

the uniqueness of the cephalostatin 1 signalling pathway since most other studies show that release of cytochrome c into the cytosol also implies Smac release which sometimes even occurs in tandem [29].

Interestingly, the release of Smac by cephalostatin 1 proceeds in a caspase-independent manner as its onset happened before caspase-9 activation and release was not affected by preincubation with the pan-caspase inhibitor zVADfmk. This observation stands in contrast to a recent study in which the release of Smac is a secondary event following cytochrome c release and caspase activation [30]. As a result, the caspase-independent release of Smac suggests that caspase activation upstream of the mitochondria is not required for cephalostatin 1-induced apoptosis. The signalling resulting in Smac release has not been identified yet but it is conceivable that JNK which is activated early in cephalostatin 1-induced apoptosis plays a role in Smac release as recently proposed [31]. Backing this theory is the very recent work of another group who showed that JNK produces a distinct Bid cleavage product in TNF $\alpha$ -induced apoptosis (jBid) which is able to induce selective Smac release without concomitant cytochrome c leakage [32]. The question how the selective release of Smac is mediated is still unanswered. Truncated Bid has been shown to induce a conformational change of Bax and Bak whereupon these trigger the release of proteins from the IMS. Obviously, jBid effects Smac release in a different manner since concomitant cytochrome c release was not detected. It is conceivable that different cleavage products of Bid lead to another form of conformational change in Bax and Bak which might result in different pore formation. Calpain has also been shown to cleave Bid at sites differing from those commonly described [33]. Beyond that, calpain can cleave Bax to produce an even more potent pro-apoptotic protein than wtBax [34]. Calpain activated by cephalostatin 1 might mediate the selective Smac release *via* an altered Bax / Bak signalling. Another model might include an interaction of cephalostatin 1 with the components of the permeability transition pore possibly leading to an opening of the PTP. Since Smac is a soluble protein within the IMS in contrast to cytochrome c and AIF that are attached to the inner

membrane [35;36], the selective release of Smac might be facilitated while cytochrome c and AIF are retained.

The hypothesis that caspase activity is not required upstream of the mitochondria raises the question if the release of Smac is required for caspase-9 activation. Recent publications propose that under certain conditions, Smac may be sufficient to initiate a caspase-9-dependent apoptotic pathway in the absence of cytochrome c and apoptosome formation [37;38]. However, regarding the data that inhibition of caspase-9 did not lead to a complete inhibition of cephalostatin 1-mediated apoptosis and taking into account that caspase-9, that is not complexed by Apaf-1, displays a markedly decreased activity [39] leads to the assumption that the common mitochondrial execution pathway routed *via* caspase-9 may not be the essential initiator of the cephalostatin 1-induced caspase cascade.

The finding, that overexpression of Bcl-x<sub>L</sub> delays both apoptosis and Smac release, indicates that Smac is pivotally involved in cephalostatin 1-induced apoptosis. Although Smac displaces XIAP from caspase-9, this does not seem to be the crucial function of Smac since obviously – as discussed above – caspase-9 does not act as initiator of cephalostatin 1-mediated apoptosis. An explanation might be provided by the studies of Riedl *et al.* [40] and Chai *et al.* [41] who present evidence for the interaction of XIAP with caspase-3 and caspase-7. Since cephalostatin 1 triggers the activation of caspase-3 and caspase-7, Smac may relieve the inhibition of caspase-3 and -7 by XIAP and thus contribute considerably to an unchallenged apoptotic progress. Such a contribution was demonstrated for receptor-mediated apoptosis in type II cells. After binding of death ligands, these cells require a mitochondrial signal for complete activation of caspase-3 which was shown to be conveyed by Smac [42;43]. Thus, cephalostatin 1 might employ a pathway different from common extrinsic and intrinsic pathways which is entirely functional only in combination with Smac activity.

### 1.3 INVOLVEMENT OF THE ENDOPLASMIC RETICULUM

The endoplasmic reticulum has only recently come into the focus of interest as major player in apoptotic processes. Several regulators of the mitochondrial pathway are found to be present also at ER membranes such as members of all three sub-groups of the Bcl-2 family [44-48]. Exclusively ER-located pro-caspases (caspase-12 [49], caspase-8L [50]) and corresponding regulators such as TRAF2 [51] and BAP31 [50] were identified. The function of the ER lumen as  $\text{Ca}^{2+}$  store mark the ER as important source of apoptotic signals. Mobilisation of  $\text{Ca}^{2+}$  is sufficient for the initiation of apoptosis in some models [52-55]. In addition, intense crosstalk between ER and mitochondria mediated by  $\text{Ca}^{2+}$  leads to a sensitisation of the latter to pro-apoptotic signals [56]. Apart from agents perturbing protein glycosylation in the ER or  $\text{Ca}^{2+}$  homeostasis [55;57;58], the ER-mediated pathway has been shown to mediate several models of drug-induced apoptosis [59;60] and ischemia / reperfusion injury [61;62].

ER stress can be identified by analysis of changes in the expression levels of distinct ER stress markers. BiP is an ER-located chaperone whose upregulation indicates a disturbance in protein processing in the ER lumen. CHOP, a C/EBP homologous transcription factor, is implied in the mediation of the apoptotic signal from the ER. Cephalostatin 1 induces rapid upregulation of both ER stress markers after 2 h indicating induction of ER stress by cephalostatin 1. In concert, caspase-12 which may act as initiator caspase for ER stress-induced apoptosis is activated markedly after 2 h. These events precede activation of caspase-9 giving rise to the idea that the cephalostatin 1-induced signalling pathway originates at the endoplasmic reticulum and that caspase-12 might act as primary initiator caspase activating caspase-9 downstream. Indeed, a recent study provided evidence of such an interaction [27]. The signal upstream of caspase-12 is not defined yet in cephalostatin 1-induced apoptosis but most probably it is mediated by calpain being activated very rapidly after 1 h as shown by Nakagawa *et al.* [63]. Caspase-7 has also been described to translocate to the ER and cleave caspase-12 there [64] but considering the

rather low signal of active caspase-7 at 2 h stimulation when caspase-12 is clearly activated, it is unlikely that caspase-7 acts as upstream signal.

As discussed in 1.2, the mitochondria are involved and have a relevant part in cephalostatin 1-induced apoptosis. However, the topmost caspase of the cascade is most probably activated at the endoplasmic reticulum. Therefore, either some kind of crosstalk is initiated between the two organelles which coordinates downstream events or cephalostatin 1 acts on both organelles in parallel. In Figure 42, the time flow of events triggered by cephalostatin 1 is depicted. The first event triggered by cephalostatin 1 is the activation of calpain but since all other events were not investigated at this early time point it cannot be excluded that they might be induced in the same time window as calpain (excepting caspase-7 and caspase-9). Calpain activation at 1 h evidences a rapid onset of ER stress. Since calpain is a  $\text{Ca}^{2+}$ -dependent protease located in the cytosol [65], an increase in cytosolic  $[\text{Ca}^{2+}]$  will presumptively have occurred before. Calcium constitutes one of the mechanisms of interaction between the ER and mitochondria. Release of  $\text{Ca}^{2+}$  into the cytosol activates the  $\text{Ca}^{2+}$ -dependent phosphatase calcineurin which in turn dephosphorylates Bad resulting in its activation [66]. Subsequently, Bad can translocate to the mitochondria and bind to the anti-apoptotic protein Bcl-2 leading to Bcl-2 inactivation. Another form of signalling consists in the direct transport from  $\text{Ca}^{2+}$  from the ER to the mitochondria which has been shown to sensitise the mitochondria for pro-apoptotic signals [67]. A third model describes a caspase cleavage product of BAP31 which can transfer the pro-apoptotic signal from the ER to the mitochondria [68]. This model, however, is unlikely for cephalostatin 1-induced apoptosis since according to the results presented here there is no time difference between activation of caspase-12 and release of Smac. In addition, Smac release proceeds independently of caspases. These findings contradict the assumption that caspase activity is required for the ER-mitochondria crosstalk.

The second scheme for the sequence of events in cephalostatin 1-mediated apoptosis assumes that Smac release as well as calpain activation and ER stress are triggered within the same time frame. This would imply that cephalostatin 1 either activates an unknown mediator that virtually immediately targets both ER and mitochondria or cephalostatin 1 interacts directly with the membranes of the two organelles, e. g. by insertion thus triggering the release of  $\text{Ca}^{2+}$ . Another approach might be an interaction with proteins guarding membrane integrity such as Bcl-2 proteins. Considering the chemical steroid structure of cephalostatin 1 which displays a hydrophobic center and two hydrophilic moieties toward the ends of the molecule it is conceivable that it is able to interact with biological membranes which are also composed of a lipophilic core surrounded by hydrophilic layers.

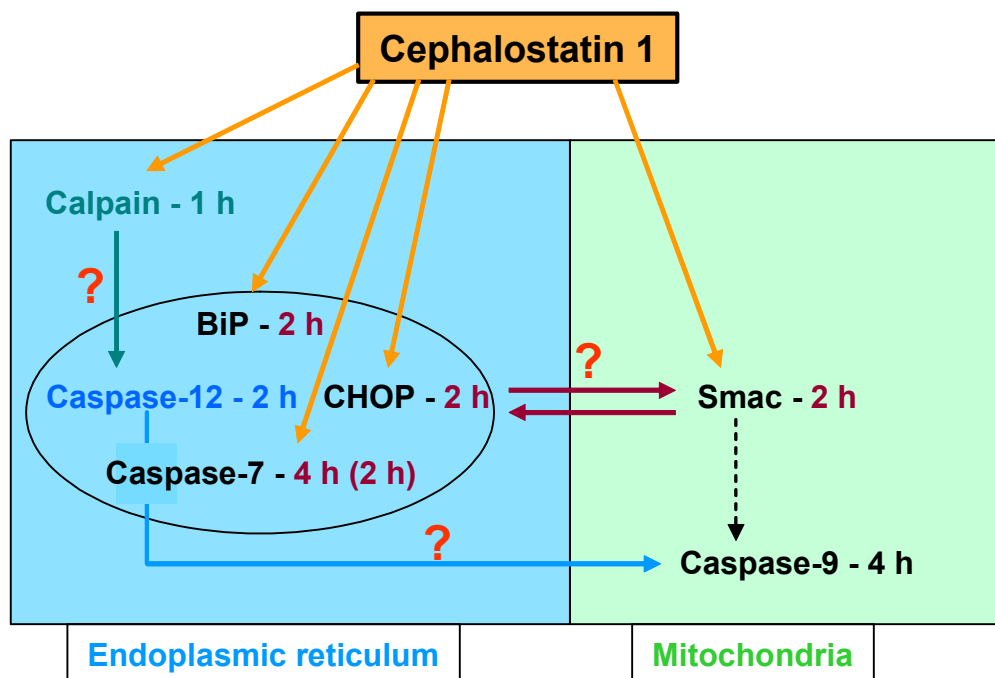


**Figure 42: Proposed time flow of cephalostatin 1-induced apoptosis initiation.**

Events at the ER are presented in the left panel, events at the mitochondria in the right panel. Question marks indicate potential interactions/activations without definite proof provided in this study.

## REGULATION OF CEPHALOSTATIN 1-INDUCED APOPTOSIS

Overexpression of Bcl-2 and Bcl-x<sub>L</sub> in cancer cells due to mutations poses a severe problem for cancer therapy since these cells, protected against mitochondrial apoptosis as well as ER-mediated apoptosis, are often resistant against chemotherapeutic agents which mainly employ the mitochondria as apoptotic mediators [69-75].

Cephalostatin 1-induced apoptosis is inhibited by Bcl-x<sub>L</sub> overexpression. However, Bcl-2 overexpression did not convey complete protection against cephalostatin 1 indicating that cephalostatin 1 initiates an inactivation mechanism.

Several mechanisms are reported to inactivate Bcl-2: activated caspases have been shown to cleave Bcl-2 generating a 23 kDa pro-apoptotic product [76;77]. Furthermore, down-regulation of Bcl-2 mRNA or Bcl-2 protein has been observed after treatment with several anti-cancer drugs [78;79]. In cephalostatin 1-induced apoptosis, total Bcl-2 levels are not altered suggesting that cleavage of the protein or alterations of mRNA levels do not apply here. In addition, Bcl-2 phosphorylation has been observed as mechanism for altering the activity of the protein. Under physiological conditions, Bcl-2 is phosphorylated on Ser<sup>70</sup> during M-phase [80] by PKC [80;81] and ERK [82]. Phosphorylation of Ser<sup>70</sup> seems to be important for the anti-apoptotic function of the protein [80] whereas hyperphosphorylation on Thr<sup>69</sup> and Ser<sup>87</sup> was proposed to inactivate Bcl-2 [83] and abrogate its protective role by impairing its interaction with the pro-apoptotic protein Bax [84]. This theory, however, is discussed intensely since recently published data present evidence against a decrease of anti-apoptotic function by Bcl-2 hyperphosphorylation [85].

Hyperphosphorylation of Bcl-2 was shown to be induced by anticancer drugs, such as anti-mitotic agents [86] and some DNA damaging chemotherapeutics [87]. However, cephalostatin 1-induced Bcl-2 hyperphosphorylation occurs independent of a mitotic arrest or DNA-damage and is sufficient for the observed Bcl-2 inactivation. Compared to taxol, the degree of

hyperphosphorylation induced by cephalostatin 1 seemed to be lower corresponding to the lower sensitivity of Bcl-2 overexpressing cells towards cephalostatin 1. Interestingly, Jurkat T cells carrying mutated phosphorylation sites (Jurkat/*mbcl-2*) displayed a higher apoptosis rate after taxol treatment compared to cephalostatin 1. This observation may be explained by an additional inactivating mechanism of taxol, such as cleavage of Bcl-2 [88].

Several previous studies have focused on the signalling pathway leading to Bcl-2 hyperphosphorylation. Among the key enzymes responsible for Bcl-2 inactivation various kinases have been described (Raf-1 [89], PKA [90], ASK [91], JNK [83], ) depending on cell type and stimulus. Activated JNK has been implied in the hyperphosphorylation of Bcl-2 in response to numerous anti-mitotic agents such as taxol, *Vinca* alkaloids or cryptophycins [92]. In some settings, JNK activation but no Bcl-2 hyperphosphorylation was evident [93] or no causal link between JNK activation and Bcl-2 hyperphosphorylation could be proven [94]. In fact, PKA was favoured as the kinase exclusively responsible for Bcl-2 hyperphosphorylation [90]. Since the specific JNK inhibitor SP600125 strongly impaired cephalostatin 1-triggered Bcl-2 hyperphosphorylation, JNK acts as the crucial kinase upstream of Bcl-2.

How does cephalostatin 1 induce JNK activation and subsequent Bcl-2 hyperphosphorylation? JNK/SAPK (stress-activated protein kinase) activation is involved in the regulation of cell cycle progression at the transition from G<sub>1</sub>- to S-phase [95]. JNK also fulfils functions in the M-phase [83]. Beyond that, it is induced by diverse extracellular stimuli such as UV irradiation, pro-inflammatory cytokines, heat shock and numerous cytotoxic agents [96]. Among these, microtubuli-interfering agents (MIA) inducing an arrest in G<sub>2</sub>/M-phase activate JNK as major pro-apoptotic player [92]. JNK activation by MIAs was often linked to Bcl-2 hyperphosphorylation suggesting that an arrest in M-phase is a crucial factor in the signalling pathway leading to Bcl-2 inactivation and subsequent apoptosis [83;97;98]. Cephalostatin 1, however, does not arrest cells in G<sub>2</sub>/M-phase contradicting the view that an arrest in M-phase may be a prerequisite for JNK activation with a subsequent Bcl-2 hyperphosphorylation and inactivation.

---

JNK activation was also found in response to DNA damaging agents [99;100]. Some of them, such as platinum compounds and doxorubicin, were shown to induce Bcl-2 hyperphosphorylation [87]. So far, the pathway leading to Bcl-2 hyperphosphorylation in DNA damage-induced apoptosis has not been investigated but involvement of JNK is conceivable. Cephalostatin 1, however, does not induce DNA damage excluding this mechanism for JNK activation.

## **VI. SUMMARY AND OUTLOOK**

The present study provides insight into the cell death signalling pathway induced by cephalostatin 1, a marine bis-steroidal compound.

### **Cephalostatin 1 triggers apoptosis in human Jurkat T cells.**

Apoptosis was shown by the formation of apoptotic bodies, DNA fragmentation and phosphatidylserine exposure. Cephalostatin 1-induced apoptosis, which proceeds time- and dose-dependently, is dependent on caspases. ,

### **Cephalostatin 1-induced apoptosis follows a novel pathway that is characterised by selective Smac release from the mitochondria and caspase-9 activation without apoptosome formation.**

Signalling involving death receptors and subsequent components of the extrinsic pathway is not required. In contrast, mitochondria are affected as evident in the loss of the membrane potential. Unexpectedly, the mitochondrial matrix does not swell but appears condensed. Although neither cytochrome c nor AIF are released, Smac is selectively translocated into the cytosol where it binds to XIAP. Thus, XIAP previously bound to caspase-9 is displaced. Caspase-9 does not associate with Apaf-1 and is activated without requirement for apoptosome formation. However, caspase-9 contributes to but is not essential for cephalostatin 1-induced apoptosis.

### **Cephalostatin 1 triggers rapidly ER stress.**

ER stress is shown by upregulation of BiP and CHOP. Calpain is activated very early which might effect the observed activation of the ER-located caspase-12.

### **Cephalostatin 1 is able to counterregulate the anti-apoptotic effect of Bcl-2.**

Overexpression of Bcl-2 confers only partial protection against cephalostatin 1. Inactivation of Bcl-2 is brought about by hyperphosphorylation mediated by JNK. The signalling upstream of JNK does involve neither an arrest in G<sub>2</sub>/M-



## VII. APPENDIX

### 1. ABBREVIATIONS

Apaf-1	Apoptosis protein-activating factor 1
ADP	Adenosine diphosphate
AFC	Amino trifluoromethyl coumarin
AIF	Apoptosis inducing factor
ANT	Adenine nucleotide translocator
ANOVA	Analysis of variance between groups
APS	Ammonium persulfate
AT pair	Adenin – thymin pair
ATP	Adenosine triphosphate
BAP	B-cell antigen receptor-associated protein
Bcl	B-cell lymphoma
BH	Bcl-2 homology
BiP	Binding protein
BIR	Baculovirus IAP repeat
BSA	Bovine serum albumin
CAPS	Cyclohexylamino-1-propane sulfonic acid
CrmA	Cytokine responsive modifier A
CAD	Caspase-activated DNase
CARD	Caspase recruitment domain
CHAPS	3-[(3-Cholamidopropyl)dimethylammonio]-1-propanesulfonate
CHOP	C/EBP homologous protein
CLSM	Confocal laser scanning microscopy
DED	Death effector domain
DEV	Asp-Glu-Val-Asp
DFF	DNA fragmentation factor
DIABLO	Direkt IAP binding protein with a low isoelectric point
DISC	Death inducing signalling complex
DMSO	Dimethyl sulfoxide

---

DNA	Desoxyribonucleic acid
DR	Death receptor
DTT	Dithiothreitol
ECL	Enhanced chemoluminescence
EDTA	Ethylenediaminetetraacetic acid
EGTA	Ethylene glycol-bis(2-aminoethylether) tetraacetic acid
EndoG	Endonuclease G
ELISA	Enzyme-linked immunosorbent assay
ER	Endoplasmic reticulum
FACS	Fluorescence-activated cell sorter
FADD	Fas-associated death domain
FCS	Foetal calf serum
FITC	Fluorescein isothiocyanate
FL-1 / FL-2	Fluorescence channel 1 / 2
FSC	Forward scatter
GADD	Growth arrest and DNA damage
GI <sub>50</sub>	50 % growth inhibition
h	Hour
HEPES	N-(2-Hydroxyethyl)piperazine-N'-(2-ethanesulfonic acid)
HFS	Hypotonic fluorochrome solution
HPLC	High performance liquid chromatography
IAP	Inhibitor of apoptosis protein
IC <sub>50</sub>	Concentration required to achieve 50 % inhibition
ICAD	Inhibitor of caspase-activated DNase
IMM	Inner mitochondrial membrane
IMS	Intermembrane space
JNK	c-jun N-terminal kinase
M phase	Mitosis phase
MIA	Microtubuli-interfering agents
mRNA	Messenger RNA
MTT	3-(4,5-dimethylthiazol-2-yl)-2,5-diphenyl tetrazolium bromide
NCI	National Cancer Institute

---

OMM	Outer mitochondrial membrane
PAA	Polyacrylamide
PARP	Poly (ADP-ribose) polymerase
PBS	Phosphate-buffered saline
PI	Propidium iodide
PMSF	Phenylmethanesulfonylfluoride
PS	Phosphatidylserine
PTP	Permeability transition pore
PVDF	Polyvinylidene fluoride
QACXG	Gln-Ala-Cys-X-Gly
RPMI	Roswell Park Memorial Institute
RT	Room temperature
SCUBA	Self-contained underwater breathing apparatus
S phase	Synthesis phase
SDS	Sodium dodecyl sulfate
SDS-PAGE	Sodium dodecyl sulfate – polyacrylamide gel electrophoresis
SE	Standard error
Smac	Second mitochondria-derived activator of caspases
SSC	Sideward scatter
TBS-T	Tris-buffered saline with Tween-20
TEMED	N, N, N', N' tetramethylethylene diamine
TNF	Tumour necrosis factor
TRADD	Trail-associated death domain
TRAF2	TNF-receptor associated factor 2
TRAIL	TNF-receptor associated apoptosis inducing ligand
UPR	Unfolded protein response
UV	Ultraviolet
VDAC	Voltage-dependent anion channel
XIAP	X-linked inhibitor of apoptosis protein
zLEHDFmk	N-benzyloxycarbonyl-Leu-Glu(OMe)-His-Asp(OMe)- fluoromethylketone
zVADfmk	N-benzyloxycarbonyl-Val-Ala-Asp-fluoromethylketone

## 2. ALPHABETICAL LIST OF COMPANIES

Agfa	Köln, Germany
Amersham Biosciences	Freiburg, Germany
BD Pharmingen	Heidelberg, Germany
BD Transduction Laboratories	Heidelberg, Germany
Becton Dickinson	Heidelberg, Germany
Biometra	Göttingen, Germany
BioRad	München, Germany
Biozol	Eching, Germany
Calbiochem	Schwalbach, Germany
Cell Signaling	Frankfurt, Germany
Chemicon	Hofheim, Germany
Coulter	Krefeld, Germany
DakoCytomation GmbH	Hamburg, Germany
GraphPad Software, Inc.	San Diego, USA
Millipore	Bedford, USA
Molecular Probes	Eugene, USA
PAA Laboratories	Cölbe, Germany
PAN Biotech	Aidenbach, Germany
Roth	Karlsruhe, Germany
Sigma-Aldrich	München, Germany
SLT Labinstruments	Crailsheim, Germany
Tecan	Crailsheim, Germany
Trevigen Inc.	Gaithersburg, MD, USA
Upstate	Lake Placid, USA
Zeiss	Munich, Germany

### 3. PUBLICATIONS

#### 3.1 ABSTRACTS

I.M. Sönning, S.T. Eichhorst, G.R. Pettit, A.M. Vollmar, V.M. Dirsch  
Cephalostatin 1-induced apoptosis is characterized by selective mitochondrial release of Smac  
Naunyn-Schmiedeberg's Archive of Pharmacology, Vol. 367, Suppl. 1

I.M. Müller, G.R. Pettit, A.M. Vollmar, V.M. Dirsch  
Cephalostatin 1 induces Bcl-2 hyperphosphorylation without prior G<sub>2</sub>/M phase arrest  
Naunyn-Schmiedeberg's Archive of Pharmacology, Vol. 369, Suppl. 1

I.M. Müller, G.R. Pettit, A.M. Vollmar, V.M. Dirsch  
Cephalostatin 1 inaktiviert Bcl-2 unabhängig von einem M-Phasenarrest oder einer DNA-Schädigung  
Doktorandentagung der Deutschen Pharmazeutischen Gesellschaft  
Freudenstadt-Lauterbach, 2004

#### 3.2 ORIGINAL PUBLICATIONS

V.M. Dirsch, I.M. Müller, S.T. Eichhorst, G.R. Pettit, Y. Kamano, M. Inoue, J-P. Xu, Y. Ichihara, G. Wanner, A.M. Vollmar  
Cephalostatin 1 selectively triggers the release of Smac/DIABLO and subsequent apoptosis that is characterized by an increased density of the mitochondrial matrix  
Cancer Res. 2003, 63, 8869-8876

I.M. Müller, V.M. Dirsch, G.R. Pettit, A.M. Vollmar  
Cephalostatin 1 inactivates Bcl-2 by hyperphosphorylation independent of M-phase arrest and DNA damage  
J.Biol.Chem., submitted

## VIII. REFERENCES

1. **Schwartzmann,G., Ratain,M.J., Cragg,G.M., Wong,J.E., Saijo,N., Parkinson,D.R., Fujiwara,Y., Pazdur,R., Newman,D.J., Dagher,R., and Di Leone,L.,** Anticancer drug discovery and development throughout the world. *J.Clin.Oncol.* 2002. **20**: 47S-59S.
2. **Faulkner,D.J.,** Marine pharmacology. *Antonie Van Leeuwenhoek* 2000. **77**: 135-145.
3. **Haygood,M.G. and Davidson,S.K.,** Small-subunit rRNA genes and in situ hybridization with oligonucleotides specific for the bacterial symbionts in the larvae of the bryozoan *Bugula neritina* and proposal of "Candidatus endobugula sertula". *Appl.Environ.Microbiol.* 1997. **63**: 4612-4616.
4. **Harrigan,G.G., Yoshida,W.Y., Moore,R.E., Nagle,D.G., Park,P.U., Biggs,J., Paul,V.J., Mooberry,S.L., Corbett,T.H., and Valeriote,F.A.,** Isolation, structure determination, and biological activity of dolastatin 12 and lyngbyastatin 1 from *Lyngbya majuscula*/*Schizothrix calcicola* cyanobacterial assemblages. *J.Nat.Prod.* 1998. **61**: 1221-1225.
5. **Newman,D.J., Cragg,G.M., and Snader,K.M.,** Natural products as sources of new drugs over the period 1981-2002. *J.Nat.Prod.* 2003. **66**: 1022-1037.
6. **Mann,J.,** Natural products in cancer chemotherapy: past, present and future. *Nat.Rev.Cancer* 2002. **2**: 143-148.
7. **Grever,M.R., Schepartz,S.A., and Chabner,B.A.,** The National Cancer Institute: cancer drug discovery and development program. *Semin.Oncol.* 1992. **19**: 622-638.

8. **Monks,A., Scudiero,D.A., Johnson,G.S., Paull,K.D., and Sausville,E.A.**, The NCI anti-cancer drug screen: a smart screen to identify effectors of novel targets. *Anticancer Drug Des* 1997. **12**: 533-541.
9. *Anticancer Drug Discovery Guide: Preclinical Screening, Clinical Trials, and Approval*. Humana Press, Totawa, NJ, USA 1997.
10. **Pettit,G.R., Inoue,M., Kamano,Y., Herald,D.L., Arm,C., Dufresne,C., Christie,N.D., Schmidt,J.M., Doubek,K.L., and Krupa,T.S.**, Isolation and structure of powerful cell growth inhibitor cephalostatin 1. *J Am Chem Soc* 1988. **110**: 2006-2007.
11. **Pettit,G.R., Inoue,M., Kamano,Y., Dufresne,C., Christie,N.D., Niven,M.L., and Herald,D.L.**, Isolation and Structure of the Hemichordate Cell Growth Inhibitors Cephalostatins 2, 3 and 4. *J Chem Soc., Chem Comm* 1988. 865-867.
12. **Pettit,G.R., Xu,J., Williams,D.M., Christie,N.D., Doubek,D.L., and Schmidt,J.M.**, Isolation and structure of cephalostatins 10 and 11. *J Nat Prod* 1994. **57**: 52-63.
13. **Pettit,G.R., Xu,J.P., Schmidt,J.M., and Boyd,M.R.**, Isolation and structure of the exceptional Pterobranchia human cancer inhibitors cephalostatins 16 and 17. *Bioorganic & Medicinal Chemistry Letters* 1995. **5**: 2027-2032.
14. **Pettit,G.R., Kamano,Y., Dufresne,C., Inoue,M., Christie,N.D., Schmidt,J.M., and Doubek,D.L.**, Isolation and structure of the unusual Indian Ocean Cephalodiscus gilchristi components, cephalostatins 5 and 6. *Can J Chem* 1989. **67**: 1509-1513.

15. **Pettit,G.R., Kamano,Y., Inoue,M., Dufresne,C., Boyd,M.R., Herald,C.L., Schmidt,J.M., Doubek,D.L., and Christie,N.D.,** Antineoplastic Agents. 214. Isolation and Structure of Cephalostatins 7-9. *J Org Chem* 1992. **57**: 429-431.
16. **Pettit,G.R., Ichihara,Y., Xu,J., Boyd,M.R., and Williams,M.D.,** Isolation and structure of the symmetrical disteroidal alkaloids cephalostatin 12 and cephalostatin 13. *Bioorganic & Medicinal Chemistry Letters* 1994. **4**: 1507-1512.
17. **Pettit,G.R., Xu,J., Ichihara,Y., Williams,D.M., and Boyd,M.R.,** Antineoplastic agents 285. Isolation and structures of cephalostatins 14 and 15. *Can J Chem* 1994. **72**: 2260-2267.
18. **Pettit,G.R., Tan,R., Xu,J., Ichihara,Y., Williams,M.D., and Boyd,M.R.,** Antineoplastic agents. 398. Isolation and structure elucidation of cephalostatins 18 and 19. *J Nat Prod* 1998. **61**: 955-958.
19.   
<http://faculty.washington.edu/bjswalla/Hemichordata/Pterobranchia/cephalodiscus%20gracilis.html>. 11-2-2004.
20. **Barrington,E.J.W.,** *The biology of hemichordata and protochordata*. Oliver & Boyd, Edinburgh, London 1965.
21. **Harrison,F.W.,** *Microscopic anatomy of invertebrates*. Wiley-Liss, New York 1997.
22. **Cameron,C.B., Garey,J.R., and Swalla,B.J.,** Evolution of the chordate body plan: new insights from phylogenetic analyses of deuterostome phyla. *Proc.Natl.Acad.Sci.U.S.A* 2000. **97**: 4469-4474.

23. **LaCour,T.G., Guo,C., Ma,S., Jeong,J.U., Boyd,M.R., Matsunaga,S., Fusetani,N., and Fuchs,P.L.**, On topography and functionality in the B-D rings of cephalostatin cytotoxins. *Bioorg.Med.Chem.Lett.* 1999. **9**: 2587-2592.
24. **Pettit,G.R.**, *Pure & Appl.Chem.* 1994. **66**: 2271.
25. **Kerr,J.F., Wyllie,A.H., and Currie,A.R.**, Apoptosis: a basic biological phenomenon with wide-ranging implications in tissue kinetics. *Br.J Cancer* 1972. **26**: 239-257.
26. **Fadok,V.A., Voelker,D.R., Campbell,P.A., Cohen,J.J., Bratton,D.L., and Henson,P.M.**, Exposure of phosphatidylserine on the surface of apoptotic lymphocytes triggers specific recognition and removal by macrophages. *J.Immunol.* 1992. **148**: 2207-2216.
27. **Verhoven,B., Schlegel,R.A., and Williamson,P.**, Mechanisms of phosphatidylserine exposure, a phagocyte recognition signal, on apoptotic T lymphocytes. *J.Exp.Med.* 1995. **182**: 1597-1601.
28. **Ellis,H.M. and Horvitz,H.R.**, Genetic control of programmed cell death in the nematode *C. elegans*. *Cell* 1986. **44**: 817-829.
29. **Sanders,E.J. and Wride,M.A.**, Programmed cell death in development. *Int.Rev.Cytol.* 1995. **163**: 105-173.
30. **Kanduc,D., Mittelman,A., Serpico,R., Sinigaglia,E., Sinha,A.A., Natale,C., Santacroce,R., Di Corcia,M.G., Lucchese,A., Dini,L., Pani,P., Santacroce,S., Simone,S., Bucci,R., and Farber,E.**, Cell death: apoptosis versus necrosis (review). *Int.J Oncol.* 2002. **21**: 165-170.

31. **Van Cruchten,S. and Van Den,B.W.**, Morphological and biochemical aspects of apoptosis, oncosis and necrosis. *Anat.Histol.Embryol.* 2002. **31**: 214-223.
32. **Zeiss,C.J.**, The apoptosis-necrosis continuum: insights from genetically altered mice. *Vet.Pathol.* 2003. **40**: 481-495.
33. **Vaux,D.L. and Korsmeyer,S.J.**, Cell death in development. *Cell* 1999. **96**: 245-254.
34. **Jameson,S.C., Hogquist,K.A., and Bevan,M.J.**, Positive selection of thymocytes. *Annu.Rev.Immunol.* 1995. **13**: 93-126.
35. **Ashton-Rickardt,P.G. and Tonegawa,S.**, A differential-avidity model for T-cell selection. *Immunol.Today* 1994. **15**: 362-366.
36. **Kerr,J.F., Gobe,G.C., Winterford,C.M., and Harmon,B.V.**, Anatomical methods in cell death. *Methods Cell Biol.* 1995. **46**: 1-27.
37. **Thornberry,N.A., Rano,T.A., Peterson,E.P., Rasper,D.M., Timkey,T., Garcia-Calvo,M., Houtzager,V.M., Nordstrom,P.A., Roy,S., Vaillancourt,J.P., Chapman,K.T., and Nicholson,D.W.**, A combinatorial approach defines specificities of members of the caspase family and granzyme B. Functional relationships established for key mediators of apoptosis. *J.Biol.Chem.* 1997. **272**: 17907-17911.
38. **Earnshaw,W.C., Martins,L.M., and Kaufmann,S.H.**, Mammalian caspases: structure, activation, substrates, and functions during apoptosis. *Annu.Rev.Biochem.* 1999. **68**: 383-424.
39. **Wolf,B.B. and Green,D.R.**, Suicidal tendencies: apoptotic cell death by caspase family proteinases. *J.Biol.Chem.* 1999. **274**: 20049-20052.

40. **Degterev,A., Boyce,M., and Yuan,J.**, A decade of caspases. *Oncogene* 2003. **22**: 8543-8567.
41. **Salvesen,G.S. and Dixit,V.M.**, Caspase activation: the induced-proximity model. *Proc.Natl.Acad.Sci.U.S.A* 1999. **96**: 10964-10967.
42. **Cohen,G.M.**, Caspases: the executioners of apoptosis. *Biochem.J* 1997. **326 ( Pt 1)**: 1-16.
43. **Levkau,B., Koyama,H., Raines,E.W., Clurman,B.E., Herren,B., Orth,K., Roberts,J.M., and Ross,R.**, Cleavage of p21Cip1/Waf1 and p27Kip1 mediates apoptosis in endothelial cells through activation of Cdk2: role of a caspase cascade. *Mol.Cell* 1998. **1**: 553-563.
44. **Cheng,E.H., Kirsch,D.G., Clem,R.J., Ravi,R., Kastan,M.B., Bedi,A., Ueno,K., and Hardwick,J.M.**, Conversion of Bcl-2 to a Bax-like death effector by caspases. *Science* 1997. **278**: 1966-1968.
45. **Clem,R.J., Cheng,E.H.Y., Karp,C.L., Kirsch,D.G., Ueno,K., Takahashi,A., Kastan,M.B., Griffin,D.E., Earnshaw,W.C., Velicuona,M.A., and Hardwick,J.M.**, Modulation of cell death by Bcl-xL through caspaseáinteraction. *PNAS* 1998. **95**: 554-559.
46. **Thornberry,N.A. and Lazebnik,Y.**, Caspases: enemies within. *Science* 1998. **281**: 1312-1316.
47. **Zhou,Q. and Salvesen,G.S.**, Viral caspase inhibitors CrmA and p35. *Methods Enzymol.* 2000. **322**: 143-154.
48. **Xue,D. and Horvitz,H.R.**, Inhibition of the *Caenorhabditis elegans* cell-death protease CED-3 by a CED-3 cleavage site in baculovirus p35 protein. *Nature* 1995. **377**: 248-251.

49. **Deveraux,Q.L., Roy,N., Stennicke,H.R., Van Arsdale,T., Zhou,Q., Srinivasula,S.M., Alnemri,E.S., Salvesen,G.S., and Reed,J.C.,** IAPs block apoptotic events induced by caspase-8 and cytochrome c by direct inhibition of distinct caspases. *EMBO J.* 1998. **17**: 2215-2223.
50. **Takahashi,R., Deveraux,Q., Tamm,I., Welsh,K., Assa-Munt,N., Salvesen,G.S., and Reed,J.C.,** A single BIR domain of XIAP sufficient for inhibiting caspases. *J.Biol.Chem.* 1998. **273**: 7787-7790.
51. **Sartorius,U., Schmitz,I., and Krammer,P.H.,** Molecular mechanisms of death-receptor-mediated apoptosis. *Chembiochem.* 2001. **2**: 20-29.
52. **Wang,S. and el Deiry,W.S.,** TRAIL and apoptosis induction by TNF-family death receptors. *Oncogene* 2003. **22**: 8628-8633.
53. **Ashkenazi,A. and Dixit,V.M.,** Death receptors: signaling and modulation. *Science* 1998. **281**: 1305-1308.
54. **Gupta,S.,** Molecular steps of death receptor and mitochondrial pathways of apoptosis. *Life Sci.* 2001. **69**: 2957-2964.
55. **Alberts,B., Bray, D., Lewis, J., Raff, M., Roberts, K., and Watson, J. D.,** *Molecular Biology of the Cell.* Garland Publishing Inc., New York 2002.
56. **Wang,X.,** The expanding role of mitochondria in apoptosis. *Genes Dev.* 2001. **15**: 2922-2933.
57. **Bratton,S.B., MacFarlane,M., Cain,K., and Cohen,G.M.,** Protein complexes activate distinct caspase cascades in death receptor and stress-induced apoptosis. *Exp.Cell Res.* 2000. **256**: 27-33.

58. **van Gurp,M., Festjens,N., van Loo,G., Saelens,X., and Vandenamee,P.**, Mitochondrial intermembrane proteins in cell death. *Biochem.Biophys.Res.Comm.* 2003. **304**: 487-497.
59. **Coultas,L. and Strasser,A.**, The role of the Bcl-2 protein family in cancer. *Semin.Cancer Biol.* 2003. **13**: 115-123.
60. **Kaufmann,S.H. and Hengartner,M.O.**, Programmed cell death: alive and well in the new millennium. *Trends Cell Biol.* 2001. **11**: 526-534.
61. **Shimizu,S., Narita,M., and Tsujimoto,Y.**, Bcl-2 family proteins regulate the release of apoptogenic cytochrome c by the mitochondrial channel VDAC. *Nature* 1999. **399**: 483-487.
62. **Marzo,I., Brenner,C., Zamzami,N., Jurgensmeier,J.M., Susin,S.A., Vieira,H.L., Prevost,M.C., Xie,Z., Matsuyama,S., Reed,J.C., and Kroemer,G.**, Bax and adenine nucleotide translocator cooperate in the mitochondrial control of apoptosis. *Science* 1998. **281**: 2027-2031.
63. **Shi,Y., Chen,J., Weng,C., Chen,R., Zheng,Y., Chen,Q., and Tang,H.**, Identification of the protein-protein contact site and interaction mode of human VDAC1 with Bcl-2 family proteins. *Biochem.Biophys.Res.Comm.* 2003. **305**: 989-996.
64. **Cory,S., Huang,D.C., and Adams,J.M.**, The Bcl-2 family: roles in cell survival and oncogenesis. *Oncogene* 2003. **22**: 8590-8607.
65. **Verhagen,A.M. and Vaux,D.L.**, Cell death regulation by the mammalian IAP antagonist Diablo/Smac. *Apoptosis*. 2002. **7**: 163-166.
66. **Wu,G., Chai,J., Suber,T.L., Wu,J.W., Du,C., Wang,X., and Shi,Y.**, Structural basis of IAP recognition by Smac/DIABLO. *Nature* 2000. **408**: 1008-1012.

67. **Okada,H., Suh,W.K., Jin,J., Woo,M., Du,C., Elia,A., Duncan,G.S., Wakeham,A., Itie,A., Lowe,S.W., Wang,X., and Mak,T.W.,** Generation and characterization of Smac/DIABLO-deficient mice. *Mol.Cell Biol.* 2002. **22**: 3509-3517.
68. **Roberts,D.L., Merrison,W., MacFarlane,M., and Cohen,G.M.,** The inhibitor of apoptosis protein-binding domain of Smac is not essential for its proapoptotic activity. *J.Cell Biol.* 2001. **153**: 221-228.
69. **Vaux,D.L. and Silke,J.,** Mammalian mitochondrial IAP binding proteins. *Biochem.Biophys.Res.Comm.* 2003. **304**: 499-504.
70. **Kaufman,R.J.,** Stress signaling from the lumen of the endoplasmic reticulum: coordination of gene transcriptional and translational controls. *Genes Dev.* 1999. **13**: 1211-1233.
71. **Breckenridge,D.G., Germain,M., Mathai,J.P., Nguyen,M., and Shore,G.C.,** Regulation of apoptosis by endoplasmic reticulum pathways. *Oncogene* 2003. **22**: 8608-8618.
72. **Oyadomari,S., Araki,E., and Mori,M.,** Endoplasmic reticulum stress-mediated apoptosis in pancreatic beta-cells. *Apoptosis.* 2002. **7**: 335-345.
73. **Ishii,H., Suzuki,Y., Kuboki,M., Morikawa,M., Inoue,M., and Kazama,M.,** Activation of calpain I in thrombin-stimulated platelets is regulated by the initial elevation of the cytosolic Ca<sup>2+</sup> concentration. *Biochem.J* 1992. **284 ( Pt 3)**: 755-760.
74. **Rizzuto,R., Pinton,P., Ferrari,D., Chami,M., Szabadkai,G., Magalhaes,P.J., Di Virgilio,F., and Pozzan,T.,** Calcium and apoptosis: facts and hypotheses. *Oncogene* 2003. **22**: 8619-8627.

75. **Nakagawa,T., Zhu,H., Morishima,N., Li,E., Xu,J., Yankner,B.A., and Yuan,J.,** Caspase-12 mediates endoplasmic-reticulum-specific apoptosis and cytotoxicity by amyloid-beta. *Nature* 2000. **403**: 98-103.
76. **Nakagawa,T. and Yuan,J.,** Cross-talk between two cysteine protease families. Activation of caspase-12 by calpain in apoptosis. *J Cell Biol.* 2000. **150**: 887-894.
77. **Yoneda,T., Imaizumi,K., Oono,K., Yui,D., Gomi,F., Katayama,T., and Tohyama,M.,** Activation of caspase-12, an endoplasmic reticulum (ER) resident caspase, through tumor necrosis factor receptor-associated factor 2-dependent mechanism in response to the ER stress. *J.Biol.Chem.* 2001. **276**: 13935-13940.
78. **Rao,R.V., Hermel,E., Castro-Obregon,S., del Rio,G., Ellerby,L.M., Ellerby,H.M., and Bredesen,D.E.,** Coupling endoplasmic reticulum stress to the cell death program. Mechanism of caspase activation. *J.Biol.Chem.* 2001. **276**: 33869-33874.
79. **Morishima,N., Nakanishi,K., Takenouchi,H., Shibata,T., and Yasuhiko,Y.,** An endoplasmic reticulum stress-specific caspase cascade in apoptosis. Cytochrome c-independent activation of caspase-9 by caspase-12. *J.Biol.Chem.* 2002. **277**: 34287-34294.
80. **Breckenridge,D.G., Nguyen,M., Kuppig,S., Reth,M., and Shore,G.C.,** The procaspase-8 isoform, procaspase-8L, recruited to the BAP31 complex at the endoplasmic reticulum. *Proc.Natl.Acad.Sci.U.S.A* 2002. **99**: 4331-4336.
81. **Thomenius,M.J. and Distelhorst,C.W.,** Bcl-2 on the endoplasmic reticulum: protecting the mitochondria from a distance. *J.Cell Sci.* 2003. **116**: 4493-4499.

82. **Mathai,J.P., Germain,M., Marcellus,R.C., and Shore,G.C.,** Induction and endoplasmic reticulum location of BIK/NBK in response to apoptotic signaling by E1A and p53. *Oncogene* 2002. **21**: 2534-2544.
  
83. **Walczak,H., Bouchon,A., Stahl,H., and Krammer,P.H.,** Tumor necrosis factor-related apoptosis-inducing ligand retains its apoptosis-inducing capacity on Bcl-2- or Bcl-xL-overexpressing chemotherapy-resistant tumor cells. *Cancer Res.* 2000. **60**: 3051-3057.
  
84. **Peter,M.E., Dhein,J., Ehret,A., Hellbardt,S., Walczak,H., Moldenhauer,G., and Krammer,P.H.,** APO-1 (CD95)-dependent and -independent antigen receptor-induced apoptosis in human T and B cell lines. *Int.Immunol.* 1995. **7**: 1873-1877.
  
85. **Yamamoto,K., Ichijo,H., and Korsmeyer,S.J.,** BCL-2 is phosphorylated and inactivated by an ASK1/Jun N-terminal protein kinase pathway normally activated at G(2)/M. *Mol.Cell Biol.* 1999. **19**: 8469-8478.
  
86. **Nicoletti,I., Migliorati,G., Pagliacci,M.C., Grignani,F., and Riccardi,C.,** A rapid and simple method for measuring thymocyte apoptosis by propidium iodide staining and flow cytometry. *J.Immunol.Methods* 1991. **139**: 271-279.
  
87. **Mosmann,T.,** Rapid colorimetric assay for cellular growth and survival: application to proliferation and cytotoxicity assays. *J.Immunol.Methods* 1983. **65**: 55-63.
  
88. **Vermes,I., Haanen,C., Steffens-Nakken,H., and Reutelingsperger,C.,** A novel assay for apoptosis. Flow cytometric detection of phosphatidylserine expression on early apoptotic cells using fluorescein labelled Annexin V. *J.Immunol.Methods* 1995. **184**: 39-51.

89. **Smiley,S.T., Reers,M., Mottola-Hartshorn,C., Lin,M., Chen,A., Smith,T.W., Steele,G.D., Jr., and Chen,L.B.,** Intracellular heterogeneity in mitochondrial membrane potentials revealed by a J-aggregate-forming lipophilic cation JC-1. *Proc.Natl.Acad.Sci.U.S.A* 1991. **88**: 3671-3675.
90. **Cossarizza,A., Ceccarelli,D., and Masini,A.,** Functional heterogeneity of an isolated mitochondrial population revealed by cytofluorometric analysis at the single organelle level. *Exp.Cell Res.* 1996. **222**: 84-94.
91. **Lydon,M.J., Keeler,K.D., and Thomas,D.B.,** Vital DNA staining and cell sorting by flow microfluorometry. *J.Cell Physiol* 1980. **102**: 175-181.
92. **Leist,M., Volbracht,C., Fava,E., and Nicotera,P.,** 1-Methyl-4-phenylpyridinium induces autocrine excitotoxicity, protease activation, and neuronal apoptosis. *Mol.Pharmacol.* 1998. **54**: 789-801.
93. **Bradford,M.M.,** A rapid and sensitive method for the quantitation of microgram quantities of protein utilizing the principle of protein-dye binding. *Anal.Biochem.* 1976. **72**: 248-254.
94. **Laemmli,U.K.,** Cleavage of structural proteins during the assembly of the head of bacteriophage T4. *Nature* 1970. **227**: 680-685.
95. **Sakahira,H., Enari,M., and Nagata,S.,** Cleavage of CAD inhibitor in CAD activation and DNA degradation during apoptosis. *Nature* 1998. **391**: 96-99.
96. **Mathiasen,I.S., Sergeev,I.N., Bastholm,L., Elling,F., Norman,A.W., and Jaattela,M.,** Calcium and calpain as key mediators of apoptosis-like death induced by vitamin D compounds in breast cancer cells. *J.Biol.Chem.* 2002.

97. **Bidere,N. and Senik,A.**, Caspase-independent apoptotic pathways in T lymphocytes: a minireview. *Apoptosis*. 2001. **6**: 371-375.
98. **Arimura,T., Kojima-Yuasa,A., Suzuki,M., Kennedy,D.O., and Matsui-Yuasa,I.**, Caspase-independent apoptosis induced by evening primrose extract in Ehrlich ascites tumor cells. *Cancer Lett.* 2003. **201**: 9-16.
99. **Slee,E.A., Adrain,C., and Martin,S.J.**, Serial killers: ordering caspase activation events in apoptosis. *Cell Death.Differ.* 1999. **6**: 1067-1074.
100. **Scarlett,J.L., Sheard,P.W., Hughes,G., Ledgerwood,E.C., Ku,H.H., and Murphy,M.P.**, Changes in mitochondrial membrane potential during staurosporine-induced apoptosis in Jurkat cells. *FEBS Lett.* 2000. **475**: 267-272.
101. **Lorz,C., Justo,P., Sanz,A., Subira,D., Egido,J., and Ortiz,A.**, Paracetamol-Induced Renal Tubular Injury: A Role for ER Stress. *J.Am.Soc.Nephrol.* 2004. **15**: 380-389.
102. **McDonnell,M.A., Wang,D., Khan,S.M., Vander Heiden,M.G., and Kelekar,A.**, Caspase-9 is activated in a cytochrome c-independent manner early during TNFalpha-induced apoptosis in murine cells. *Cell Death.Differ.* 2003. **10**: 1005-1015.
103. **Rao,R.V., Castro-Obregon,S., Frankowski,H., Schuler,M., Stoka,V., del Rio,G., Bredesen,D.E., and Ellerby,H.M.**, Coupling Endoplasmic Reticulum Stress to the Cell Death Program. AN Apaf-1-INDEPENDENT INTRINSIC PATHWAY. *J.Biol.Chem.* 2002. **277**: 21836-21842.

104. **Kaufmann,S.H. and Vaux,D.L.**, Alterations in the apoptotic machinery and their potential role in anticancer drug resistance. *Oncogene* 2003. **22**: 7414-7430.
105. **Saleem,A., Datta,R., Yuan,Z.M., Kharbanda,S., and Kufe,D.**, Involvement of stress-activated protein kinase in the cellular response to 1-beta-D-arabinofuranosylcytosine and other DNA-damaging agents. *Cell Growth Differ.* 1995. **6**: 1651-1658.
106. **Pratesi,G., Polizzi,D., Perego,P., Dal Bo,L., and Zunino,F.**, Bcl-2 phosphorylation in a human breast carcinoma xenograft: a common event in response to effective DNA-damaging drugs. *Biochem.Pharmacol.* 2000. **60**: 77-82.
107. **Duksin,D. and Mahoney,W.C.**, Relationship of the structure and biological activity of the natural homologues of tunicamycin. *J.Biol.Chem.* 1982. **257**: 3105-3109.
108. **Goll,D.E., Thompson,V.F., Li,H., Wei,W., and Cong,J.**, The calpain system. *Physiol Rev.* 2003. **83**: 731-801.
109. **Bao,J.J., Le,X.F., Wang,R.Y., Yuan,J., Wang,L., Atkinson,E.N., LaPushin,R., Andreeff,M., Fang,B., Yu,Y., and Bast,R.C., Jr.**, Reexpression of the tumor suppressor gene ARHI induces apoptosis in ovarian and breast cancer cells through a caspase-independent calpain-dependent pathway. *Cancer Res.* 2002. **62**: 7264-7272.
110. **Broker,L.E., Huisman,C., Span,S.W., Rodriguez,J.A., Kruyt,F.A., and Giaccone,G.**, Cathepsin B mediates caspase-independent cell death induced by microtubule stabilizing agents in non-small cell lung cancer cells. *Cancer Res.* 2004. **64**: 27-30.

111. **Takuma,K., Kiriu,M., Mori,K., Lee,E., Enomoto,R., Baba,A., and Matsuda,T.,** Roles of cathepsins in reperfusion-induced apoptosis in cultured astrocytes. *Neurochem.Int.* 2003. **42**: 153-159.
112. **Lambert,C., Apel,K., Biesalski,H.K., and Frank,J.,** 2-methoxyestradiol induces caspase-independent, mitochondria-centered apoptosis in DS-sarcoma cells. *Int.J.Cancer* 2004. **108**: 493-501.
113. **Liu,T., Brouha,B., and Grossman,D.,** Rapid induction of mitochondrial events and caspase-independent apoptosis in Survivin-targeted melanoma cells. *Oncogene* 2004. **23**: 39-48.
114. **Shih,C.M., Ko,W.C., Wu,J.S., Wei,Y.H., Wang,L.F., Chang,E.E., Lo,T.Y., Cheng,H.H., and Chen,C.T.,** Mediating of caspase-independent apoptosis by cadmium through the mitochondria-ROS pathway in MRC-5 fibroblasts. *J.Cell Biochem.* 2004. **91**: 384-397.
115. **Murahashi,H., Azuma,H., Zamzami,N., Furuya,K.J., Ikebuchi,K., Yamaguchi,M., Yamada,Y., Sato,N., Fujihara,M., Kroemer,G., and Ikeda,H.,** Possible contribution of apoptosis-inducing factor (AIF) and reactive oxygen species (ROS) to UVB-induced caspase-independent cell death in the T cell line Jurkat. *J.Leukoc.Biol.* 2003. **73**: 399-406.
116. **Alonso,M., Tamasdan,C., Miller,D.C., and Newcomb,E.W.,** Flavopiridol induces apoptosis in glioma cell lines independent of retinoblastoma and p53 tumor suppressor pathway alterations by a caspase-independent pathway. *Mol.Cancer Ther.* 2003. **2**: 139-150.
117. **Boya,P., Gonzalez-Polo,R.A., Poncet,D., Andreau,K., Vieira,H.L., Roumier,T., Perfettini,J.L., and Kroemer,G.,** Mitochondrial membrane permeabilization is a critical step of lysosome-initiated apoptosis induced by hydroxychloroquine. *Oncogene* 2003. **22**: 3927-3936.

118. **Selznick,L.A., Zheng,T.S., Flavell,R.A., Rakic,P., and Roth,K.A.,** Amyloid beta-induced neuronal death is bax-dependent but caspase-independent. *J.Neuropathol.Exp.Neurol.* 2000. **59**: 271-279.
119. **Perfettini,J.L., Reed,J.C., Israel,N., Martinou,J.C., Dautry-Varsat,A., and Ojcius,D.M.,** Role of Bcl-2 family members in caspase-independent apoptosis during Chlamydia infection. *Infect.Immun.* 2002. **70**: 55-61.
120. **Kaufmann,S.H. and Earnshaw,W.C.,** Induction of apoptosis by cancer chemotherapy. *Exp.Cell Res* 2000. **256**: 42-49.
121. **Slee,E.A., Harte,M.T., Kluck,R.M., Wolf,B.B., Casiano,C.A., Newmeyer,D.D., Wang,H.G., Reed,J.C., Nicholson,D.W., Alnemri,E.S., Green,D.R., and Martin,S.J.,** Ordering the cytochrome c-initiated caspase cascade: hierarchical activation of caspases-2, -3, -6, -7, -8, and -10 in a caspase-9-dependent manner. *J.Cell Biol.* 1999. **144**: 281-292.
122. **Wesselborg,S., Engels,I.H., Rossmann,E., Los,M., and Schulze-Osthoff,K.,** Anticancer drugs induce caspase-8/FLICE activation and apoptosis in the absence of CD95 receptor/ligand interaction. *Blood* 1999. **93**: 3053-3063.
123. **Zamzami,N. and Kroemer,G.,** The mitochondrion in apoptosis: how Pandora's box opens. *Nat.Rev.Mol.Cell Biol.* 2001. **2**: 67-71.
124. **Wei,M.C., Lindsten,T., Mootha,V.K., Weiler,S., Gross,A., Ashiya,M., Thompson,C.B., and Korsmeyer,S.J.,** tBID, a membrane-targeted death ligand, oligomerizes BAK to release cytochrome c. *Genes Dev.* 2000. **14**: 2060-2071.

125. **Eskes,R., Desagher,S., Antonsson,B., and Martinou,J.C.,** Bid induces the oligomerization and insertion of Bax into the outer mitochondrial membrane. *Mol.Cell Biol.* 2000. **20**: 929-935.
126. **He,L. and Lemasters,J.J.,** Regulated and unregulated mitochondrial permeability transition pores: a new paradigm of pore structure and function? *FEBS Lett.* 2002. **512**: 1-7.
127. **Gottlieb,E., Armour,S.M., Harris,M.H., and Thompson,C.B.,** Mitochondrial membrane potential regulates matrix configuration and cytochrome c release during apoptosis. *Cell Death.Differ.* 2003. **10**: 709-717.
128. **Du,C., Fang,M., Li,Y., Li,L., and Wang,X.,** Smac, a mitochondrial protein that promotes cytochrome c-dependent caspase activation by eliminating IAP inhibition. *Cell* 2000. **102**: 33-42.
129. **Adrain,C., Creagh,E.M., and Martin,S.J.,** Apoptosis-associated release of Smac/DIABLO from mitochondria requires active caspases and is blocked by Bcl-2. *EMBO J.* 2001. **20**: 6627-6636.
130. **Chauhan,D., Li,G., Hideshima,T., Podar,K., Mitsiades,C., Mitsiades,N., Munshi,N., Kharbanda,S., and Anderson,K.C.,** JNK-dependent Release of Mitochondrial Protein, Smac, during Apoptosis in Multiple Myeloma (MM) Cells. *J.Biol.Chem.* 2003. **278**: 17593-17596.
131. **Deng,Y., Ren,X., Yang,L., Lin,Y., and Wu,X.,** A JNK-dependent pathway is required for TNFalpha-induced apoptosis. *Cell* 2003. **115**: 61-70.

132. **Chauhan,D., Hideshima,T., Rosen,S., Reed,J.C., Kharbanda,S., and Anderson,K.C.,** Apaf-1/cytochrome c-independent and Smac-dependent induction of apoptosis in multiple myeloma (MM) cells. *J.Biol.Chem.* 2001. **276**: 24453-24456.
133. **McNeish,I.A., Bell,S., McKay,T., Tenev,T., Marani,M., and Lemoine,N.R.,** Expression of Smac/DIABLO in ovarian carcinoma cells induces apoptosis via a caspase-9-mediated pathway. *Exp.Cell Res.* 2003. **286**: 186-198.
134. **Rodriguez,J. and Lazebnik,Y.,** Caspase-9 and APAF-1 form an active holoenzyme. *Genes Dev.* 1999. **13**: 3179-3184.
135. **Riedl,S.J., Renatus,M., Schwarzenbacher,R., Zhou,Q., Sun,C., Fesik,S.W., Liddington,R.C., and Salvesen,G.S.,** Structural basis for the inhibition of caspase-3 by XIAP. *Cell* 2001. **104**: 791-800.
136. **Chai,J., Shiozaki,E., Srinivasula,S.M., Wu,Q., Datta,P., Alnemri,E.S., Shi,Y., and Dataa,P.,** Structural basis of caspase-7 inhibition by XIAP. *Cell* 2001. **104**: 769-780.
137. **Sun,X.M., Bratton,S.B., Butterworth,M., MacFarlane,M., and Cohen,G.M.,** Bcl-2 and Bcl-xL inhibit CD95-mediated apoptosis by preventing mitochondrial release of Smac/DIABLO and subsequent inactivation of X-linked inhibitor-of-apoptosis protein. *J.Biol.Chem.* 2002. **277**: 11345-11351.
138. **Deng,Y., Lin,Y., and Wu,X.,** TRAIL-induced apoptosis requires Bax-dependent mitochondrial release of Smac/DIABLO. *Genes Dev.* 2002. **16**: 33-45.

139. **Akao,Y., Otsuki,Y., Kataoka,S., Ito,Y., and Tsujimoto,Y.,** Multiple subcellular localization of bcl-2: detection in nuclear outer membrane, endoplasmic reticulum membrane, and mitochondrial membranes. *Cancer Res.* 1994. **54**: 2468-2471.
140. **Ng,F.W. and Shore,G.C.,** Bcl-XL cooperatively associates with the Bap31 complex in the endoplasmic reticulum, dependent on procaspase-8 and Ced-4 adaptor. *J.Biol.Chem.* 1998. **273**: 3140-3143.
141. **Germain,M., Mathai,J.P., and Shore,G.C.,** BH-3-only BIK functions at the endoplasmic reticulum to stimulate cytochrome c release from mitochondria. *J.Biol.Chem.* 2002. **277**: 18053-18060.
142. **Mund,T., Gewies,A., Schoenfeld,N., Bauer,M.K., and Grimm,S.,** Spike, a novel BH3-only protein, regulates apoptosis at the endoplasmic reticulum. *FASEB J.* 2003. **17**: 696-698.
143. **Zong,W.X., Li,C., Hatzivassiliou,G., Lindsten,T., Yu,Q.C., Yuan,J., and Thompson,C.B.,** Bax and Bak can localize to the endoplasmic reticulum to initiate apoptosis. *J.Cell Biol.* 2003. **162**: 59-69.
144. **Wertz,I.E. and Dixit,V.M.,** Characterization of calcium release-activated apoptosis of LNCaP prostate cancer cells. *J.Biol.Chem.* 2000. **275**: 11470-11477.
145. **Pan,Z., Damron,D., Nieminen,A.L., Bhat,M.B., and Ma,J.,** Depletion of intracellular Ca<sup>2+</sup> by caffeine and ryanodine induces apoptosis of chinese hamster ovary cells transfected with ryanodine receptor. *J.Biol.Chem.* 2000. **275**: 19978-19984.
146. **Tagliarino,C., Pink,J.J., Dubyak,G.R., Nieminen,A.L., and Boothman,D.A.,** Calcium is a key signaling molecule in beta-lapachone-mediated cell death. *J.Biol.Chem.* 2001. **276**: 19150-19159.

147. **Kaneko,Y. and Tsukamoto,A.**, Thapsigargin-induced persistent intracellular calcium pool depletion and apoptosis in human hepatoma cells. *Cancer Lett.* 1994. **79**: 147-155.
148. **Csordas,G. and Hajnoczky,G.**, Sorting of calcium signals at the junctions of endoplasmic reticulum and mitochondria. *Cell Calcium* 2001. **29**: 249-262.
149. **Hacki,J., Egger,L., Monney,L., Conus,S., Rosse,T., Fellay,I., and Borner,C.**, Apoptotic crosstalk between the endoplasmic reticulum and mitochondria controlled by Bcl-2. *Oncogene* 2000. **19**: 2286-2295.
150. **Lu,T., Xu,Y., Mericle,M.T., and Mellgren,R.L.**, Participation of the conventional calpains in apoptosis. *Biochim.Biophys.Acta* 2002. **1590**: 16-26.
151. **Tinhofer,I., Anether,G., Senfter,M., Pfaller,K., Bernhard,D., Hara,M., and Greil,R.**, Stressful death of T-ALL tumor cells following treatment with the antitumor agent Tetrocarcin-A. *FASEB J.* 2002.
152. **Reddy,R.K., Mao,C., Baumeister,P., Austin,R.C., Kaufman,R.J., and Lee,A.S.**, Endoplasmic reticulum chaperone protein GRP78 protects cells from apoptosis induced by topoisomerase inhibitors: role of ATP binding site in suppression of caspase-7 activation. *J.Biol.Chem.* 2003. **278**: 20915-20924.
153. **Mouw,G., Zechel,J.L., Gamboa,J., Lust,W.D., Selman,W.R., and Ratcheson,R.A.**, Activation of caspase-12, an endoplasmic reticulum resident caspase, after permanent focal ischemia in rat. *Neuroreport* 2003. **14**: 183-186.

154. **Hayashi,T., Saito,A., Okuno,S., Ferrand-Drake,M., Dodd,R.L., Nishi,T., Maier,C.M., Kinouchi,H., and Chan,P.H.,** Oxidative damage to the endoplasmic reticulum is implicated in ischemic neuronal cell death. *J.Cereb.Blood Flow Metab* 2003. **23**: 1117-1128.
155. **Wang,H.G., Pathan,N., Ethell,I.M., Krajewski,S., Yamaguchi,Y., Shibasaki,F., McKeon,F., Bobo,T., Franke,T.F., and Reed,J.C.,** Ca<sup>2+</sup>-induced apoptosis through calcineurin dephosphorylation of BAD. *Science* 1999. **284**: 339-343.
156. **Hajnoczky,G., Csordas,G., Madesh,M., and Pacher,P.,** Control of apoptosis by IP(3) and ryanodine receptor driven calcium signals. *Cell Calcium* 2000. **28**: 349-363.
157. **Breckenridge,D.G., Stojanovic,M., Marcellus,R.C., and Shore,G.C.,** Caspase cleavage product of BAP31 induces mitochondrial fission through endoplasmic reticulum calcium signals, enhancing cytochrome c release to the cytosol. *J.Cell Biol.* 2003. **160**: 1115-1127.
158. **Tyagi,D., Sharma,B.S., Gupta,S.K., Kaul,D., Vasishta,R.K., and Khosla,V.K.,** Expression of Bcl2 proto-oncogene in primary tumors of the central nervous system. *Neurol.India* 2002. **50**: 290-294.
159. **Nor,J.E., Christensen,J., Liu,J., Peters,M., Mooney,D.J., Strieter,R.M., and Polverini,P.J.,** Up-Regulation of Bcl-2 in microvascular endothelial cells enhances intratumoral angiogenesis and accelerates tumor growth. *Cancer Res.* 2001. **61**: 2183-2188.
160. **Domen,J. and Weissman,I.L.,** Hematopoietic stem cells and other hematopoietic cells show broad resistance to chemotherapeutic agents in vivo when overexpressing bcl-2. *Exp.Hematol.* 2003. **31**: 631-639.

161. **Reed,J.C.**, Bcl-2 family proteins: regulators of apoptosis and chemoresistance in hematologic malignancies. *Semin.Hematol.* 1997. **34**: 9-19.
162. **Biroccio,A., Benassi,B., D'Agnano,I., D'Angelo,C., Buglioni,S., Mottolese,M., Ricciotti,A., Citro,G., Cosimelli,M., Ramsay,R.G., Calabretta,B., and Zupi,G.**, c-Myb and Bcl-x overexpression predicts poor prognosis in colorectal cancer: clinical and experimental findings. *Am.J.Pathol.* 2001. **158**: 1289-1299.
163. **Lebedeva,I., Rando,R., Ojwang,J., Cossum,P., and Stein,C.A.**, Bcl-xL in prostate cancer cells: effects of overexpression and down-regulation on chemosensitivity. *Cancer Res.* 2000. **60**: 6052-6060.
164. **Liu,R., Page,C., Beidler,D.R., Wicha,M.S., and Nunez,G.**, Overexpression of Bcl-x(L) promotes chemotherapy resistance of mammary tumors in a syngeneic mouse model. *Am.J.Pathol.* 1999. **155**: 1861-1867.
165. **Fadeel,B., Hassan,Z., Hellstrom-Lindberg,E., Henter,J.I., Orrenius,S., and Zhivotovsky,B.**, Cleavage of Bcl-2 is an early event in chemotherapy-induced apoptosis of human myeloid leukemia cells. *Leukemia* 1999. **13**: 719-728.
166. **Del Bello,B., Valentini,M.A., Zunino,F., Comporti,M., and Maellaro,E.**, Cleavage of Bcl-2 in oxidant- and cisplatin-induced apoptosis of human melanoma cells. *Oncogene* 2001. **20**: 4591-4595.
167. **Sawada,M., Nakashima,S., Banno,Y., Yamakawa,H., Hayashi,K., Takenaka,K., Nishimura,Y., Sakai,N., and Nozawa,Y.**, Ordering of ceramide formation, caspase activation, and Bax/Bcl-2 expression during etoposide-induced apoptosis in C6 glioma cells. *Cell Death.Differ.* 2000. **7**: 761-772.

168. **Bandyopadhyay,S., Sengupta,T.K., Fernandes,D.J., and Spicer,E.K.**, Taxol- and okadaic acid-induced destabilization of bcl-2 mRNA is associated with decreased binding of proteins to a bcl-2 instability element. *Biochem.Pharmacol.* 2003. **66**: 1151-1162.
169. **Ito,T., Deng,X., Carr,B., and May,W.S.**, Bcl-2 phosphorylation required for anti-apoptosis function. *J.Biol.Chem.* 1997. **272**: 11671-11673.
170. **May,W.S., Tyler,P.G., Ito,T., Armstrong,D.K., Qatsha,K.A., and Davidson,N.E.**, Interleukin-3 and bryostatin-1 mediate hyperphosphorylation of BCL2 alpha in association with suppression of apoptosis. *J.Biol.Chem.* 1994. **269**: 26865-26870.
171. **Deng,X., Ruvolo,P., Carr,B., and May,W.S., Jr.**, Survival function of ERK1/2 as IL-3-activated, staurosporine-resistant Bcl2 kinases. *Proc.Natl.Acad.Sci.U.S.A* 2000. **97**: 1578-1583.
172. **Scatena,C.D., Stewart,Z.A., Mays,D., Tang,L.J., Keefer,C.J., Leach,S.D., and Pietenpol,J.A.**, Mitotic phosphorylation of Bcl-2 during normal cell cycle progression and Taxol-induced growth arrest. *J.Biol.Chem.* 1998. **273**: 30777-30784.
173. **Deng,X., Gao,F., Flagg,T., and May,W.S., Jr.**, Mono- and multisite phosphorylation enhances Bcl2's antiapoptotic function and inhibition of cell cycle entry functions. *Proc.Natl.Acad.Sci.U.S.A* 2004. **101**: 153-158.
174. **Ruvolo,P.P., Deng,X., and May,W.S.**, Phosphorylation of Bcl2 and regulation of apoptosis. *Leukemia* 2001. **15**: 515-522.

175. **Blagosklonny,M.V., Chuman,Y., Bergan,R.C., and Fojo,T.,** Mitogen-activated protein kinase pathway is dispensable for microtubule-active drug-induced Raf-1/Bcl-2 phosphorylation and apoptosis in leukemia cells. *Leukemia* 1999. **13**: 1028-1036.
176. **Blagosklonny,M.V., Giannakakou,P., el Deiry,W.S., Kingston,D.G., Higgs,P.I., Neckers,L., and Fojo,T.,** Raf-1/bcl-2 phosphorylation: a step from microtubule damage to cell death. *Cancer Res.* 1997. **57**: 130-135.
177. **Srivastava,R.K., Mi,Q.S., Hardwick,J.M., and Longo,D.L.,** Deletion of the loop region of Bcl-2 completely blocks paclitaxel-induced apoptosis. *Proc.Natl.Acad.Sci.U.S.A* 1999. **96**: 3775-3780.
178. **Tang,C., Willingham,M.C., Reed,J.C., Miyashita,T., Ray,S., Ponnathpur,V., Huang,Y., Mahoney,M.E., Bullock,G., and Bhalla,K.,** High levels of p26BCL-2 oncoprotein retard taxol-induced apoptosis in human pre-B leukemia cells. *Leukemia* 1994. **8**: 1960-1969.
179. **Mollinedo,F. and Gajate,C.,** Microtubules, microtubule-interfering agents and apoptosis. *Apoptosis.* 2003. **8**: 413-450.
180. **Figuroa-Masot,X.A., Hetman,M., Higgins,M.J., Kokot,N., and Xia,Z.,** Taxol induces apoptosis in cortical neurons by a mechanism independent of Bcl-2 phosphorylation. *J.Neurosci.* 2001. **21**: 4657-4667.
181. **Wang,T.H., Popp,D.M., Wang,H.S., Saitoh,M., Mural,J.G., Henley,D.C., Ichijo,H., and Wimalasena,J.,** Microtubule dysfunction induced by paclitaxel initiates apoptosis through both c-Jun N-terminal kinase (JNK)-dependent and -independent pathways in ovarian cancer cells. *J.Biol.Chem.* 1999. **274**: 8208-8216.

182. **MacCorkle-Chosnek,R.A., VanHooser,A., Goodrich,D.W., Brinkley,B.R., and Tan,T.H.**, Cell cycle regulation of c-Jun N-terminal kinase activity at the centrosomes. *Biochem.Biophys.Res.Commun.* 2001. **289**: 173-180.
183. **Minden,A. and Karin,M.**, Regulation and function of the JNK subgroup of MAP kinases. *Biochim.Biophys.Acta* 1997. **1333**: F85-104.
184. **Tseng,C.J., Wang,Y.J., Liang,Y.C., Jeng,J.H., Lee,W.S., Lin,J.K., Chen,C.H., Liu,I.C., and Ho,Y.S.**, Microtubule damaging agents induce apoptosis in HL 60 cells and G2/M cell cycle arrest in HT 29 cells. *Toxicology* 2002. **175**: 123-142.
185. **Fan,M., Goodwin,M., Vu,T., Brantley-Finley,C., Gaarde,W.A., and Chambers,T.C.**, Vinblastine-induced phosphorylation of Bcl-2 and Bcl-XL is mediated by JNK and occurs in parallel with inactivation of the Raf-1/MEK/ERK cascade. *J.Biol.Chem.* 2000. **275**: 29980-29985.
186. **Hayakawa,J., Depatie,C., Ohmichi,M., and Mercola,D.**, The activation of c-Jun NH2-terminal kinase (JNK) by DNA-damaging agents serves to promote drug resistance via activating transcription factor 2 (ATF2)-dependent enhanced DNA repair. *J.Biol.Chem.* 2003. **278**: 20582-20592.

## **IX. ACKNOWLEDGEMENTS**

First and foremost, I am very grateful to Prof. Dr. Angelika M. Vollmar for the opportunity to perform this project in her laboratories. Her enthusiasm for “my” extraordinary compound was a constant source of inspiration.

I am very much obliged to PD Dr. Verena M. Dirsch for her support, helpful discussions and guidance throughout the course of this work.

Special thanks go to my thesis committee, especially Prof. Dr. E. Wagner for acting as coreferee.

I am very thankful to Prof. Dr. G. Wanner for the transmission electron microscopic analyses and the great support with the interpretation of the results.

My dearest thanks go to my “Boxenluder” Thomas for the great time in the lab and for never applying “Jetzt nicht” to my problems, no matter if they were about computers, bikes or life. I am deeply indebted to Kathi and Elke for their unlimited support. Sincere thanks also to H-P, Thommäß, Nancy and Anita for the fun and cheers, the scientific and non-scientific discussions and for being there. A great thank you goes to our technical staff – Conny, Elfriede, Hanna, Lila, Rita and Uschi. Additional thanks to all the other members of the institute not named here for the great atmosphere, especially to the PBII-team for many successful student courses.

Special thanks go to Alex and Claudia for keeping their faith in me and for their support over the distance.

Final acknowledgements go to my family and Andi for their constant help and encouragement.

## **X. CURRICULUM VITAE**

### **Persönliche Daten**

Name: Irina Melanie Müller  
Geburtsdatum, -ort: 21.02.1975 in Forchheim  
Staatsangehörigkeit: deutsch

---

### **Schulbildung**

1981 – 1985 Grundschule Forchheim  
1985 – 1994 Herder-Gymnasium Forchheim

---

### **Studium und Promotion**

1994 – 2001 Studium der Biologie  
Friedrich-Alexander-Universität Erlangen-Nürnberg  
1996 Vordiplom  
2001 Abschluss als Dipl. Biol. Univ.  
1997 – 1998 Studium der Applied Biosciences  
Glasgow Caledonian University, Glasgow, Schottland  
1998 Abschluss als Bachelor of Sciences  
2001 – 2004 Dissertation am Lehrstuhl von Prof. Dr. A. M.  
Vollmar, Zentrum für Pharmaforschung, Department  
Pharmazie, LMU München

